Biochemical and functional analysis of innexin2-containing gap junction channels during organogenesis in *Drosophila*

Dissertation

zur

Erlangung des Doktorgrades (Dr. rer. nat.)

der

Mathematisch-Naturwissenschaftlichen Fakultät

der

Rheinischen Friedrich-Wilhelms-Universität Bonn

vorgelegt von

Hildegard Lechner

aus

Bonn

Bonn 2008

Angefertigt mit Genehmigung der Mathematisch-Naturwissenschaftlichen Fakultät der Rheinischen Friedrich-Wilhelms-Universität Bonn

Erscheinungsjahr: 2009

1. Gutachter: Prof. Dr. rer. nat. M. Hoch
2. Gutachter: Prof. Dr. rer. nat. T. Lang

Tag der Promotion: 17.03.2009

Parts of this work are published in a scientific journal:

Lechner, H., Josten, F., Fuss, B., Bauer, R., Hoch, M. (2007). Cross regulation of intercellular gap junction communication and paracrine signaling pathways during organogenesis in *Drosophila*. Dev Biol. 310: 23-34.

Other publications:

Bauer, R., Weimbs, A., Lechner H., Hoch, M. (2006). *D*E-cadherin, a core component of the adherens junction complex modifies subcellular localization of the *Drosophila* gap junction protein innexin2. Cell Commun. Adhes. 13: 103-114.

Lehmann, C., Lechner, H., Löer, B., Knieps, M., Herrmann, S., Famulok, M., Bauer, R., Hoch, M. (2006). Heteromerization of innexin gap junction proteins regulates epithelial tissue organization in *Drosophila*. Mol. Biol. Cell. 17: 1676-1685.

Bauer, R., Löer, B., Ostrowski, K., Martini, J., Weimbs, A., Lechner, H., Hoch, M. (2005). Intercellular communication: the *Drosophila* innexin multiprotein family of gap junction proteins. Chem. Biol. 12: 515-526.

Abbreviations

A.bidest	*Aqua bidestillata*
Å	Angstrom
aa	Amino acid
Ab	Antibody
amp	Ampicillin
AP	Alkaline phosphatase
APS	Ammoniumpersulfate
BCIP	5-bromo-4-chloro-3-indolyl-phosphate
BFA	Brefeldin A
BiP	Binding protein
bp	Base pairs
cDNA	Coding deoxyribonucleid acid
CT	Carboxyterminus
D.m.	*Drosophila melanogaster*
DMSO	Diemethylsulfoxide
dNTP	Deoxyribonucleoside Triphosphate
DOC	sodium deoxycholate
DTT	Dithiothreitol
e.g.	exemplī grātia (*latin*); for example
ECL	Enhanced chemiluminescence
et al.	*et aliter*
Fig	Figure
fkh	Forkhead
g	Gravity
g	Gram
h	Hour/s
HRP	Horseradish peroxidase
hs	Heat shock
IF	Immunofluorescence
IgG	Immunoglobulin G
inx	Innexin
IP	immunoprecipitation
kD	Kilo Dalton
l	Liter
LB	Luria-Bertani Medium
M	Molarity

mg	Milligram
min	Minute/s
ml	Milliliter
mm	Millimeter
*m*RNA	Messenger ribonucleid acid
NaOH	Natriumhydroxide
NBT	Nito blue tetrazolium chloride
NEM	*N*-ethylmaleimide
NT	Aminoterminus
OD	Optical density
PBS	Phosphate buffered saline
PCR	Polymerase-chain-reaction
PDI	Protein disulfid isomerase
pH	The negative of the logarithm to the base 10 of the concentration of hydrogen ions
PMSF	Phenylmethylsulfonyl fluoride
PVDF	Polyvinylidene flouride
*q*RT-PCR	Quantitative real time polymerase-chain-reaction
rpm	Revolutions per minute
RT	Room temperature
SDS	Sodium dodecyl sulfate,
TAE	Tris-acetate-EDTA
TE	Tris-EDTA
TEMED	N,N,N`, N`-tetramethylethylenediamine
TMA/DPH	1-(4-trimethylammoniumphenyl)-6-phenyl-1,3,5-hexatriene p-toluenesulfonate
U	Unit
UV	Ultraviolett
V	Volt
v/v	Volume per volume
w/v	Weight per volume
WB	Western Blot
Wt	Wild type
µ	Micro
µl	Microliter

Table of Contents

1 Introduction

During development, embryonic tissues are formed in a specific manner resulting in highly ordered organisms, in which different organs take over pivotal tasks concerning metabolism and homoeostasis. Once the three germ layers are established, cells start to interact with each other and rearrange themselves to produce a variety of tissues and organs. Different procedures of tissue remodeling occur, such as tissue infolding and tissue elongation; the spatio-temporal control of these morphogenetic processes is responsible for the organisation of different body plans, as well as for organogenesis (Pilot and Lecuit, 2005).

The central problem of organogenesis is the specification of a correct cell behaviour in the appropriate group of cells. First, groups of cells are specified such that they follow a given morphogenetic pathway; second, the morphogenetic process is executed through changes in the cell architecture and/or polarity (Pilot and Lecuit, 2005). To ensure that all processes, which are necessary for the formation of a specialised tissue or organ are executed in a precise spatio-temporal manner, a complicated network of cell communication and signalling is required. This network integrates all single processes into a coordinated program that guarantees proper function of the developing organ.

1.1 Mechanisms of cell-cell communication

Cell communication mechanisms are strongly dependent on the synthesis of extracellular and intracellular molecules which are produced by cells to inform or signal to their neighbouring cells, or to cells that are further away. The perception of those molecules by other cells premises the existence of appliances that enable further processing of the information and in addition enable response to the signal. Appliances that take over those roles are first of all cell-surface receptor proteins, which bind extracellular molecules. Upon binding of the signal molecule to the receptor (= perception of the signal), the information is processed by a number of intracellular proteins that forward the message to the corresponding part of the cell where the response initiated. Response can be given in terms of alterations in gene expression profiles, ion channel permeability, metabolism, or rearrangements of the cytoskeleton.

A distinction is made on whether the signal molecules remain bound to the surface of a neighbouring cell (juxtacrine signaling) or whether the molecule is secreted (paracrine signalling). Propagation of signals by juxtacrine signalling is only possible when cells are in direct contact with each other. Secreted molecules induce paracrine signalling resulting in processing of the information by a responding cell in the vicinity of the emitting cell.

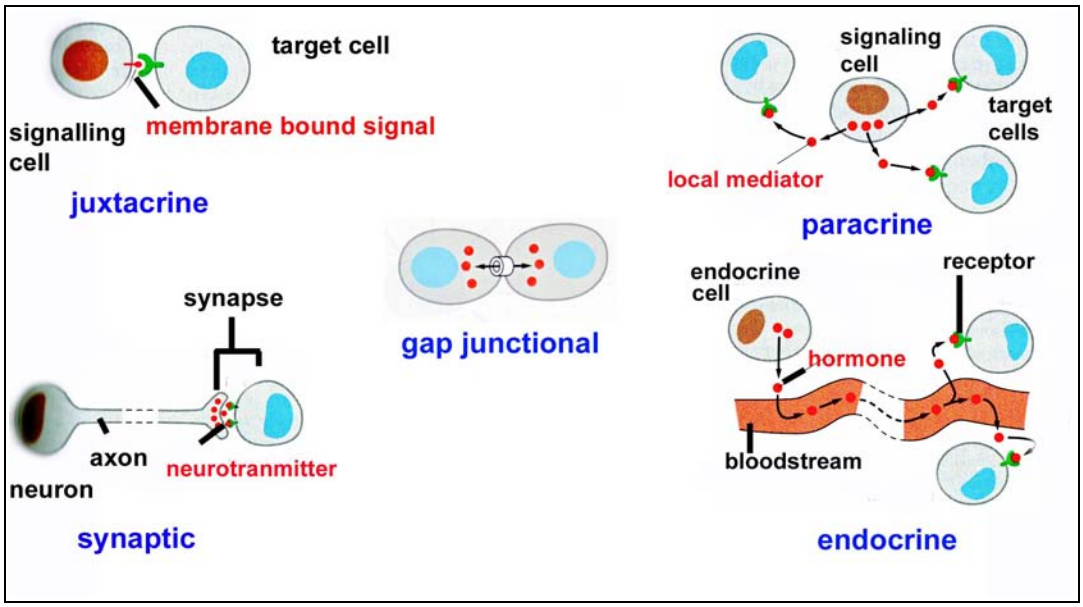

Fig. 1-1 Major mechanisms of cell communication. Schematic drawing of the five major signalling pathways that cells use for short-range and long distance communication. Synaptic and endocrine pathways enable cell communication over great distances within an organism, whereas juxtacrine, gap junctional and paracrine signalling enable direct or short range communication. (Modified after Alberts et al., 2004)

Long distance communication within an organism is mediated via synaptic and endocrine signalling. The signals mediated by hormones or an action-potentials are transmitted to different locations within an organism where they are further processed, for example by the release of neurotransmitters at the synapse between a neuronal cell and a target cell.

Another way to coordinate the activities of neighbouring cells is the usage of gap junctions. These specialised intercellular channels directly connect the cytoplasms of two cells and enable the exchange of small intracellular mediators, second messenger, like calcium and cyclic AMP. Gap junctions are one of the three major junctional complexes between epithelial cells (Fig. 1-1; Alberts et al., 2004).

1.1.1 Cross talk between cell communication mechanisms

Mechanisms of cell communication described in the previous section do normally not take place isolated from each other but instead, can be influenced by each other. Many examples for an elaborate interplay of signalling pathways has been elucidated so far. One example is the influence of the well conserved paracrine Wnt/Wingless signalling pathway on the expression of gap junction proteins in various tissues. The activation of the Wnt/wingless cascade by ligand binding had been shown to activate the transcription of gap junction constituting proteins in vertebrates and invertebrates (Fig. 1-2; Ai et al., 2000; Bauer et al., 2004; van der Heyden et al., 1998). Another example is the cross regulatory effect of the paracrine signalling pathways wingless and hedgehog which act in cooperation with the juxtacrine Notch and epidermal growth factor (EGF) signalling pathways in the epidermal differentiation of segment specification in *Drosophila melanongaster* (Sanson, 2001). With the potential of a regulatory dependency among different signalling pathways, information processing is improved and becomes more complex, resulting in refined patterns within organs and tissues.

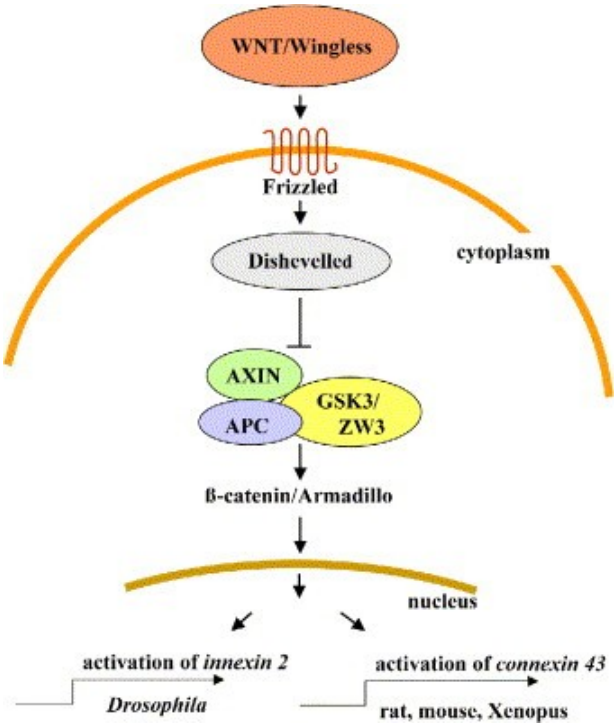

Fig. 1-2 Cross talk between cell communication mechanisms. Wnt/wingless signalling has an effect on gap junction protein expression. Activation of the conserved paracrine Wnt/wingless signaling pathway results in transcriptional activation of gap junction protein expression, leading to an enhanced direct intracellular communication within a specialised tissue. (After Bauer et al., 2005)

1.2 Epithelia and polarity

Cell communication networks program the formation of specialised tissues and organs within an organism resulting in the existence of many different cell types that enable crucial procedures including homoeostasis, which are needed to survive. One class of cells that is important for the separation of tissues and organs against the body cavity, providing a kind of barrier function, are the epithelial cells (Giepmans et al., 2008). They arise from the different germ layers during embryonic development. For instance, epithelia deriving from the ectoderm form the epidermis, endodermal epithelia (and ectodermal epithelia in *Drosophila*) are needed for lining of the gastrointestinal tract, whereas mesodermal cells form epithelia that line the inner body cavity. One characteristic of all epithelial cells is their highly organised architecture along the apico-basal axis. Cell polarity is defined as the asymmetry in cell shape, protein distribution and cell function. This architecture is set via different kinds of cellular junctions that guarantee the unique properties of those cells (Bryant and Mostov, 2008).

1.2.1 Epithelial junctions

The segregation of apical from basal plasma membrane constituents is widely believed to be mediated and controlled by lateral cell–cell adhesion junctions, which are therefore often considered to be the primary epithelial polarity landmark (Yeaman et al., 1999).
In general, cellular junctions equip epithelial cells with various specialised features, which make the epithelium to one of the most robust tissue layers (Fig. 1-3).

The initially mentioned adherens junctions serve for instance as cellular anchors that connect the cells within an organ or specialized tissue. They are associated with the actin cytoskeleton and are involved in adhesion (sticking cells together or sticking cells to surfaces). Conversely, members of a family of calcium ion-dependent cell adhesion molecules called cadherins, mediate the attachment between cells at adherens junctions. Adherens junctions also transduce signals into and out of the cell thereby influencing a variety of cellular behaviours including proliferation and differentiation. Some protein components of this type of junctions can shuttle to and from the nucleus, where they are thought to play a role in regulating gene expression (Niessen, 2007).

A second type of epithelial junctions are the tight junctions of the vertebrates and their invertebrate counterparts, the septate junctions. This essential type of cellular junction is

required in differentiated epithelial cells for polarised transport of proteins, intercellular integrity and signalling. Additionally, it provides fence function against the surrounding tissues (Eckert et al., 2008).

The third group of epithelial junctions which enables cellular communication are the gap junctions. They are established by proteins of the pannexin, innexin or connexin family of proteins in the animal kingdom.

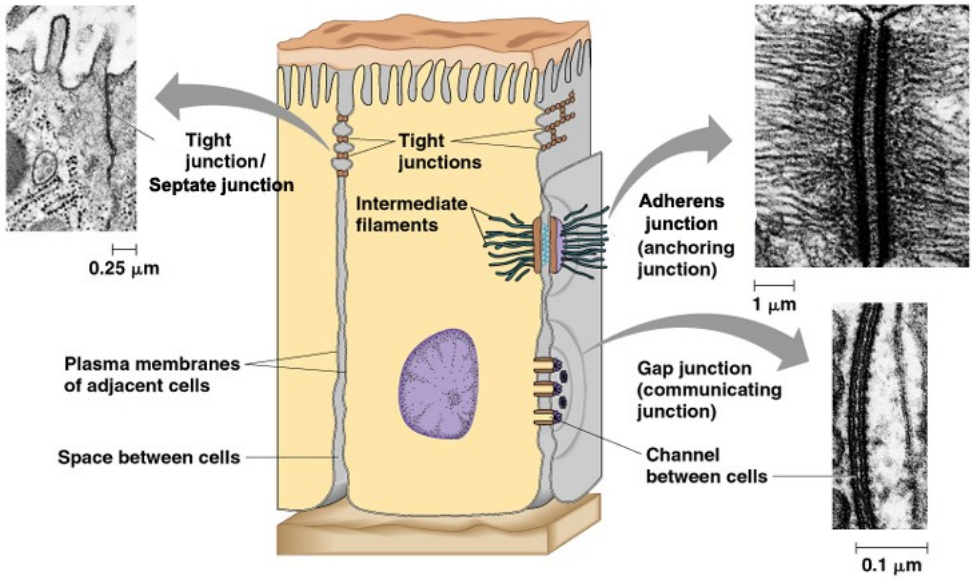

Fig. 1-3 Overview of epithelial junctions. Three types of epithelial junctions are established between two epithelial cells. Tight juctions (vertebrates) or septate junctions (invertebrates) provide fence function. Adherens junctions with intermediate filaments (only in vertebrates) are the anchoring junctions and gap junctions are the communicating junctions. (Campell et al., 1999; after Orci and Perrelet, 1975).

Whereas vertebrates express connexins and pannexins, the invertebrate gap junctions are build by the protein family of innexins. Gap junctions assure direct cell to cell communication via the exchange of ions and small metabolites within a tissue, an important prerequisite during development and homoeostasis. The pores of connexin channels have been studied extensively over the time and seem to be sufficiently wide (nominally ~12Å) to be permeable to a variety of cytoplasmic molecules. There is evidence for permeation through at least some types of connexin channels of virtually all soluble second messengers, amino acids, nucleotides, calcium ions, glucose and its metabolites (Harris et al., 2007).

1.2.1.1 Connexins

Connexin proteins construct intercellular gap junction channels that connect the cytoplasms of adjacent cells by the formation of two hemichannels, each consisting of a hexameric

assembly of connexin proteins. The composition of a hemichannel and the resulting gap junction channel is highly mutable. Homomeric hemichannels consist of six connexin protein subunits of one isoform, whereas heteromeric hemichannels exhibit the presence of two different connexin isoforms in one hemichannel. Finally, homotypic gap junction channels are constructed by two homomeric hemichannels of the same type and heterotypic channels form by combinations of different hemichannel types (Fig. 1-4; Mese et al., 2007). The variety of possible hemichannel arrangements is provided by the plurality of connexin isoforms. Meanwhile, 20 connexin isoforms have been isolated in mice and 21 isoforms in humans (Söhl and Willecke, 2004). Various connexin proteins are expressed in overlapping patterns throughout tissues and organs, whereas others are found only in specialised tissues. This enables a specification of gap junction channel permeability needed in different tissues.

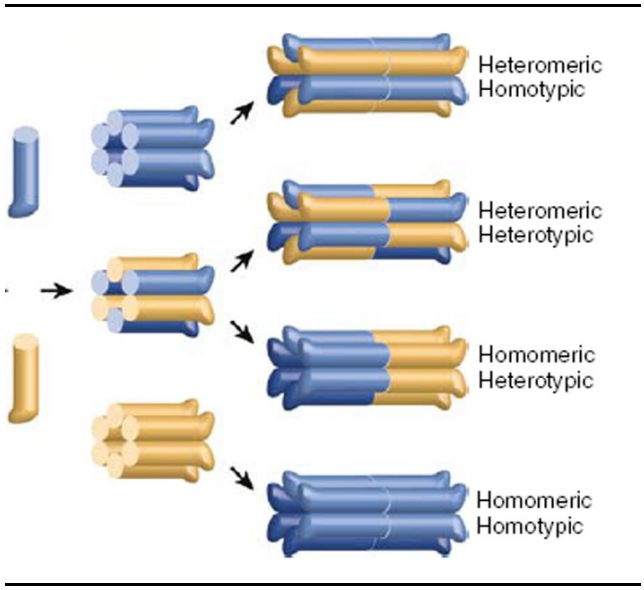

Fig. 1-4 Assembly of vertebrate gap junction channels. Hexameric hemichannels are formed by connexins. Two hemichannels build an intercellular gap junction channel that connects the cytoplasms of two adjacent cells. Nomenclature divides hemichannels that are constructed by one connexin isoform only as homomeric, hemichannels consisting of different connexin isoforms heteromeric. Gap junction channels are called homotypic when both hemichannels have the same composition, heterotypic, when it assembles from two different hemichannel subsets. (After Mese et al., 2007)

1.2.1.2 Innexins

Whereas connexins are the building blocks for gap junctions in vertebrates, innexins are the gap junction constituting proteins of the invertebrates (innexin, invertebrate connexin). They were first identified in the *Caenorhabditis elegans* and *Drosophila melanogaster*. Meanwhile, their existence has been proven in several other invertebrate species (Bauer et al., 2005)

with different amounts of isoforms in each species. The protein super family of innexins comprises eight members in *Drosophila* (Fig. 1-5).

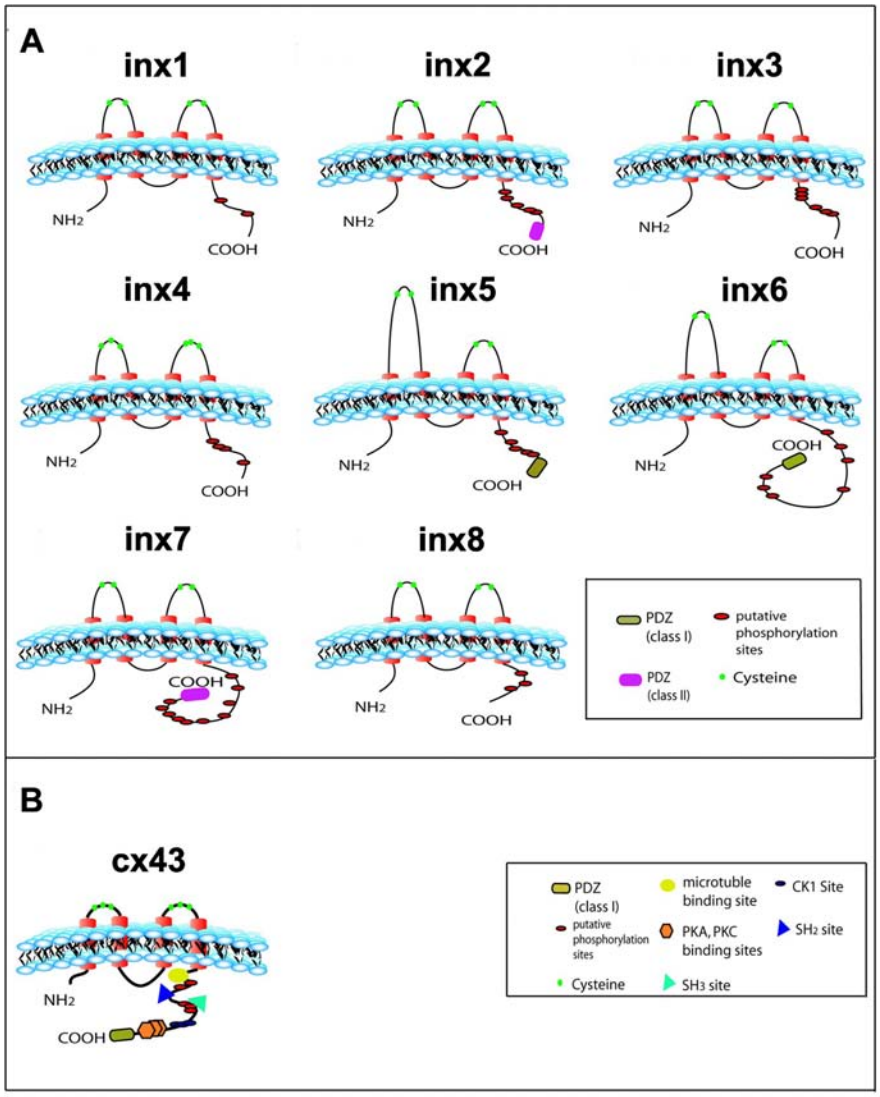

Fig.1-5 Conserved topology of gap junction proteins. Innexins and connexins show the same overall protein topology, although both families do not exhibit sequence homologies. The topology of the eight members of the innexin gap junction protein family are depicted in (**A**) compared to the topology of connexin43, as representative isoform for connexins (**B**). Both families exhibit topologies containing four transmembrne membranes (red), two extracellular loops with conserved cysteines (three cysteine residues for connexins and two in innexin sequence (green; exception inx4 with three residues) and cytoplasmic located N- and C-termini. Potential phosphorylation sites and protein interactions sites of C-termini are marked with different symbols, see legend. (After Bauer et al., 2005)

Despite of lacking sequence homology to the vertebrate connexins, all innexin proteins share a gap junction common architecture with four transmembrane domains, two extra-cellular loops, cytoplasmic located amino- and carboxy-termini as well as two, conserved cysteine-

residues in their extracellular loops; exception to the rule provides the germ line specific innexin4, which contains three cysteine residues (Fig. 1-5; Bauer et al., 2005). So far, no biochemical data exist concerning the oligomerisation process and nature of innexin hemichannels. Both of these issues are subject to the present thesis.

Nevertheless, innexins as gap junction constituting proteins have been found indispensible for a number of developmental processes, for instance the establishment of the left-right neuronal asymmetry in *C*.elegans (Chuang et al., 2007), the development of the embryonic nervous system and the formation of the posterior foregut of *Drosophila* (Bauer et al., 2004, Lechner et al., 2007, Ostrowski et al., 2008).

1.2.1.3 Pannexins

Connexins were considered for a long time to be the only class of the vertebrate proteins capable of gap junction formation, until additional candidates for this function with no homology to connexins, termed pannexins, were discovered in vertebrates (Panchin, 2005). In contrast, vertebrate pannexins and invertebrate innexins reveal partial sequence homology (Baranova et al., 2004).

Both, the human and the mouse genomes contain three pannexin-encoding genes. A first evidence that vertebrate pannexins may serve as gap junction constituting proteins was provided by Bruzzone and coworkers (Bruzzone et al., 2003), when they demonstrated that in paired oocytes, rodent pannexin1 alone and in combination with pannexin2, induced the formation of intercellular channels. Meanwhile, biochemical studies also provide evidence for a hexameric composition of pannexin hemichannels (Boassa et al., 2007). Functional assays in cultured cells, transiently expressing panx1 and panx3, were incapable of forming intercellular channels, but assembled into functional cell surface channels (Penuela, et al 2007). These proteins probably play an important biological role as single membrane channels. Pannexin function is only poorly understood. Initial expression analyses have been shown that they are expressed in neuronal structures of the mouse brain (Meier et al., 2006).

1.2.2 Vertebrate gap junction life cycle

Vertebrate gap junction protein biosynthesis and assembly are strictly regulated processes for the reason that the half life of intercellular junctions is with only a few hours relatively short and must be therefore processed in a highly ordered fashion (Musil et al., 2000). For instance, connexin43 the best-studied connexin isoform has a half-life of only 1.5-5 hours

(Leithe and Rivedal, 2007). Most connexins are cotranslationally integrated into the endoplasmic reticulum (ER) membrane. Misfolded connexins are targeted for ER associated degradation (ERAD). The oligomerisation of six connexins into a hemichannel is thought to be accomplished in an advancing manner starting in the endoplasmic reticulum and ending in the trans-Golgi network (Musil and Goodenough, 1993; Sarma et al., 2002; Laird, 2006). Some members of the connexin family show that complete oligomerisation is delayed until the connexin passes through the intermediate compartment and reaches the distal elements of the Golgi apparatus, namely trans-Golgi network (TGN; Laird, 2006). Hexameric hemichannels (= connexons) are subsequently transported to the targeting membrane via vesicles, which are transported through microtubules (Shaw et al., 2007). Connexons may function as hemichannels or laterally diffuse in a closed state to sites of cell-cell apposition where they dock with connexons from an opposing cell. In conjunction with cadherin-based cell adhesion, gap-junction channels cluster into plaques, open and exchange secondary messengers. Connexin-binding proteins have been identified, and it is likely that these binding proteins regulate plaque formation and stability, possibly by acting as scaffolds to cytoskeletal elements (Laird, 2006). After having functioned as intercellular channels or hemichannels, gap junctions are degraded by formation of annular junctions (Piehl et al., 2007), which either fuse with the lysosome or are targeted to the proteosomal pathway (Leithe et al., 2007). Whole gap junction plaques and fragments of those are internalised into one of two adjacent cells as a double-membrane structure commonly referred to as annular junction. Other pathways for connexin internalisation may exist in which connexons disassemble and enter the cell by classical endocytic pathways (Fig. 1-6).

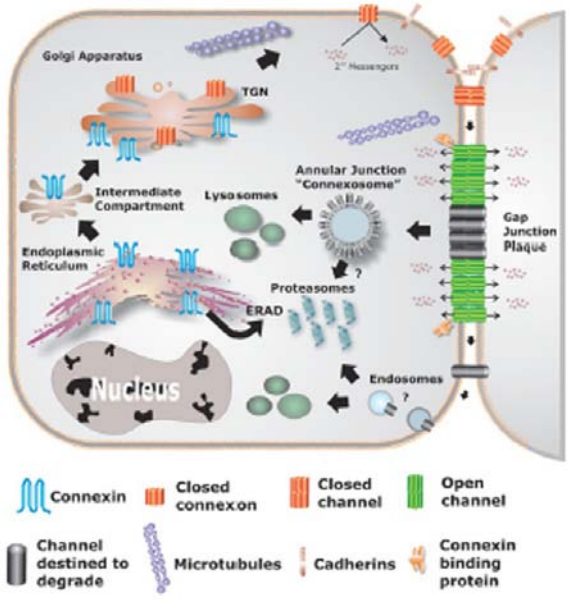

Fig. 1-6 Life cycle of vertebrate gap junctions. For details, see text. (After Laird, 2006).

The continuous synthesis and degradation of connexins through these processes serve as mechanisms for the quick adaptation of tissues to changing environmental conditions.

1.3 Regulation of membrane trafficking in epithelial cells

As presented in the previous section, gap junction proteins that take over their function at the plasma membrane of epithelial cells, have to travel along the secretory pathway to their place of destination.

In general, polarized epithelial cells are exposed to mechanical stress frequently and need to assure that protein turnover at the different membrane domains takes place in highly ordered fashion because of the perpetually ongoing cycles of protein delivery and degradation. Therefore, different pathways are established in those cells to ensure an adequate protein delivery to the different domains. This is achieved mainly by the existence of two delivery pathways, one that ensures trafficking of membrane proteins to the apical site of the cell and one that enables transport of proteins to baso-lateral plasma membrane domains. Proteins determined tor the targeting to different domains of the plasma membrane have to undergo a sorting process before membrane trafficking, which is accomplished within a specialised organelle, the trans-Golgi-network.

1.3.1 Sorting of cargo in the trans-Golgi network

The Golgi apparatus is know as the most important organelle for the selective sorting process of proteins. The delivery of most proteins to their place of destination within a cell is mediated by transport vesicles, so called post-Golgi-carriers, which arise from membranes of the trans-Golgi-network (TGN) that do not contain Golgi-resident enzymes. Because of their different size and shape, the resulting protein transporters differ, therefore also called pleiomorphic structures. Post Golgi carriers emerge after initial separation of cargo proteins from Golgi resident proteins from the last cisternae of the Golgi-complex and are most likely formed by a pulling force mediated by microtubule-base motors like kinesin (Luini et al., 2008). The resulting curvature of the emerging vesicles is not completely understood yet. Two hypotheses try to explain the shaping of the vesicles. One claims that additional proteins are involved (Antonny, 2006), the other mechanism argues for alterations in the lipid composition of those membrane in vesicle bending (De Matteis and Godi, 2004). A

combination of both mechanisms is also conceivable. Fission of the carrier from the cisternal membrane finally takes place at the thinnest part of the vesicle precursor. Movements of motor proteins along the cytoskeleton towards the periphery of the cell provide the necessary tension to induce fission and separation of the post Golgi transporter from the TGN (Fig. 1-7)

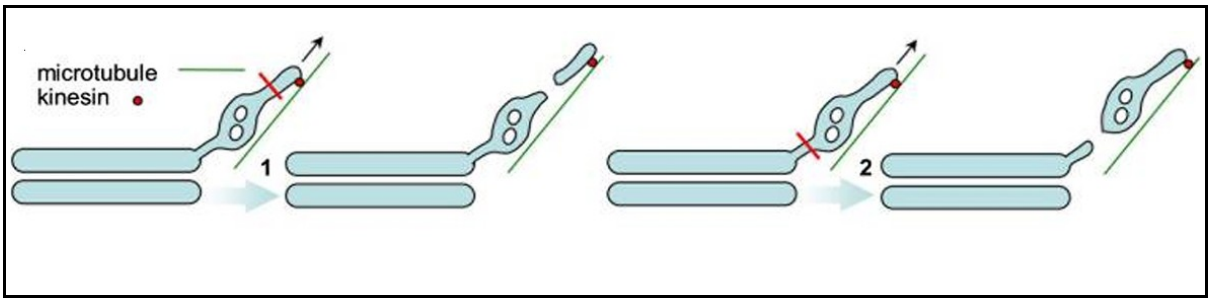

Fig. 1-7 Fission of transport vesicles from the TGN. Membranes from the trans-Golgi cisterna are pulled along microtubules (green line) by kinesin (red dot). Fission of the vesicle takes place at the thinnest part of the stretched membrane (red line). Fission close to the tip leads to the formation of smaller carriers (1), whereas fission at the bottom of the emerging structure results in larger vesicles (2). (After Luini et al., 2008).

Allocation of the right delivery pathway (apical or baso-lateral) for the cargo, which is appointed to different domains of polarised cells, requires different characteristics within the composition of the transported protein.

1.3.2 Apical transport

Proteins that are designated for apical membrane insertion usually contain ectodomain signals like N- or O-linked glycans, a special organisation of trans membrane domains or are equipped with glycosylphosophatidylinositol-anchors (GPI-anchored proteins). One or more of these attributes are recognised by the delivery machinery of the cell and transport is initiated after exit of proteins from the trans Golgi network (TGN). A common mechanism here is the clustering of proteins within glycolipid raft domains or other carriers, that recognise attached glycans via lectins (Fölsch, 2008). Lectins are named after their role in the recognition and selection of carbohydrate moieties of proteins (lectin derives from the latin word *legere*, meaning to select). They are grouped into two different types with a one group localising mainly in intracellularly in luminal compartments, which is responsible for sorting and trafficking of glycoproteins in the secretory and other pathways. The other group of lectins is found outside of the cell and is either secreted or localised to the plasma membrane (Dodd et al., 2001).

1.3.3 Baso-lateral transport

Transport of proteins to the baso-lateral membrane domain of epithelial cells is accomplished at the initial phase by the recognition of a signal sequence encoded in the cytoplasmic tail of transmembrane proteins. This motif has been found to be either tyrosine or di-leucine based and seems to be dominant over apical transport mechanism information. Cytosolic adaptor proteins (AP-1, AP-3, AP-4) are bound to this motif in the TGN and build, once they arrived at the plasma membrane a hetero-tetrameric complex by binding AP-2. This complex is also interacting with clathrin during endocytosis later on (Ellis et al., 2006). Two potential trafficking routes to the baso-lateral membrane domain are discussed, first an indirect route which is executed via recycling endosomes and a direct route. Less is known about the direct sorting at the TGN, because many baso-lateral proteins travel through the TGN only once, while they are typically recycled many times (Fölsch, 2008).
The idea of the recycling endosome as a new type of cargo sorter for baso-lateral proteins came up in the recent years. Little is known so far about the trafficking between TGN and the recycling endosome. It is known that polarised columnar epithelial cells express the epithelial cell-specific adaptor complex AP-1B (Ohno et al., 1999). AP-1B plays an important role in baso-lateral sorting from recycling endosomes. On the one hand it interacts directly with the baso-lateral cargo, and on the other hand facilitates membrane recruitment of subunits of the exocyst complex for incorporation in the AP-1B vesicle.

1.3.3.1 Exocyst complex

The exocyst is an octameric protein complex being involved in vesicular trafficking, specifically in tethering and spatial targeting of post-Golgi vesicles to the plasma membrane prior to vesicle fusion. Subunits are sec3, sec5, sec6, sec8, sec10, sec15, exo70 and exo84. Mutations of each member have been shown to prevent exocytosis and to arrest growth of the daughter cell and cytokinesis. The resulting phenotypes of all subunits were similar and biochemical studies led to the assumption that they act in concert to mediate exocytosis of baso-lateral proteins (Murthy et al., 2004).
The complex is implicated in a number of cell processes, including exocytosis and also cell migration and growth. It was discovered initially in yeast during a screen for regulators of exocytosis (TerBrush et al., 1996; Novick et al., 1980) and was later on found in various other species from invertebrates, like *Drosophila*, to mammals. Components of the exocyst complex are localised to sites of active exocytosis, where they mediate the targeting and tethering of post-Golgi secretory vesicles for subsequent membrane fusion (Murthy et al.,

2003).

Targeting of LDL-receptors to the baso-lateral membrane was the first functional study showing the involvement of the exocyst complex in anterograde trafficking of membrane proteins (Grindstaff et al., 1998). Fusion activity of exocyst complex mediated protein delivery is observed only in the upper third of the basolateral membrane domain immediately below the tight junctions (Kreizer et al., 2003). Assembly of the exocyst complex at the fusion site might be regulated by ralA, a small GTPase that seems to directly interact with the exocyst subunits sec5 and exo84.

Two possible mechanisms exist by which the exocyst complex may mediate vesicle tethering or docking at the plasma membrane. In the first mechanism, the exocyst complex may exist as two subcomplexes. One subcomplex interacts with secretory vesicles, while the other subcomplex is recruited to specific plasma membrane domains. Interaction between these two halves of the complex enables vesicle docking at the plasma membrane.A second mechanism suggests that the entire exocyst complex may be recruited to the plasma membrane where it mediates vesicle docking. Exocyst subunit positive vesicles have been shown to colocalise with microtubuli, arguing for a microtubule dependent trafficking to the membrane. In addition, members of the exocyst complex may take over the transfer of vesicles from the microtubule to cortical the actin-network to enable vesicle fusion with plasma membrane. It is not clear how many events take place between the transfer of secretory vesicles from microtubules, at the vicinity of the plasma membrane, to the fusion of these vesicles at the plasma membrane (Wang and Hu, 2006). Evidence exists that secretory vesicles have to go through both microtubule and actin networks to reach the plasma membrane (Langford, 1995, Goode et al., 2000).

Cargo vesicles are transported along the microtubule-network and the actin cytoskeleton by motor proteins to reach their target membranes or compartments within the cell. Selection of specific cargo proteins by motor proteins is accomplished either by a direct interaction between the the cargo protein and the motor protein or is mediated, as mentioned above, via binding of adaptor proteins to the cargo protein.

1.4 Actin and microtubule dependent transport of vesicles

The transport of secretory vesicles, organelles and protein complexes is an essential intracellular process. Disturbance of the machinery by mutations of motor proteins that are necessary for the accomplishment of trafficking along the cytoskeleton leads in humans to severe diseases like amyotrophic lateral sclerosis, parapalegia and Griscelli syndrome type 1

(Ross et al., 2008). Whereas microtubules serve as trafficking routes for long distance travelling of cargo to the plasma membrane, actin filaments are mainly involved in transport processes that occur beneath the plasma membrane (Fig. 1-8; Rogers et al., 2000).

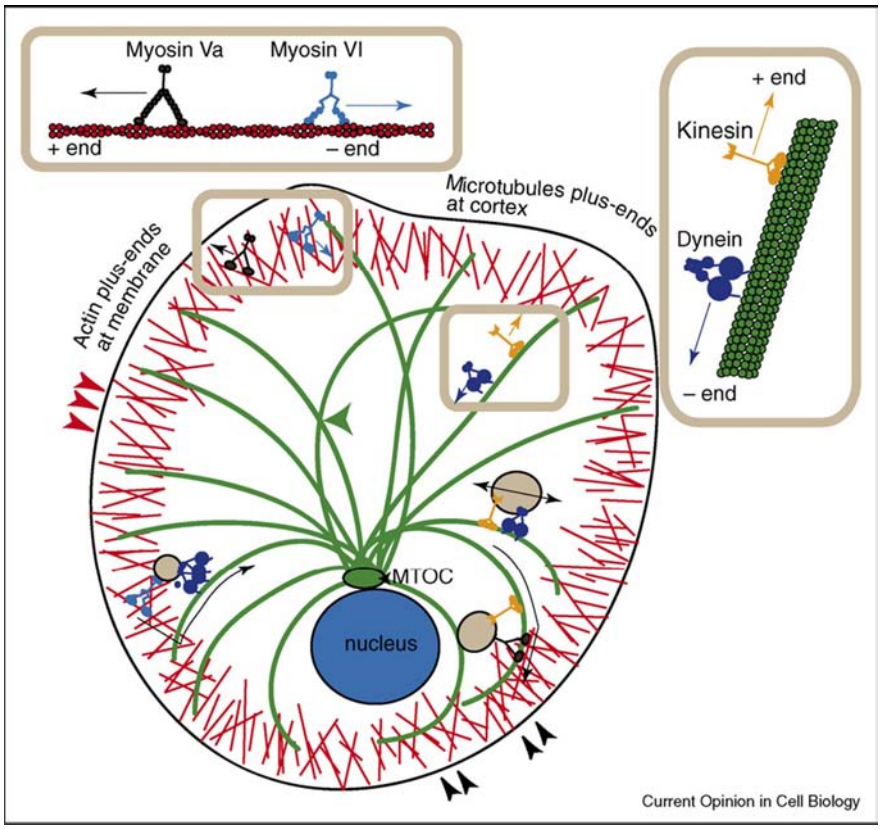

Fig.1-8 Motor proteins and vesicular cargo transport in the cell. Actin filaments (red) and microtubules (green) provide a network within the cytoplasm of a cell that is used to traffic vesicles from one place to another within the cell. Motor proteins assure these movements. Kinesin (yellow) enables transport along microtubules to the plus end, Dynein (blue) to the minus end. Myosin motor proteins allow movements of vesicles along actin filaments. Myosin Va directs cargo in plus direction, Myosin VI directs cargo in minus direction. Actin filament plus ends are oriented to the plasma membrane and microtubule plus ends orient to the cell cortex. (After Ross et al., 2008).

1.4.1 Microtubule organisation

Microtubules are polymers of subunits from α-and ß-tubulin proteins. The smallest subunit of a microtubule itself is a heterodimer formed by both tubulin isoforms. Both tubulin proteins contain GTP binding sites. The resulting microtubule is a hollow and stiff cylindrical structure formed by 13 parallel protofilaments, each composed of the above mentioned heterodimers in an alternating order. Each protofilament is assembled from subunits that all point in one direction resulting in a structural polarity with α-tubulins directed to the one end, termed minus end and ß-tubulins oriented to the other end, termed plus end (Fig.1-9). Nucleation, as

the initial step in the biogenesis of microtubules, paraphrases a spontaneous process where short oligomers are composed of subunits, that remain unstable as long it is not stabilised by additional subunits (Desai and Mitchison, 1997).

Microtubule nucleation begins at the minus ends, whereas the plus end is growing end orients towards the cell periphery. The minus end of microtubules is anchored to the microtubule-organisation center (MOTC), the centrosome, which located near the nucleus of the cell, in most animal cells (Fig. 1-8). A γ-tubulin ring complex, which is part of the MOTC, has been shown to mediate the initial step of nucleation (Raynaud-Messina et al., 2007). Microtubules are in a process of ongoing renewal by which polymers maintain a constant length. One process that controls a constant polymer length is termed “treadmilling” and includes growing of the plus end by the recruitment of heteromeric subunits on the one end and shedding of subunits from the minus end. To ensure that renewal takes place in a steady-state fashion, GTP hydrolysis along the way of incorporation of new subunits is a crucial process. The other process, called dynamic instability describes a mechanism in which the individual microtubule ends switch between a phase of relatively slow sustained growth and a phase of relatively rapid shortening (Margolis and Wilson, 1998).

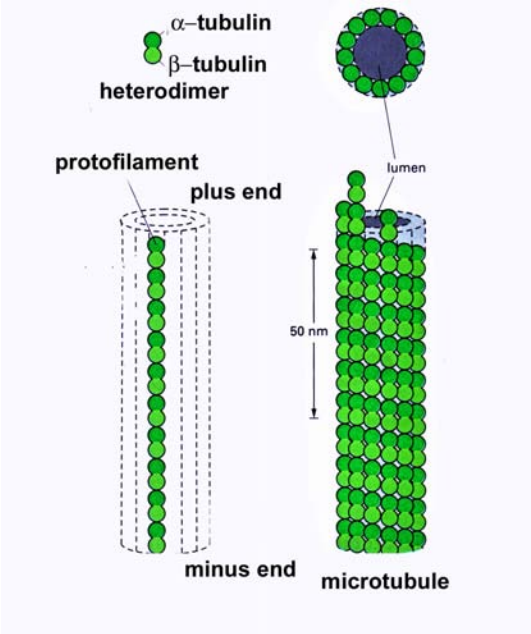

Fig. 1-8 Structure of microtubules and their organisation. The smallest unit within a microtubule is a heterodimer consisting of one α- and one β-tubulin protein. Subunits oligomerise in a nucleation process and are stabilised by addition of further subunits, a protofilament results. 13 parallel protofilaments build a hollow cylindrical tube, one microtubule.

1.4.2 Microtubule based motors and transport of cargo

Motor proteins, driving the movement of cargo along microtubules, are members of the kinesin and dynein super families. Both are microtubule activated ATPases, which provide the driving forces along microtubular movements.

Kinesin causes movements towards the microtubule plus end, whereas dynein enables movements to the microtubule minus end. Kinesin is a hetero-tetramer composed of two alpha- and beta- subunits. The alpha-subunits contain ATP binding site in their N-terminal heads, whereas the tail domain mediates binding to membrane vesicles or other structures (Fig.1-7).

Cytoplasmic dynein consists of two heavy chains and multiple intermediate and one light chain. Dynein cannot transport cargo on its own, like kinesin does, but needs to build a complex with other proteins, the so called dynactin-complex, that links vesicles to the motor protein. Kinesin and the dynein complexes are distinguished by the filament substrates, the direction of movements, the objects they move and the regulation of movement. Kinesin and dynein are not able to convert the ATP provided energy into movements themselves, but need accessory components, the microtubule associated proteins (MAPs; Schroer and Sheetz, 1991). MAPs are a family of proteins that bind to and stabilise microtubules. Whereas some MAPs bind specifically to the microtubule plus ends or the minus ends, many MAPs bind along the microtubule lattice (Halpain and Dehmelt, 2006).

1.4.3 Actin organisation

In contrast to the organisation of microtubules where nucleation takes place mostly near the nucleus in the cytoplasm, actin filament nucleation is accomplished frequently below the plasma membrane. This is also the reason for observations of highest actin-filament densities within in the cell. The area just below the plasma membrane is called cell cortex. Its function is to determine shape and movement of the cell surface and is involved in trafficking of scaffold proteins to the plasma membrane (Ross et al., 2008).

Actin subunits are monomeric globular proteins with a binding capacity for ATP, which provides energy for the process of actin filament formation. One actin filament consists of two parallel protofilaments that are twisted around each other in right handed helix, which provide flexibility to the filament. Those single filaments are crosslinked and bundled with each other within the cell. Actin needs several binding proteins that promote or inhibit polymerisation.

Treadmilling and dynamic instability also regulate the steady-state growth and shrinkage of actin-filaments as described for microtubules in section 1.4.1. with the difference, that ATP is the driving force in this process.

1.4.4 Actin based motors and transport of cargo

The large family of myosins has been implicated in movements of the actin cytoskeleton. This superfamily consists of 20 members among organisms (Krendel and Mooseker, 2000). The family members myosin I, myosin II, myosin V and myosin VI are the best investigated ones. Myosin II is involved in muscle contraction, whereas Myosin I, V and VI take part in cytoskeleton-membrane interactions like the transport of transport vesicles.

Myosins consist of one or two heavy chains and a different number of light chains, with regulatory functions. One characteristic of all myosins is a specialised head, neck and tail domain within all myosin heavy chains. All head domains are equipped with ATPase activity, which promotes the hydrolysis ATP that binds to the neck region. The tail region of myosins I V and VI bind the plasma membrane or the membranes of intercellular vesicles. Myosin movement is carried out towards the actin-filament plus end by most of the myosins, with the exception myosin VI, which moves to the minus end (Fig. 1-7; Ross et al.,2008).

1.5 Objective of research

Innexin2 as one representative member of the *Drosophila melanogaster* innexin gap junction family was investigated in this work to understand nature and assembly of *Drosophila* gap junction hemichannels biochemically, using various approaches of density gradient centrifugation. In addition, trafficking of innexin2 containing hemichannels to the plasma membrane was analysed by a combination of experiments performed in cell culture and *Drosophila*. Furthermore, the influence of innexin2 function on the organogenesis of a specialised part of the posterior foregut of *Drosophila*, the proventriculus, was investigated. Here, the influence of innexin2-dependent gap junctional communication on paracrine signalling pathways was studied that are involved in morphogenetic movements and organ formation.

2 Material

2.1 Chemicals

All materials used are purchased with the quality grade *pro analysi* from Biomol, BioRad, Boehringer, Faust, Invitrogen, Macherey & Nagel, Promega, Pierce, Qiagen and Roth.

2.2 Expendables

Common laboratory equipment	Faust (Meckenheim), Schütt (Göttingen)
1,5ml / 2ml test tubes	Roth
PCR-reaction tubes, thick-walled	Eppendorf (Hamburg)
Plastic wares	Greiner (Solingen)
X-ray films	Fuji Medical X-Ray Film Super RX; BW Plus

2.3 Equipment

autoclave	H+P Varioklav steam-sterilisator EP-2 with microprocessor
binocular	Olympus S2X 12; Olympus S2 40
centrifuges	Biofuge Pico, Heraeus Eppendorf centrifuge 5415R; Hettich centrifuge Rotina 46R
confocal-laser scanning microscopes	Leica TCS SP2, ZEISS LSM 710
electro-pipette	Accu-jet; Brand
electrophoretic transfer cell	Trans Blot, BioRad

Fluorescence microscope	Zeiss Axiovert M200 with ApoTome
gel-documentation system	Biozym, Alpha Digi Doc
incubator for bacteria	Memmert, Model 400
microwave	Samsung, 1000W
nucleic acid electrophoresis	PEQLAB
optical microscope	Olympus Ax70 with camera Olympus U-TVO.5xC-2; Color View Soft Imaging System
PCR-Cycler	MJ Research PTC-200 Peltier Thermal Cycler
photometer	BioRad SmartSpec Plus
power supply unit	Bio-Rad Power Pac 200
protein gel electrophoresis	Mini-Protean 3 Cell, BioRad
scales	Sartorius BL 150 S; Sartorius B211 D
test-tube rotator	Snijders
thermo mixer	Eppendorf Thermomixer comfort
ultracentrifuge	Beckman Coulter OptimaTM LE-80 K
ultrasound device	Bandelin SONOPLUS HD2070
vortexer	Vortex Genie2 (Scientific industries)

water bath	Julabo TBW22
x-ray film developer	Curix 60, AGFA

2.4 Standards and Kits

Company	Item	Purpose
BioRad	All Blue prestained Protein Standard	Molecular weight determination of proteins
Boehringer / Roche	DNA Molecular Weight Marker X	Molecular weight determination of DNA-fragments;
	PCR Nucleotide Mix	PCR component
Macherey & Nagel	Nucleospin Plasmid Midi Kit	Purification of plasmid DNA
	NucleoSpin Extract II	Extraction and purification of DNA fragments
	NucleoSpin RNA II	Extraction and purification RNA from tissues and cells
Pierce	ECL kit	Detection of Western Blot via chemiluminescence
	Cell surface biotinylation kit	Biotinylation of cell surface exposed proteins
Promega	Canine microsomal membranes	*In vitro* oligomerisation of proteins
	Rabbit Reticulocyte Lysate System, nuclease treated	i*n vitro* translation from *m*RNA
	Ribomax Large Scale RNA Production Systems	*in vitro* transcription, *m*RNA synthesis
Qiagen	QuantiTect Reverse cDNA-Synthesis Transcription Kit	cDNA synthesis

2.5 Antibodies

2.5.1 Primary antibodies

Antibody	Species	Source	Concentration
Armadillo	mouse	DSBH	1:5
BIP	mouse	S. Roth	1:1000
alpha-Spectrin	mouse	DSHB	1:10
*D*E-Cadherin	goat	Santa Cruz	1:30
Disc -large	mouse	DSHB	1:10
GFP (FI)	rabbit	Santa Cruz	1:100
DIG	sheep	Boehringer/Roche	1:500
DIG-AP	mouse	Boehringer/Roche	1:2000
FasciclinII	mouse	DSHB	1:10
GFP (B2)	mouse	Santa Cruz	1:50 1:500 (WB)
Hedgehog	rabbit	T. Tabata	1:50
Innexin2-CS	guinea pig	Davids	1:50
Innexin2-CT (KLRH)	rabbit	Davids	1:40 1:400 (WB)
Innexin2-CT (REM)	rabbit	Davids	1:40
Innexin3-CS	rabbit	Davids	1:100 1:400 (WB)
Myc (9E10)	mouse	Santa Cruz	1: 200 1: 600 (WB)
Rab 5	rabbit	M. Gonazales-Gaitan	1:50 1:200 (WB)
ß-galactosidase	mouse	Promega	1:500

Antibody	Species	Source	Concentration
ß -tubulin (E7)	mouse	DSHB	1.200 1:5000 (WB)
Sec6	guinea pig	U. Tepass	1:100
Sxl	mouse	DSHB	1:10
Syx	mouse	DSHB	1:600 (WB)

(DSHB; Developmental Studies Hybridoma Bank; WB; Western Blot)

2.5.2 Secondary antibodies

Antibody	Species	Source	Concentration
rabbit-HRP	donkey	Santa Cruz	1:15000 (WB)
mouse-HRP	donkey	Santa Cruz	1:15000 (WB)
guinea pig-HRP	donkey	Santa Cruz	1:15000 (WB)
rabbit-Cy3	donkey	Dianova	1:200/1:300 (IF cells)
mouse-Cy3	donkey	Dianova	1:200/1:300 (IF cells)
guinea pig-Cy3	donkey	Dianova	1:200/1:300 (IF cells)
rabbit-Alexa 488	donkey	Molecular Probes	1:100/1:200 (IF cells)
mouse-Alexa 488	donkey	Molecular Probes	1:100/1:200 (IF cells)
guinea pig Cy2	goat	Dianova	1:100/1:200 (IF cells)
Mouse-Alexa 633	goat	Molecular Probes	1:100
rabbit-Alexa 633	donkey	Molecular Probes	1:000
sheep-Biotin	goat	Sigma	1:300

(IF; immunofluorescent staining of cultured cells)

2.6 Solutions

Agarose gel loading buffer (5x)	0.1% bromophenol blue, 0.1% xylene cyanol, 15% ficoll, 10% glycerine
Alkaline solution I (plasmid preparation)	50 mM glucose, 25 mM Tris-Cl (pH 8.0),10 mM EDTA (pH 8.0)
Alkaline solution II (plasmid preparation)	0.2 N NaOH, 1% (w/v) SDS
Alkaline solution III (plasmid preparation)	60 ml 5 M potassium acetate, 11.5 ml glacial acetic acid, 28 ml A.bidest
Ampicillin	50 mg / ml ampicillin in A.bidest for stock solution, working concentration 50 µg / ml
AP-buffer	100 mM NaCl, 50 mM $MgCl_2$, 1 M Tris; pH 9.5, 0.1% Tween-20
Apple juice agar	1 l Apple juice, 100 g sugar, 85 g agar, 40 ml nipagine (15%), 3 l A.bidest
Coomassie staining solution	0.25 g Coomassie Brilliant blue R-250 in 90 ml of methanol : H_2O (1:1, v/v) and 10 ml glacial acetic acid
EDTA (0.5M, pH 8.0)	186.1 g EDTA to 800 ml H_2O .adjust pH to 8.0 with NaOH, autoclave
Homogenisation medium (cells/embryos)	10 mM HEPES, 25 mM EDTA, 100 mM NaCl, pH 7.4
Hybridisation buffer	50% deionized formamide, 5 x SSC, 100 µg/ml tRNA, Heparin 5 µg / ml, 0.1% Tween-20
Incubation buffer	136.8 mM NaCl, 5.36 mM KCl, 0.336 mM Na_2PO_4, 0.345 mM KH_2PO_4, 0.6 mM $MgSO_4$, 2.7 mM $CaCl_2$, 20 mM HEPES, adjusted to pH 7.5 (supplemented with 10 mM NEM and 200 µM PMSF)
Injection buffer	5 mM KCl, 0.1 mM $NaPO_4$, pH 6.8
Nipagine-solution	147 ml ethanol, 63 ml A. bidest, 21 g nipagine
PBS (20x)	2.6 M NaCl, 10mM Na_2HPO_4, 60 mM NaH_2PO_4
PBT	1x PBS + 0.1% Tween 20
Proteinase K	20 mg / ml proteinase K in 50% glycerol, 10 mM Tris; pH 7.8, store at - 20°C

RF-1 solution (chemocompetent bacteria)	100 mM $RbCl_2$; 50 mM $MnCl_2$; 30 mM KOAc; 10 mM $CaCl_2$; 15% v/v Glycerin; pH 5.8
RF-2 solution (chemocompetent bacteria)	10 mM Mops, pH 7,0; 10 mM $RbCl_2$; 10 mM $CaCl_2$; 15% v/v Glycerin
RIPA buffer	100 mM NaCl, 1% IGEPAL CA-630, 0.5% DOC, 0.1% SDS, 50 mM Tris (pH 8.0) + protease inhibitor cocktail
SDS gel-loading buffer	50 mM Tris-Cl (pH 6.8), 100 mM DTT, 2% (w/v) SDS, 0.1% bromophenol blue, 10% glycerol
Solubilisation buffer	20 mM EDTA, 10 mM DTT, 2% (w/v) n-dodecyl ß-D-maltoside, 20mM triethanolamine (TEA); pH 9.2
Sonication buffer	120 mM potassiumglutamate, 10 mM EDTA (pH 8.5), 20 mM potassiumacetate, 4 mM $MgCl_2$, 2 mM ATP, 0.5 mM DTT, 20 mM HEPES; pH 7.2
TAE-Buffer (50x)	2 M Tris-acetate (pH 8.0), 50 mM EDTA
TBS (10x)	0.5 M Tris-HCl, 1.5M NaCl; pH 7.5
TE	10 mM Tris-HCl, 1 mM EDTA; pH 8.0
TX-100 (20%)	2 ml TX-100 in 8 ml A.bidest.
Transfer buffer	25 mM Tris-base, 192 mM glycine, 10% methanol
Tris-glycine electrophoresis buffer	25 mM Tris-base , 250 mM glycine, 0.1% SDS

2.7 Enzymes and Buffers

Boehringer, Roche	Complete, Protease-Inhibitor-cocktail
	Alkaline Shrimp-Phosphatase (SAP)
	DNase; RNase
	10 x dephosphorylation buffer
	T4-DNA ligase
	10 x ligation-buffer
	Restriction endonucleases

Fermentas	Restriction-endonucleases
Promega	*Pfu*-Polymerase
Invitrogen	SYBR green

2.8 Plasmids

Vector	plasmid source
pAc/V5-His B	Invitrogen, Karlsruhe
pBluescriptII	Stratagene, Heidelberg
pCRII-Topo	Invitrogen, Karlsruhe
pCS+	Dave Turner, Ralph Rupp
pMJ-Green	AG Willecke, Bonn
pMT/V5-His B,C	Invitrogen, Karlsruhe
pUAST AG	AG Hoch (R. Bauer)
pWiz	Carthew lab
pTOPO	Invitrogen, Karlsruhe

2.8.1 LD clones

(from Berkeley *Drosophila* Genome Project)

Clone	Gene	Characteristics
SD03467	sec5	SD library; tissue source: *Drosophila* Schneider L2-cells; vector: pOT2

Clone	Gene	Characteristics
LD24661	sec6	LD library; tissue source: *D.m.*-embryo (0-22 Std. old); vector: pBluescript SK(+/-)
RE55430	sec15	RE library; tissue source: *D.m.*-embryo (0-22 Std. old); vector: pFLC-I

2.9 Oligonucleotides

2.9.1 Cloning primers

Primer name	Sequence (5`->3´)	Melting temperature Tm (°C)
inx2NTstart-EcoRI	GGA ATT CCA AAA TGT TTG ATG TCT TTG GGT CCG TC	68.3
inx2deltaCTmycstop - XbaI	GCT CTA GAG CTT ACA GAT CCT CAG AGA TCA GTT TCT GCT CGA TAA GCG ATA	84.7
sec5T7RNAiF1	TAA TAC GAC TCA CTA TAG GGC AAG CTA CAC GGC AAT GAG	77.0
sec5T7RNAiR1	TAA TAC GAC TCA CTA TAG GGA AAT GTC TGG CGA AAT GTC	76.0
sec6T7RNAiF1	TAA TAC GAC TCA CTA TAG GGC TTC AGC GCC TGT CAT A	77.0
sec6T7RNAiR1	TAA TAC GAC TCA CTA TAG GGA AGT TAT TGG GTC GCA GGT G	77.0
sec15T7RNAiF1	TAA TAC GAC TCA CTA TAG GGA ACA TTC CGT TCG ATC CTT G	76.0
sec15T7RNAiR1	TAA TAC GAC TCA CTA TAG GGC GAC GGA TGT TTT CCT TGA	76.0
inx2 start koz-EcoRI	GGA ATT CCC ACC ATG TTT GAT GTC TTT GGG TCC	74.0
inx2stop-ApaI	CGG GCC CGT TAG GCG TCG AAG GGC CGC TTG TG	83.0
inx2myc stop-ApaI	CGG GCC CGT TACAGA TCC TCT TCA GAG ATG AGT TTC TGC TCG GCG TCG AAG GCC CGC TTG TG	92.0

2.9.2 Sequencing-primers

All sequencing analyses were done by 4Base lab GmbH, Reutlingen and GATC, Konstanz

The following oligonucleotides were used for sequencing:

Primer name	Sequence (5`->3´)
CMV	CAA ATG GGC GGT AGG CGT GTA
pCDNA3.1/BGH rev	TAG AAG GCA CAG TCG AGG
pEGFP-RP	AAC AGC TCC TCG CCC TTG
pUAST F1	GTG AAC ACG TCG CTA AG
pUAST R1	GCG GTT GCC TGC TGA GA
SP6 (Standard)	ATT TAG GTG ACA CTA TA
T3 (Standard)	ATT AAC CCT CAC TAA AGG GA
T7 (Standard)	AAT ACG ACT CAC TAT AGG

2.9.3 RT-PCR primers

Primer name	Sequence (5`->3`)	Efficiency at 59°C annealing temperature
inx2-Sy-F1	CCT ACT CCG AGC CCG TTC C	100%
inx2-Sy-R1	TGC CCA GCT GAT AGA GCA GG	
wg-Sy-F1	GTG CAA GCT GTG TCG GAC CA	100%
wg-Sy-R1	AGA ACG AAGAGG CCG GCT TC	
hh-Sy-R1	CAA AGG GCT TGA ACTCGC C	98.3%
hh-Sy-R1	CAA AGG GCT TGA ACTCGC C	
Dl-Sy-F1	GCT GTT TTC TCC GTTGCG AT	100%
Dl-Sy-R1	GCG TCG TCC TTT TCCTGA GC	
rp49-Real- F1	GTG CAC CGC AAG TGC TTC TAA	100%
rp49-Real-R1	TGC TGC ACT CCA AAC TTC CAC	
act-Sy-F1	GCT AAG CTG TCG CAC AAA TG	98.7%
act-Sy-R1	GTT CGA TCC GTA ACC GATGT	
sec5-AV-F1	CAT CGA GCC CTC CAT GTA TCT	100%
sec5-AV-R1	CCA ACC AAA TTA TCG CAG CAC	

Primer name	Sequence (5`->3`)	Efficiency at 59°C annealing temperature
sec6-AV-F1	TTC TTT GAG AAA ATC GCG CC	100%
sec6-AV-R1	ACG AGC AGT TCG ATA TCC GAG	
sec15-AV-F1	CTG TGC CTG GTC TAA AGG AAG G	90.9%
sec15-AV-R1	CAT GGA AAT ACG TGC TCC ATT C	

2.10 *In situ* probes

Name of probe	Amount per reaction
innexin2 (pBluescript SK+)	4 µl
hedgehog (pBluescript KS+)	10 µl
*otp (*pBluescript KS+*)*	2 µl

2.11 Organisms

2.11.1 Bacterial strains

***E. coli* XL1 Blue MRF** ∆(mcrA)183, ∆ (mcrCB-hsdSMR-mrr), endA1, gyrA96, lac(F−, proAB, lacIF*q*Z∆M15, TN10(tet*r*), recA1, relA1, thi-1 (Stratagene, Heidelberg)

***E. coli* DH5α:** F$^-$, φ80d*lacZ*ΔM15, Δ(*lacZYA-argF*)U169, *deoR*, *recA*1, *endA*1, *hsdR*17(rk$^-$, mk$^+$), *phoA*, *supE*44, λ$^-$, *thi*-1, *gyrA*96, *relA*1 (Invitrogen)

2.11.2 Fly strains

Fly strain	genotype	chromosome	source
double balancer	y w; Sp /CyO ftz lacZ; Dr / TM3; dominant marker Sp and Dr	II. +III.	stock collection
hh^{IJ35}	*hh^{IJ35}* / Ubx-lacZ	III.	stock collection

kropf P(x)16	P(x)16/ FM7; kr::GFP	X.	stock collection
Gal4-strains	**genotype**	**chromosome**	**source**
fkh-Gal4	w; p[14-3 Gal4, fkh1 e+2]/ TM3, Sb Ubx lacZ	III.	stock collection
hs-Gal4	P[GAL4-Hsp70];w	X.	stock collection
prd-Gal4	y w; p[w+;prd::Gal4]3	III.	stock collection
twi-Gal4	P{GAL4-twi.2xPE}2 ,w	III.	Bloomington
twi-Gal4	P[GAL4-twi.G]108.4, w	I.	Bloomington
UAS-strains	**genotype**	**chromosome**	**source**
UAS- *WIZinx2ttt 5.1*	w; P[UAS-inx2 dsRNA]	III.	diploma thesis H. Lechner
UAS-*inx2-1*	w;P[UAS-inx2]	II.	stock collection
UAS-*inx2ΔCTmyc*	w;P[UAS-inx2ΔCT]	II. +III.	produced during PhD thesis
UAS-*sec6*	w;P[UAS-sec6]/TM3, Sb	III.	provided by U. Tepass
UAS-*sec6*	w;P[UAS-sec6]/SM6	II.	provided by U. Tepass
UAS-*wgHA*	w; P[UAS-UAS wg HA]	II.	stock collection

2.11.3 Cell lines

HeLa cells cell line derivative of cervical cancer explant, (source: Willecke lab, Bonn)

SL2 cells embryonic *Drosophila* Schneider cell line

SL2 inx2-myc embryonic *Drosophila* Schneider cell line, stably transfected with pMTVinx2myc for inducible over expression of innexin2 fusion protein with myc-tag

SL2 inx2-gfp embryonic Drosophila Schneider cell line, stably transfected with pMTVinx2GFP for inducible over expression of innexin2 fusion protein with gfp-tag

2.12 Media for the cultivation of organisms

2.12.1 Media for bacterial cultures

LB-agar:

10 g NaCl; 10 g tryptophan; 5 g yeast extract; 20 g agar; add 1 l A.bidest, adjust pH to7.0, with 5 M NaOH; autoclave

LB-ampicillin-agar:

1 l LB-agar autoclaved, cooled to 60°C, addition of 1 ml ampicillin (50 mg / ml sterile filtrated)

LB-chloramphenicol-agar:

1 l LB-agar autoclaved, cooled to 60 °C , addition of 3 ml chloramphenicol (10 mg / ml; sterile filtrated)

2.12.2 Media for fly cultivation

2.12.2.1 Fly food (for 11 l)

90 g fiber-agar; 165 g yeast; 615 g maize flour; 1 l treacle; 200 ml 10% nipagine-solution. While dissolving fiber-agar in 8 l A.bidest, yeast and maize-flour are mixed with 3.3 l A.bidest, which is then applied to the dissolved agar and boiled. Treacle is added and the food is cooked for 15 min while stirring. After that, the food is cooled down to 60°C , nipagine-solution is added and the food is filled into food vials.

2.12.2.2 Apple juice agar plates

4 l A.bidest are boiled with 85 g agar and cooled down to 65° C. 1 l apple juice is mixed with 100 g sugar and heated to 65°C. 40 ml nipagine-solution are added to the apple juice-sugar mixture followed by the combination of agar and apple-juice mixture. The fluid agar is distributed on petri-dishes and cooled down at RT until the agar is solid.

3 Methods

3.1 Isolation of plasmids from *E.coli*

3.1.1 Analytical preparation

2 ml of rich medium (LB) containing the appropriate antibiotic are inoculated with a single colony of transformed bacteria and are incubated in the culture overnight at 37°C with vigorous shaking. 1.5 ml of the culture are filled into a microcentrifuge tube and centrifuged at maximum speed for 30 sec at 4°C in a microcentrifuge. The bacterial pellet is resuspended in 100 µl ice cold alkaline lysis solution I by vigorous vortexing, followed by the addition of 200 µl freshly prepared alkaline lysis solution II to each vial and mixing. The tubes are stored on ice for 2 min. After incubation 150 µl of alkaline solution III are added and the mixture is stored on ice for further 5 min followed by centrifugation at maximum speed at 4°C. The supernatant is transferred to a fresh tube. The DNA is now either precipitated directly by the addition of two volumes ethanol (100%) at RT and then pelleted by centrifugation, or is extracted from the solution using Phenol / Chloroform purification. The DNA pellet is washed with 1 ml of 70% ethanol and DNA is recovered after 2 min centrifugation at 4°C. After that, DNA is dried leaving the tube inverted at RT until the ethanol has evaporated.

3.1.2 Preparative scale

(Nucleo Bond® PC AX100 Kit (Macherey Nagel)

Quantitative plasmid preparations are carried out following the manufacturer´s protocol. An overnight culture of a single colony containing the plasmid of interest is set up with 50 ml of rich Medium (LB) supplemented with the adequate antibiotic and grown overnight at 37°C in a bacterial shaker. The culture is pelleted the following day by centrifugation at 4500 x *g* for 15 min at 4°C. The supernatant is discarded and the pellet is dissolved in 4 ml S1 buffer containing RNAse A, followed by addition of 4 ml S2 to the suspension and inversion of the tube 6-8 times and 5 min incubation at RT for 2-3 min. Then, 4 ml of prechilled S3 buffer is added and the suspension directly mixed and incubated 5 min on ice. In between the column

is equilibrated with 2,5 ml N2 buffer. A funnel is set onto the column containing a NucleoBond® Folded Filter and the lysate is applied onto the filter. The flow through is discarded and the column washed with 10 ml N3 buffer. After discarding the flow through the column is set onto a fresh 50 ml tube and 5 ml Elution buffer N5 are added to the column. After elution of the purified plasmids, the DNA is precipitated by adding 3.5 ml isopropanol and centrifugation is carried out at 4500 x *g* for 60 min at 4°C. The DNA pellet is washed with 5 ml 70% ethanol, centrifuged again for 15 min and is dried at RT after careful removal of the ethanol. Plasmids are later reconstituted by dissolving the pellet in A.bidest or TE buffer and the plasmid yield is determined by UV spectrophotometry.

3.2 Isolation of RNA from tissues

(Nucleospin RNA 2 Kit, Macherey & Nagel)

Isolation of total RNA from embryos and cultured cells is performed according the manufacturer instructions. For isolation of RNA from embryos, specimen are collected in a close-meshed sieve, washed with PBS and transferred to a 2 ml microcentrifuge tube, the supernatant is discarded. 50-100 embryos are homogenised in 600 µl RA1 buffer supplemented with 6 µl ß-mercaptoethanol using an electrical homogenisation device. The suspension is loaded on a NucleoSpinFilter® and centrifuged for 1 min at 11000 x *g* at RT to reduce viscosity and clear the lysate. The flow through is transferred to fresh tube and mixed with 600 ml 70% ethanol. The suspension is transferred onto a NucleoSpin® RNA II Column and further processed according to the manual. Purified RNA is resuspended in 60 µl A.bidest devoid of RNAse and stored at -80°C. The concentration and quality of the isolated RNA is determined by agarose gel electrophoresis and UV spectrophotometry.

3.3 cDNA synthesis and *q*RT-PCR set up

3.3.1 cDNA synthesis

(Qiagen QuantiTect Reverse Transcription Kit)

Reverse transcription of *m*RNA into cDNA is performed using the Quantitect Kit purchased from Qiagen. Reactions are carried out as described in the manual. For one reaction only half the amount given in the protocol is used and RNA template input is 0.5 µg. Each cDNA reaction is diluted to a total volume of 50 µl with A.bidest prior analysis. For each isolated

RNA a control reaction is conducted where the transcriptase is substituted by A.bidest to exclude remaining DNA contaminations later on.

3.3.2 *q*RT-PCR analysis

For real-time PCR analyses each reaction consisted of cDNA template (1 µl of 1:100 diluted cDNA first strand reaction), forward and reverse primers (200 nM final concentrations, primer sequences see section 2.9.3) and iQ SYBR Green Supermix (BIO-RAD) in a total volume of 25 µl. Three reactions per template are prepared in parallel and are repeated with isolated RNA samples from different egg collections. The experiments are performed with iQ5 Real-Time PCR Detection System from BIO-RAD. Expressions of actin 5C (Act5C,act) and Ribosomal protein L32 (RpL32, rp49) are used as reference genes for normalisation (Fuss et al., 2006). Standard control PCR reactions are carried out to test for contaminations. Real-time PCR is analysed using BIO-RAD iQ5 Optical System software (version 1.1.1442.OCR), following the instruction provided by the supplier, and Microsoft Excel.

3.4 Agarose-gel electrophoresis

To separate DNA, 1% agarose is dissolved in 1x TAE buffer and boiled in the microwave until the agarose is melted completely. The fluid agarose is cooled down to 65°C and poured into a gel slayer. SYBR safe (Invitrogen). A DNA/RNA intercalating dye is added to the fluid agarose at a concentration of 1 µg / ml and is distributed with a pipette tip throughout the agarose. A comb is inserted into the slay to generate slots. After hardening, the gel is transferred into the electrophoresis chamber containing TAE buffer and the comb is removed. DNA, supplemented with loading dye is applied to one of the slots. After that, the chamber is voltage connected and the DNA is separated on the gel at constant voltage. Following separation of DNA, the gel is taken out and DNA, visible through SYBRsafe, is analysed with UV light.

3.5 Polymerase-chain-reaction (PCR)

PCR is an iterative process, consisting of three elements: denaturation of a template by heat (30 sec, 94°C), annealing of oligonucleotide primers to their single stranded target sequence (30 sec, 54°C - 59°C) and extension of annealed primers by a thermostable DNA polymerase

(1 - 2 min for a product length of up to 1.5 kb, 72°C) resulting in an amplification of template DNA (30 cycles). *Pfu*-polymerase (Promega) is used to amplify DNA for molecular cloning. The following components are mixed in a 0.5 ml microcentrifuge tube:

10 x Pfu-polymerase buffer	5.0 µl
20 mM dNTPs mix	2.0 µl
20 µM forward primer	2.0 µl
20 µM reverse primer	2.0 µl
Template DNA	< 0,5 µg
Pfu -Polymerase (3 U / µl)	0.42 µl
A.bidest	ad 50µl

3.6 Purification of DNA

3.6.1 Purification of DNA-fragments
(NucleoSpin Extract II, Macherey Nagel)

After PCR or restriction, DNA is purified from salts, oligonucleotides, enzymes or agarose. The purification is performed according to the user manual. Purified DNA is eluted from the column using 15 - 30 µl A.bidest.

3.6.2 Ethanol precipitation of DNA using sodium-acetate

Precipitation with ethanol is carried out to recover nucleic acids from aqueous solutions. DNA is precipitated by the addition of 1/10 volume 3 M sodium-acetate and 2.5 volumes of 100% ethanol followed by mixing of the solution and storage on ice for at least 15 min to allow the precipitate of DNA to form. DNA is recovered by maximal speed centrifugation at 4°C for 10 min. The supernatant is aspirated and the pellet washed with 70% ethanol and re-centrifuged for 2 min at maximum speed and 4°C. The DNA-pellet is air-dried and resuspended in A.bidest or TE.

3.6.3 Photometric determination of the DNA concentration

DNA quantification is performed using spectrophotometry. Measurements of 1:25 or 1:50 (DNA : TE or A.bidest) dilutions are taken at wavelengths of 260 nm and 280 nm. The reading at 260 nm allows the calculation of DNA concentration. An OD of 1 corresponds to 50 µg / ml for double stranded DNA. The ratio between the readings at 260 nm : 280 nm provides to estimate the purity of the nucleic acid. Pure preparations should have values of approximately 1.8 - 2.0.

Calculation of the DNA concentration:

$$\text{cDNA [µg/µl]} = \frac{\text{OD 260nm x 50 µg/ml x dilution factor}}{1000}$$

3.7 Molecular cloning of DNA-fragments

3.7.1 Restriction of DNA fragments and plasmids

Restriction enzymes are molecular scissors that cut DNA at specific sites. In order to cleave DNA the following set up is chosen: 1 µg DNA is mixed in a microcentrifuge tube with 2 µl of a 10 x restriction buffer (enzyme dependent) and 3-5 U of the corresponding enzyme following incubation at 37°C for 2 - 3 h. After incubation the enzyme is heat inactivated for 15 min at 65°C. For double digestions, using different enzymes, a suitable buffer must be chosen in which both enzymes are active.

3.7.2 Plasmid restriction and dephosphorylation

Integration of DNA fragments into plasmids requires the opening of the double stranded plasmid DNA. This is accomplished by restriction of the plasmid of interest with identical restriction enzymes used for DNA-fragment cleavage. To avoid closure of the restricted plasmid, dephosphorylation of overhanging 5`phosphate residues is carried out using an shrimp alkaline phosphatase (SAP). An amount of 100 ng plasmid DNA is therefore incubated with 1 U / µl SAP in the corresponding reaction buffer in a volume of 20 µl and

incubated 30 min at 37°C, followed by heat inactivation of the phosphatase at 65°C for 15 min.

3.7.3 Ligation of DNA fragments

The T4 DNA ligase catalyses the formation of phosphodiester bonds between juxtaposed 5'-phosphate and 3'-hydroxyl termini in duplex DNA or RNA with blunt or cohesive-end termini, to integrate restricted DNA fragments stably into plasmids, resulting in a closed ring structure which can be transformed into competent bacteria later on for amplification. For a 20 µl reaction, the ratio of input between vector DNA (100 ng) and insert DNA (300 ng) is 1 : 3. 2 µl of a 10 x ligation buffer and 1U of T4-DNA-ligase and the volume is adjusted to 20 µl with A.bidest. The reaction is incubated afterwards at 16°C over night.

3.7.4 TOPO cloning
(TOPO® PCR Cloning, Invitrogen)

TOPO® cloning uses the enzyme DNA *topoisomerase I*, which functions both as a restriction enzyme and as a ligase. Its biological role is to cleave and rejoin DNA during replication. *Vaccinia* virus *topoisomerase I* specifically recognises the pentameric sequence *5´*-(C/T)CCTT-*3´* and forms a covalent bond with the phosphate group attached to the *3´* thymidine. It cleaves one DNA strand, enabling the DNA to unwind. The enzyme then religates the ends of the cleaved strand and releases itself from the DNA. To avoid the religating activity of topoisomerase, TOPO® vectors are provided linearised with topoisomerase I covalently bound to each 3´ phosphate. This enables the vectors to readily ligate DNA sequences with compatible ends. The ligation is complete in only 5 minutes at room temperature. For one reaction 0.5 µl DNA, 1 µl salt solution, 1 µl pCRII-TOPO-Vector and 2.5 µl A. bidest are mixed by pipetting and the mixture incubated for 5 min at RT. 2 µl of this reaction are mixed to 100 µl of “One Shot” competent bacteria and are incubated 20 min on ice followed by a heat shock at 42°C for 30 sec for the transformation of bacteria. To amplify bacteria, 250 µl preheated LB medium is added to the tube and incubated at 37°C for 1h. In the meantime LB-agar- plates containing the appropriate antibiotic are covered with X-Gal solution, a substrate for *ß-galactosidase* encoded by the *lacZ* gene in the vector, and the plates are dried at 37°C. After that 50 µl of the transformed bacteria are streaked on each plate and the plates cultured over night at 37°C. At the next day, white colonies, where the *lacZ* gene of the vector is deleted by the insert DNA, can be picked an analysed further.

3.7.5 Preparation and transformation of chemocompetent bacteria

3.7.5.1 Preparation of chemocompetent bacteria

10 ml LB-medium are inoculated with a single colony of bacteria (strain DH5α) and are incubated overnight at 37°C in a bacteria shaker. A volume of 2 ml of this preparatory culture are transferred to 50 µl of fresh LB-medium and incubated at 37°C in the shaker until the optical density (OD at 550 nm) has reached 0.5. Bacteria are pelleted by centrifugation (15 min, 1000 x *g*, 4°C). The pellet is resuspended in 1/3 of initial volume ice cold RF-1 solution. This suspension is incubated for 15 min on ice before centrifugation at 1000 x *g* and 4°C. The pellet is resuspended in 1/12 of initial volume RF-2 solution and incubated for 15 min at 4°C. Bacteria are divided in portions of 200 µl in microcentrifuge tubes and stored at -80°C.

3.7.5.2 Transformation of chemocompetent bacteria

For one transformation reaction of 100 ng plasmid DNA into chemocompetent bacteria, an amount of 100 µl of chemocompetent bacteria are thawed at 4°C and mixed in a 1.5 ml microcentrifuge tube with the DNA by pipetting followed by incubation on ice for 30 min. During this step plasmids adsorb to the bacterial membranes. Afterwards a heat shock at 42°C is applied for 2 min, which results in plasmid acceptance through instable bacterial membranes. Next, the transformed bacteria are cooled down on ice and 1 ml of preheated LB-medium is added. The tube is incubated shaking (800 rpm) at 37°C allowing the bacteria to amplify. After incubation, the bacteria are pelleted by centrifugation at 13000 x *g* for 10 sec, supernatant is discarded and bacteria are resuspended in the reflux. The whole suspension is streaked on LB-agar plates containing the suitable antibiotic. The plates are cultured at 37°C over night.

3.8 Biochemical Methods

3.8.1 Cell culture

3.8.1.1 Cultivation of HeLa cells

HeLa cells are cultured in 75 ml cell culture flasks in DMEM (low glucose) medium supplemented with 10% FCS and 1% antibiotic (penicillin/streptomycin) at 37°C and under 7% CO_2 gassing. They are splitted twice a week in a 1:3 ratio. Therefore cells are washed twice with PBS followed by the addition of 1 ml trypsin and incubation for several minutes until cells loose adhesion to flask bottom. Cells are harvested by several strikes against the

flask and dilution in fresh medium.

3.8.1.2 Cultivation of SL2 cells

SL2 cells are cultured in 75 ml cell culture flasks in Schneiders Mediums containing 10% FCS and 1% penicillin/streptomycin. Cells are splitted twice a week in a 1 : 5 ratio by exchange of medium and knocking off cells from the flask bottom.

3.8.1.3 Transient transfection of HeLa cells

HeLa cells are sowed one day before transfection in the appropriate density in 6 -, 24 - or 6 - well plates or on 100 mm dishes. All transfections are done with Lipofectamine 2000 (Invitrogen) in OPTIMEM (Invitrogen). Each transfection reaction is set up as described in the manual. After 6 h incubation the transfection medium is aspirated and fresh DMEM + 10% FCS is added. Cells are harvested for further analyses 24-48 h post transfection.

	24 well	**6 well**	**100mm**
plating density	2 x 10^5	5 x 10^5	2 x 10^6
DNA	0.1-0.8 µg	1-4 µg	15-20 µg
DNA : Lipfectamine ratio	1:2 - 1:3	1:2 - 1:3	1:2 - 1:3

3.8.1.4 RNAi treatment of cultured SL2 cells

Knock down experiments using RNA interference (RNAi) is a successful tool to specifically reduce transcripts levels in cells. One advantage is that *Drosophila* uses this mechanism to defend against pathogens in nature. Therefore, RNAi treatment of *Drosophila* cells is an easy approach and double stranded RNA is applied directly to the cells without the usage of transfection agents. For the accomplishment of RNAi experiments SL2-inx2 myc cells are plated in a density of 1 x 10^6 cells on 6 - well dishes containing a coverslip in serum free medium. Cells are allowed to deposit on the surface of the dish for 2 h. After that, double stranded RNA (double stranded RNA synthesis is described in section 3.8.10.1) is applied. The amounts that are used vary between 30-50 µg per sample. After incubation for 30 min at 25 °C medium containing FCS is added the incubation is carried out for 3 days. After incubation the coverslip is carefully taken out and cells grown the coverslip are fixed with 4% PFA followed by immunhistochemistry. The remaining cells are harvested using a cell scraper and are transfered to a 1.5 ml microcentrifuge tube following RNA extraction in order to analyse the knock down efficiency by *q*RT-PCR.

3.8.2 Immunohistochemistry of cultured cells

Antigens of fixed cultured cells are commonly detected by detection with antigen specific antibodies (primary antibodies), which are later visualised by secondary antibodies coupled to a fluorescent dye. The detection of fluorescent immuno-complexes is accomplished by imaging with a confocal microscope or conventional fluorescence microscopy. Therefore, cells cultured on coverslips are fixed for 10 min at RT in 4% PFA followed by 2 x 5 min washes with PBS. Accessibility of the antibodies to the antigens is enhanced by permeabilisation with 0.2% TX-100 in PBS for 5 min at RT. Further washes of the cells with PBS follow to remove the permeabilisation solution. Next, blocking of cells in PBS + 1%BSA for 20 min is carried out. After removal of the blocking solution, primary antibody dilutions (in blocking solution) are applied on the coverslips and antibodies are incubated for 30 min at RT on a rocking table following 2 x 5 min washes in PBS and 2 x 10 min washes in PBS + 1% BSA. Now cells can be incubated with the secondary antibody, which is diluted in blocking solution. Incubation is carried out in the dark for 30 min on a rocking table. Several washes with PBS follow the antibody incubation. After that, coverslips are mounted on microscopy slides with Vectashield Hard Set (with or without DAPI, as a nuclear probe).

3.8.3 Preparation of protein extracts

3.8.3.1 Preparation of protein extracts from cultured cells (native and denaturing)

Cells are washed twice with PBS before further processing. Cells are harvested from 100 mm plates with a cell scraper, transferred to a falcon tube and pelleted at 1000 x g at 4°C for 10 min. The supernatant is discarded and the pellet homogenised in homogenisation medium or RIPA buffer (depending on whether native or denaturing conditions are chosen) using a tight fitting Dounce Homogenisator. RIPA extracts are further treated for 1 min in a ultrasound bath until the lysate becomes clear. Extracts are centrifuged at 10000 x *g* for 10 min at 4°C to pellet debris. The resulting supernatant, containing cellular proteins is stored at -80°C until further usage.

3.8.3.2 Preparation of protein extracts from *D. melanogaster* embryos

Embryos are collected in a close-meshed filter, washed with PBS and transferred to a prechilled Dounce Homogenisator with a brush and the appropriate homogenisation medium is added. The lysate is prepared with 15 - 20 strokes with a tight fitting pestle. RIPA extracts are further treated for 2 min in a ultrasound bath until the lysate becomes clear. The homogenate is transferred into microcentrifuge tube and centrifuged at 10000 x *g* for 20 min

and 4°C. The supernatant is transferred to fresh microcentrifuge tube and further fractionated or stored at -80°C.

3.8.3.3 Dephosphorylation of proteins

Calf intestine alkaline phosphatase is used for dephosphorylation serine, threonine and tyrosine residues in proteins. For the dephosphorylation of proteins, *Drosophila* embryonic extracts (without phosphatase inhibitor) are incubated with the calf alkaline shrimp phosphatase (CIAP, Roche) following the manufactures protocol for at least 30 min at 37°C. The reaction is stopped by the addition of SDS gel-loading buffer and heating of the sample for 5 min at 96°C.

3.8.4 Identification of protein concentration using BCA-Test (BCA Protein Assay, Pierce)

The BCA Protein Assay is used to determine the protein concentration of protein extracts. It combines the reduction of Cu^{2+} to Cu^{1+} by protein in an alkaline medium with the highly sensitive and selective colorimetric detection of the cuprous cation (Cu^{1+}) by bicinchoninic acid. The first step is the chelation of copper with protein in an alkaline environment to form a blue-colored complex. In the second step BCA, a highly sensitive and selective colorimetric detection reagent reacts with the cuprous cation (Cu^{1+}) that is formed in step one. The purple-colored reaction product is formed by chelation of two molecules of BCA with one cuprous ion. The BCA/copper complex is water-soluble and exhibits a strong linear absorbance at 562 nm with increasing protein concentrations. Reactions and standard curves for different buffers are carried out as described in the manual using half the volume given for one reaction. 950 µl of working reagent is diluted with either 50 µl of the homogenisation buffer (blank value determination) or 46 µl homogenisation buffer supplemented with 4 µl of the protein extract (equals a 12.5 fold dilution). After incubation for 30 min at 37°C protein contents are calculated from spectrophotometry measurements at 562 nm.

3.8.5 Gel electrophoresis and transfer of proteins

3.8.5.1 SDS-PAGE and native PAGE

Proteins are usually separated on polyacrylamide gels. Polyacrylamide can be used in different concentrations resulting in variable pore sizes to efficiently separate proteins of

different sizes. In this thesis, the acrylamide concentration of the resolving gel varied from 6 to 15% depending on the protein analysed. SDS-PAGE is carried out when denaturing conditions are required to separate proteins according their size. Basic native PAGE, where no SDS is added to the gel and proteins are separated according to their charge and hydrodynamic size, is used to analyze the composition of oligomeric acidic and neutral proteins (protocol by Lebendiker, 2000). Here the pH of the running buffer is adjusted to 8.9 and SDS is exchanged by A.bidest. Electrophoresis is carried out at 80 - 150 V.

Composition / resolving gel (5 ml)	**SDS-acrylamide-gel (10%)**	**Native gel (10%)**
H_2O	1.9 ml	1.95 ml
30% acrylamide mix	1.7 ml	1.7 ml
1.5 M Tris pH 8.8	1.30 ml	1.3 ml
SDS (10% stock)	0.05 ml	--------
APS	0.05 ml	0.05 ml
TEMED	0.003 ml	0.006 ml

Composition / stacking gel (1 ml)	**SDS-acrylamide-gel (5%)**	**Native gel (5%)**
H_2O	0.68 ml	0.69 ml
30% acrylamide mix	0.17 ml	0.17 ml
1.5 M Tris pH 6.8	0.13 ml	0.13 ml
SDS (10% stock)	0.01 ml	--------
APS	0.01 ml	0.01 ml
TEMED	0.001 ml	0.002 ml

3.8.5.2 Staining polyacrylamide gels with Coomassie Brilliant Blue

Polyacrylamide gels with electrophoretically separated proteins are immersed in 5 volumes of staining solution for at least 4 h at RT followed by removal of stain and destaining by soaking gel in methanol : acetic acid solution without the dye for further 4 - 8 h. Now, destaining of the gels follows: the destaining solution is exchanged 3-4 times after 15 min incubation. After destaining, gels are stored in A.bidest in a sealed plastic bag or dried under vacuum with heat (65°C) on whatman paper for 2 h.

3.8.5.3 Western Blotting using a tank system

In order to make proteins accessible for antibody detection, separated proteins on a polyacrylamide gel are transfered to a membrane made of nitrocellulose or PVDF. The membrane, moistened with methanol (PVDF) or water (nitrocellulose) and equilibrated in transfer buffer, is placed on the gel and is layered in between a stack of whatman papers and two foam pads moistened in transfer buffer in between a tank transfer cassette holder. The membrane is oriented to the anode, whereas the gel is oriented to the cathode. Then the holder and an ice-block are placed in the tank blotting apparatus and the tank filled with transfer buffer. Electro blotting is carried out at 100 V for 1 – 2 h depending on protein size. After that, the transfer efficiency of total protein is analysed by Ponceau S (Sigma-Aldrich) red staining of proteins on the membrane and discoloration with TBST.

3.8.5.4 Antibody binding and ECL detection

After transfer of proteins to the PVDF or nitrocellulose membrane, incubation with 5% milk powder in TBST is carried out for at least 2 h, followed by over night incubation with the primary antibodies diluted in TBST at 4°C. Next day, the membrane is washed several times for 5 min in TBST before incubation with the second antibody for 1 h at RT, recognising the F_c region of the bound first antibody. After antibody incubation, the blot is washed several times with TBST. The second antibody is coupled to HRP that produces chemiluminescence when converting an ECL substrate. The signal becomes visible when X-ray films are laid onto the membrane in the dark for different exposure times (20 s - 10 min) . X-ray films are developed in a Curix60 developer.

3.8.6 Co-Immunoprecipitation

(Immunoprecipitation Starter Pack, GE Healthcare)

Immunoprecipitation is a highly specific and effective technique for analytical separation of target antigens from cell homogenates with the help of Sepharose A/G beads. Co-immunoprecipitation means that interacting proteins of the pulled antigen can be identified by antibody detection in addition using Western Blot analysis. Cell- or embryonic RIPA- extracts, a highly stringent homogenisation medium. Per reaction 300 - 500 µg of the protein lysate are diluted in 500 µl RIPA buffer. In parallel, sepharose beads are prepared as described in the manual. In the next step, the lysate is precleared by the addition of 50 µl sepharose and mixing for 1 h at 4°C. Beads are precipitated by centrifugation at 12000 x *g* at 4°C for 20 sec.

The supernatant is transferred to a fresh microcentrifuge tubes and the antibody is added at a concentration between 1 - 4 µg per reaction. As a control reaction, the appropriate normal IgG antibodies of different species are applied in parallel samples at the same concentration. Samples are incubated for 3 h at 4°C. The resulting immune complex is precipitated by the addition and incubation of 40 µl beads and incubation for 2 h at 4°C followed by centrifugation to pellet beads with the bound immune complex. The pellet is washed three times with 1 ml lysis buffer and centrifuged at 12000 x *g* for 20 sec between each wash. The final pellet is suspended in 30 µl sample buffer, heated for 3 min at 95°C and pelleted again. The supernatant is analysed by SDS-PAGE and Western blot.

3.8.6.1 Co-immunoprecipitation with crosslinked antibody sepharose complexes

To prevent that IgG chains from the precipitating antibody become visible after immunoblotting, antibodies can be coupled to the used sepharose with the help of dimethylpimelimidatdihydrochlorid (DMP), a crosslinking agent. To perform crosslinking, 60 µl of sepharose beads are washed 3 times with 0.1 M sodium-phosphate buffer (pH 7.0) and are pelleted after each wash by centrifugation (see above). The antibody is diluted in 500 µl sodium-phosphate buffer, added to the sepharose and the mixture is incubated rotating for 1h at 4°C. After that, the complexes of antibody and sepharose are sedimented by centrifugation (30 sec at, 12000 x *g*, 4°C) and are washed with 300 µl 0.2 M triethanolamine (pH 8.2). For the following crosslinking procedure, the complexes are incubated in 500 µl 20 mM DMP in 0.2 M triethanolamine (pH 8.2) for 45 min at RT followed by one wash in 0.2 M triethanolamine and three additional washes in RIPA buffer. Now, the RIPA protein extract is added as described in section 3.8.6 and incubated over night. The following washing steps are done also as described above. The final pellet is suspended in 30 ml sample buffer and heated for 10 min at 65°C.

3.8.7 Cell surface biotinylation and pulldown assay

(Cell surface biotinylation kit, Pierce)

Expression of proteins at the plasma membrane can be assayed using cell surface biotinylation when lysines are exposed at the cell surface. Adherent cells are first labeled with Sulfo-NHS-SS-Biotin, a cleavable biotinylation reagent. Efficient labeling requires accessible lysine residues, sufficient sequence with extracellular exposure and minimal steric hindrance. The cells are subsequently lysed with a mild detergent and then labeled proteins are isolated

with the help of column containing NeutrAvidin Gel. The bound proteins are released by incubating the resin with SDS-PAGE sample buffer containing 50 mM DTT. The reducing agent cleaves the disulfide bond within the biotin label, and nearly 100% of the bound proteins are recovered. Isolated proteins are analysed by Western blot.

The biotinylation procedure of SL2 cells expressing inx2-myc for 48 h is performed as described in the manual using half of the amounts given for one reaction.

3.8.8 Fractionation of cells via density gradient centrifugation

Density gradient centrifugation is applied to separate different organelles in order to study their subcellular contents and to separate different oligomeric assemblies from each other. In this thesis different approaches are undertaken that applied density gradient centrifugation. Subcellular fractionation of organelles using discontinuous systems is accomplished in order to enrich different kinds of cellular membranes. For this purpose, protocols by Quigley (1976) and Love and colleagues (1998) are followed in order to separate a cytoplasmic fraction from a plasma membrane (PM), endoplasmic reticulum (ER) and vesicle fraction to study innexin2 localisation. In order to isolate membranes of PM and ER, a total membrane fraction is isolated from SL2 cells (4 confluent 100 mm dishes), obtained by high speed centrifugation and separation in a discontinuous sucrose gradient (20%, 40%, 60% (w/v) sucrose) and centrifugation at 100000 x *g* , 3 h. The fresh lysate is centrifuged 8 min at 600 x *g* and 4°C to remove cell debris and nuclei. The postnuclear supernatant is used for the isolation of the total membrane fraction and centrifuged at 100000 x *g* for 90 min and 4°C. The supernatant constitutes the cytoplasmic fraction, whereas the pellet contains all membranes. The resulting membrane pellet is suspended in homogenisation medium and layered onto the discontinuous gradient followed by centrifugation at 100000 x *g* for 3 h at 4°C. Discrete bands of subcellular membranes are removed from the gradient between two sucrose layers, diluted with homogenisation medium and washed by centrifugation at 100000 x g for 1h. Pellets are dissolved in homogenisation medium or sample buffer, followed by SDS-PAGE and Western blot analysis. Cloudy membrane accumulations corresponding to the PM fraction float between 20% and 40% sucrose, whereas the ER / mitochondrial fraction is harvested between 40-60% sucrose. Vesicles float to the top of the gradient.

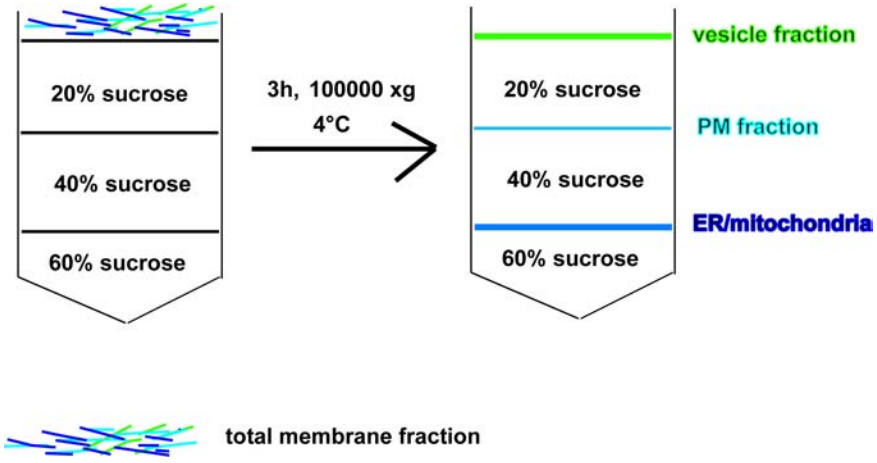

Fig. 3-1 Schematic drawing of endoplasmic reticulum and plasma membrane fractionation (after Quigley, 1976).

A second approach to isolate vesicles is a carried out using a discontinuous gradient made with Optiprep (Love et al., 1998). Cells (2 ml of a SL2 cell pellet) are washed in PBS and ST- (0.2 M sucrose, 10 mM Tris, pH 7.2) buffer, resuspended in 4 ml of ST per 1 ml of cell pellet, frozen in liquid nitrogen, and kept at -80°C until needed. Cells are thawed in a water bath at room temperature and transferred on ice immediately after thawing.

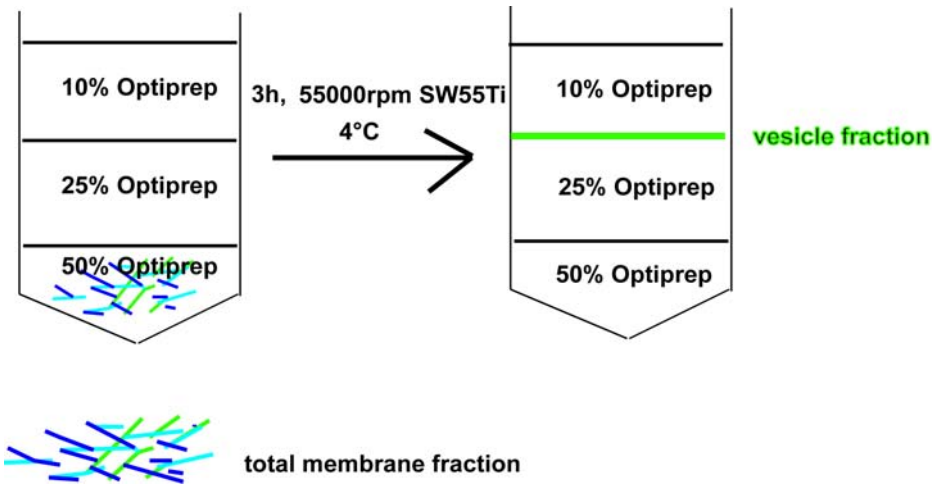

Fig. 3-2 Schematic drawing of vesicle purification (after Love et al., 1998).

Permeabilised cells are pelleted by 5 min of centrifugation at 1,000 *g* at 4°C. Vesicles remain in the supernatant. To separate vesicles from cytosol, all membranes are pelleted by ultracentrifugation (90 min at 100000 x *g*) and are resuspended in 0.8 ml KHM buffer (150

mM KCl, 10 mM Hepes, pH 7.2, 2.5 mM MgOAc). 1.2 ml of 50% iodixanol ("optiprep") in HM (10 mM Hepes, pH 7.2, 2.5 mM MgOAc) is added, and the mixture is overlaid in an SW55 tube (Beckman) with 2 ml of 25% iodixanol in KHM and 1 ml of 10% iodixanol in KHM. Vesicles are floating to the 10% / 25% interface during a 3 h centrifugation at 55,000 rpm in an SW55ti swing out rotor (Beckman Coulter) at 4°C. The vesicle membrane fraction isolated using a syringe from the interface.

3.8.9 TX-100 solubilisation and continuous density gradient centrifugation

3.8.9.1 TX-100 solubilsation

Acquisition of Triton X-100 insolubility is a useful assay for gap junction channel assembly of different connexins (VanSlyke and Musil, 2000). The ability to separate plasma membrane integrated gap junctions from native forms of connexin oligomers by this method is dependent on the detergent, temperature and the buffer composition of the solubilisation reaction. For this reason the protocol by VanSlyke and Musil is carried out strictly.

Production of a protein lysate from embryos or cultured cells is accomplished using incubation buffer and a Dounce Homogenisator (see 3.8.2). After that, 20% TX-100 is added to the the suspension to a final concentration of 1% and the tube is vortexed vigorously. The sample is incubated for 30 to 40 min at 4°C. Half the volume is removed from the sample and reserved as a sample of total lysate (= TX-100 soluble + insoluble). The remaining homogenate is spun at 100000 x *g* for 50 min at 4°C (36800 rpm in a 70Ti rotor, Beckman). The TX-100 solubilised extract is collected without disturbing the pellet. The pellet containing the TX-100 insoluble membrane fraction is resuspended with 50-100 µl incubation buffer depending on the pellet size. Its is homogenized with a micro pistil or a 26 gauge needle attached to a 1 ml syringe. Different protein fractions are kept at -80°C.

3.8.9.2 Velocity sedimentation of innexins in sucrose gradients

This procedure to fractionate innexin oligomers along sucrose gradients is adopted from studies about the assembly of the nicotinic acetylcholine receptor by Koval and colleagues (Koval et al., 1997) and from assembly studies of connexins (VanSlyke and Musil, 2000). Two stock solutions of sucrose are premixed with incubation buffer (5% and 20% w/v). 2 ml of each of the premixed solutions are added to the appropriate chamber of a gradient maker and continuous 5-20% sucrose gradients are prepared and chilled to 4°C. Gradients are overlaid with 0.5 ml - 0.75 ml (0.5 - 1 µg / µl) of TX-100 solubilised extract and gradients are spun at 250000 x *g* for 12 h in an SW55 swinging bucket rotor. In parallel, additional

gradients are loaded with 100 µg of purified ovalbumin (45 kD) or catalase (250 kD), purchased from Sigma to assess their sedimentation as markers for monomeric or hexameric assemblies, respectively. After centrifugation, fractions of 500 µl volume are collected from the top of the gradient, following sucrose concentration measurement with a refractometer. Protein is precipitated from each fraction using methanol/chloroform precipitation.

3.8.9.3 Precipitation of Proteins using methanol / chloroform extraction (after Wessel and Fluegge)

Quantitative precipitation of dilute protein samples, containing salts and detergents as TX-100, for immunoblotting analysis is done by the dilution of the protein sample with 4 volumes methanol and vortexing of the mixture followed by the addition of 1 volume chloroform and vortexing. Finally, 3 volumes of A.bidest are added and the mixture is vortexed another time. Next, centrifugation is carried out at 4500 x *g* for 15 min. The precipitated proteins are discovered in the interface between two phases. The upper phase is discarded and 3 volumes of methanol are added following mixture of the sample and centrifugation at 4500 x *g* for 15 min to pellet the precipitated proteins. The supernatant is removed completely and the pellet is dried under vacuum at 37°C for 5 min. The purified and concentrated protein can be further analysed by immunoblot analysis.

3.8.9.4 Oligomerisation assay

Sodium dodecyl sulfate (SDS) is a detergent, which is commonly used to resolve non-covalent bindings in and between proteins. In the oligomerisation assay TX-100 solubilised protein-lysates are incubated with various concentrations of SDS, which leads to the decay of oligomeric proteins into their monomeric form (Diez et al., 1999). In this thesis SDS is applied to the TX-100 solubilised lysates at concentrations between 0.6% and 2% (w/v) for 1 h at RT followed by velocity sedimentation in sucrose gradients and Western blot analysis. Results are compared to untreated controls.

3.8.10 *In vitro* transcription and translation

3.8.10.1 *In vitro* transcription (RIBOMAX large scale , Promega)

To generate *m*RNA for *in vitro* translation experiments or to synthesis of double stranded RNA, 5 µg of a linearised plasmid (e.g. pBSinx2full) containing T7, SP6 or T3 promotor *5`-prime* of the inserted cDNA are mixed with 30 µl rNTP Mix, 20 µl 5 x transcription buffer, 10 µl

enzyme Mix T7, T3 or SP6, filled to 100 µl with A.bidest and are incubated for 4 h at 37°C. In the following step DNA digestion is carried out with 4.5 U DNase RQ1 for 15 min at 37°C and phenol/chloroform extraction of the synthesised *m*RNA. The resulting RNA pellet is dried and suspended in 80 µl RNAse free A.bidest.

For the generation of double stranded RNA for RNAi treatment of SL2 cells, the DNA digestion is stopped by 5 min incubation at 70°C after *in vitro* transcription following refrigeration of the sample at RT, resulting in annealing of double stranded RNA.

3.8.10.2 *In vitro* translation and oligomerisation of proteins (Rabbit Reticulocyte Lysate System, Nuclease Treated, Canine Microsomal Membranes; Promega)

Rabbit reticulocyte lysate translation systems are utilised in the identification of *m*RNA species, the characterisation of their protein products and the investigation of transcriptional and translational control. Rabbit reticulocyte lysate is prepared from New Zealand white rabbits. After the reticulocytes are lysed, the extract is treated with micrococcal nuclease to destroy endogenous *m*RNA and thus reduce background translation to a minimum. The lysate contains the cellular components necessary for protein synthesis (*t*RNA, ribosomes, amino acids, initiation, elongation and termination factors). Microsomal vesicles are used to study co-translational and initial post-translational processing of proteins and has been used successfully for *in vitro* assembly of different connexin isoforms (Ahmad et al., 1999; Falk et al., 2001). The following components are mixed for one reaction:

17.5 µl Rabbit reticulocyte lysate

0.5 µl Amino acid mix without methionine

1.8 µl Microsomal membranes

1-3 µl *m*RNA

2.0 µl ^{35}S Methionine (1,200 Ci / mmol at 10 mCi / ml)

ad 25.0 µl H_2O

The sample is incubated at 30°C over night. Analyses are carried out using SDS-PAGE followed by autoradiography and density gradient centrifugation followed by liquid scintillation counting or SDS-PAGE.

3.8.10.3 Solubilisation of microsomal membranes

Solubilisation of microsomal membranes is done to release inserted proteins and analyse their contents (Ahmad et al., 1999). After the synthesis of innexin2 protein with the help of reticulocyte lysate and in the presence of microsomes, the translation mixture is incubated for 2 h in a solubilisation buffer. Samples are centrifuged at 12000 x *g* at 4°C for 15 min and the supernatant is subsequently loaded on preformed 5–20% (w/v) linear sucrose gradients prepared in 20 mM EDTA, 10 mM DTT, 0.2% n-dodecyl ß-D-maltoside and 20 mM TEA (pH 9.2). After centrifugation at 150000 x *g* for 18 h at 4 °C, ten 0.5 ml fractions are collected and proteins dialysed against water in Microcon filter devices.

3.9 Drug treatment of *Drosophila* ovaries and cells

Ovaries of 24 h fertilised female flies are dissected in Schneiders Medium. Drugs are added at the appropriate concentrations (Colchicine or BFA: 20 µg / ml) and incubated at RT while rotating as required (Colchicine for 30 min, BFA for 4 h). In parallel, controls are incubated with the solvents only, that are used to dissolve the drug, to exclude unspecific effects during incubation. The treatment is stopped by fixation in formaldehyde.

3.10 Membrane sheet preparation from HeLa cells

Membrane sheets from basal cell membranes can be obtained by applying an ultrasound pulse to the cultured cells on a coverslip followed by and immediate fixation in 4%PFA. Therefore HeLa-cells are grown on 25 mm coverslips coated with poly-L-lysine. The coverslip is transferred to the bottom of a dish containing sonication-buffer. One pulse (1 sec) of ultrasound is applied and the coverslip is immediately fixed in 4% PFA for 90 min. After that, PFA is removed and 50 mM NH_4Cl_2 is added for 20 min incubation, followed by several washes with PBS (Sieber et al., 2007) The preparation can be used for conventional antibody staining of cells (see section 3.8.2).

3.11 Fly work with *Drosophila melanogaster*

3.11.1 Fly stock keeping

Breeding of *Drosophila melanogaster* stocks is accomplished using standard methods (Roberts et al., 1986).

3.11.2 Fixation of *Drosophila* embryos

Embryos are transferred from agar plates with A.bidest and a brush into a close mesh. The embryos are dechorionated with 6% sodium-hypochloride, washed with A.bidest and are fixed for 5 min in heptane : 37% formaldehyde (1 : 1). To remove the vitelline membrane, the lower phase of fixation solution is discarded and 10 ml methanol are added. The sample is mixed by vortexing for 1 min. Fixed embryos sink down to the bottom of the vial. After accumulation of fixed embryos at the bottom of the vial, the whole solution is aspirated carefully and embryos are washed twice with methanol. Fixed specimen can be stored at -20°C in methanol.

3.11.3 Antibody staining of *Drosophila* embryos

An appropriate number of embryos is transferred into fresh 1,5 ml microcentrifuge tubes (this will be approximately 25-50 ml settled volume of embryos) and the methanol from surface of embryos is removed. To rehydrate the fixed embryos, washes with 70%, 50% and 30% methanol (in PBS) follow (5 min each). After that, embryos are washed twice with PBT for 10 min before they are incubated in 2% donkey serum in PBT for 20 min to block unspecific antibody binding later on. The primary antibody is diluted in 2% donkey serum in PBT and incubated overnight at 4°C while rotating. The next day, primary antibody is removed and saved at 4°C (depending on the antibody titer, it can be re-used multiple times). The embryos are washed 4 x 10 min in PBT, followed by 20 min incubation in PBT+ 2% donkey serum. The second antibody (coupled to a fluorophor or an enzyme, which creates a signal when a substrate is added) is diluted in blocking solution and incubated 2 h at RT while rotating followed by 4 x 10min washes with PBT. Embryos are mounted in Gelmount on microscope slides and kept at 4°C until imaging.

3.11.4 Antibody staining of *Drosophila* ovaries

Dissected ovaries are fixed in 4% PFA in PBT + 0.3% TX-100 for 30 min. The following steps are performed as described in section 3.11.3. with the exception that PBS is supplemented with 0.3% TX-100 instead of 0.1% Tween and mounting is done using Vectashield Hard Set with or without DAPI.

3.11.5 *In situ* hybridisation of *Drosophila* embryos (chemical)

In situ hybridisation is unique in its ability to reveal patterns of gene expression with cellular resolution. Embryos are fixed in such a way that all *m*RNA being transcribed at the time is retained by hybridisation with a probe labeled so that it can be detected by chromogenic stains or fluorescence.
In a first step, an appropriate probe has to be synthesised that is able to specifically recognise corresponding *m*RNA fragments. To enable hybridisation of the probe to the target *m*RNA, a probe is designed in the antisense direction of the corresponding *m*RNA. As a control, a sense probe is also synthesised, which should not bind to the mRNA of interest.
For the synthesis of the probe the following components are mixed in a microcentrifuge tube:

1 µg linearised plasmid containing cDNA
2 µl 10 x transcription buffer
2 µl 10 x nucleotide mix (with digoxigenin-UTP)
20U RNAse inhibitor
40 U T7, SP6 or T3 polymerase

Incubation of the mixture is done for 2 h at 37°C followed by DNase I treatment (40 U) at 37°C for 15 min. The reaction is stopped by adding 2 µl 200 mM EDTA, pH 8.0. The synthesised RNA is precipitated with 2.5 µl M LiCl and 75 µl pre-chilled ethanol. The precipitated RNA is spun down at 13000 x *g* for 10 min and redissolved in 100 µl of RNAse-free water. The quality of the obtained RNA is checked on a 0.8% agarose gel in TBE. RNA probes are stored at -20°C until usage.

In situ hybridisation of the synthesised probe is accomplished as outlined below:
Embryos are fixed in 4% PFA following the protocol given in section 3.11.2., and rehydrated through 70%, 50%, 30% methanol in PBT. Incubation with a 1:800 dilution of a 20 mg/ml proteinase K stock for 2.5 min follows to make the tissue accessible for the RNA probe. After

this step, embryos are rinsed 2 x 1 min in PBT and fixed again for 5 min in 4% PFA, before 2 x 1 min washes in PBT and a final wash in PBT : hybridisation buffer (1 : 1) follow. Pre-hybridisation is done at 60°C in a water bath for at least 1 h in hybridisation buffer. After that the buffer is removed completely and exchanged by 200 µl fresh hybridisation buffer containing the heat denaturated probe (denaturation at 80°C for 5 min in a small volume hybridisation buffer). The probe is diluted depending on RNA amount between 1:100 and 1:0000. Hybridisation is carried out over night at 60°C in a water bath.

Next day, the hybridisation buffer containing the probe is removed and the embryos are washed in fresh hybridisation buffer for 2 x 20 min ,1 x 20 min in PBT : hybridisation buffer (1 :1) at 60°C, followed by 5 x 20 min washes in PBT at RT.

Hybridised specimens are then incubated with anti-DIG antibody, diluted 1:2000 for 1 h. After removal of the antibody solutions, the embryos are washed 4 x 20 min in PBT followed by washes in AP buffer for 2 x 1 min. Next, 1 ml of AP buffer is mixed with 20 µl NBT / BCIP, a substrate which reacts with the alkaline phosphatase coupled to the anti-DIG antibody, resulting in a blue precipitation at sites where the probe has bound. The solution is added to the embryos and the appearance of stain is monitored carefully using a binocular to avoid over-staining. The reaction is stopped with several rinses in PBT.

Dehydration of the stained embryos is carried out through 30%, 50%, 70% and 100% ethanol for 5 min each. Specimen are mounted in Canada-balm on a microscope slide and covered with a coverslip. Hardening of the sample takes 12 - 24 h before analysis with a light microscope is possible.

3.11.6 Fluorescence *in situ* hybridisation combined with antibody staining

Detection of *m*RNA and protein in the same embryo can be accomplished using a combination of both techniques. For this purpose, embryos are treated during the first day of the experiment as outlined in section 3.11.5. After hybridisation of the probe with *m*RNA, embryos are washed for 2 x 20 min at 60°C in hybridisation buffer : PBT (1:1) and for 4 x 20 min in PBT to remove the unbound probe completely. Incubation with an anti-DIG antibody (sheep) is done for 1 h in PBT + 2% donkey serum followed by several washes with PBT (2 x 5 min, 1 x 10 min, 2 x 5 min) and incubation with an anti-sheep-biotin antibody in PBT +2% donkey serum for 2 h. Extensive rinses in PBT follow (2 x 5 min, 1 x 10 min, 2 x 5 min). While rinsing the embryos, ABC reagent (Vectastain) is prepared by mixing 5 µl of component A with 5 µl of component B with 490 µl PBT and pre-incubation at RT follows for 30 min while rotating. After that, the ABC-mixture is applied to the the embryos and incubated 45 min on the rotating wheel and afterwards washed with PBT (as before). Detection of the labeled

probe is performed by the addition of 100 µl TSA-Cy3 (1:250 in Amplification Diluent; Perkin Elmer) and a 20 min incubation following 4 x 10 min washes in PBT and blocking in PBT + 2% donkey serum. Specimens are ready for fluorescent antibody staining as described in 3.11.3. Secondary antibodies may not be coupled to Cy3.

3.11.7 *Drosophila* crossing experiments

In several experiments using *Drosophila melanogaster*, crossing of different strains has to be accomplished beforehand. To set these crossings only virgins of one strain are collected and crossed to males of a different strain. Identification of virgins is done time defined. A breeding vial with pupae is kept at 18°C and hatched female flies are collected within 18 h. The vial has to be screened for virgins every 4 h hours at 25°C. Virgins are collected in fresh breeding vials and are kept at 18°C until crossing.

3.11.8 The GAL4-UAS system in *Drosophila melanogaster*

The Gal4-UAS system is an ectopic expression system to overexpress transgenes in a certain temporal and spatial manner in *Drosophila* (Brand and Perrimon, 1993). The coding sequence of a yeast transcription factor, Gal4, is cloned 3` prime of certain enhancers and is introduced stably in the fly via germ line transformation. Transgenic flies (activator strains) can be kept stably. Another strain of flies (effector strain) carries the upstream activation sequence (UAS) for Gal4 in front of a transgene. When both strains are crossed, Gal4 is expressed and binds to UAS, which leads to the transcription of the inserted trangene 3`prime of the UAS.

3.11.9 Germ line transformation

P-elements are mobile genetic elements in *Drosophila* that can be used genetically as tools to create transgenes and mutations. P-elements have a length of 2.9 kb and are flanked at their ends by repeated sequences of 31 bp, which encode for a transposase that catalyses the mobilisation and integration of P-elements into the genome. This kind of mobilisation is limited to the germ line cells because soma cells express an inhibitor of transposases due to differential splicing. Modified P-Elements are used as transformation-vectors for *Drosophila*.

(Rubin and Spradling, 1982). Two differently modified P-elements are used in this case, one encodes a transposase lacking inverted repeats, which prevents the integration in the genome and is not passed over to the next generation (= helper plasmid). A second P-element containing the inverted repeats carries in between the gene of interest and a marker gene. The transposase of this P-element is deleted. To generate P-element transformed fly strains, embryos in the cellular blastoderm stadium are injected with a mixture of both elements at the posterior pole plasma, where later on the precursors of germ line cells differentiate. After the pole cells have integrated both vectors, germ cells are transformed and the progeny of those flies carries the transgene in all cells. Those transgene flies are detected via a marker, usually a marker that results in a different eye color (in this thesis embryos from flies with white colored eyes (w^- strain) are injected. *white* served as marker for transgenesis, resulting in red colored eyes after transformation).

The mixture for injection contains 2.5 µg helper plasmid and 7.5 µg (precipitated with ethanol and sodium-acetate) of the vector with the gene of interest in 50 µl injection buffer.

4 Results

4.1 *Drosophila* gap junction hemichannel assembly

Vertebrate gap junction hemichannel formation has been studied extensively over the past years. Several biochemical and functional studies showed the hexameric nature of those channels (Van Slyke and Musil, 2000; Ahmad et al., 2001). Non such studies have been undertaken to investigate the oligomeric status of *Drosophila* gap junction hemichannels.

In order to investigate the oligomeric composition of *Drosophila* innexin gap junction hemichannels that do not exhibit sequence homology on the amino acid level to their vertebrate connexin analogues, various biochemical approaches were undertaken to clarify the issue of innexin gap junction hemichannel formation. Innexin2 as one of eight gap junction constituting family members in *Drosophila* was used to analyse assembly of innexin hemichannels.

Results presented on the investigation of oligomerisation of innexin2 in the first part of this doctorate thesis continued initial studies during the Diploma thesis (Lechner, 2004) and proof first evidence for the existence of hexameric hemichannels that contain innexin2.

4.1.1 Innexin2 is contained in hexameric hemichannels that show TX-100 insolubility upon plasma membrane integration

Triton X-100 ($C_{14}H_{22}O(C_2H_4O)_n$) is a nonionic surfactant that is used routinely to permeabilise eukaryotic cell membranes. It was used by Musil and Goodenough previously in order to separate phosophorylated membrane integrated gap junction connexin43 hemichannels from unphosphorylated native connexin43 hemichannels that have not been integrated in the plasma membrane yet (Musil and Goodenough, 1991). For this assay, native protein-lysates of communication-competent normal rat kidney cells were incubated with 1% Triton X-100 (TX-100) for 30 min at 4°C in incubation buffer and were subsequently centrifuged at 100000 x *g* at 4°C. The resulting pellet contained mainly membranes enriched with TX-100 insoluble proteins containing hexameric connexons, whereas the supernatant comprised all solubilised proteins including native oligomers of connexin43 (Fig. 4-1)

In order to study innexin oligomerisation and membrane integration such an experiment was done with *Drosophila* native embryonic lysates prepared from 0-16h old wild type specimen.

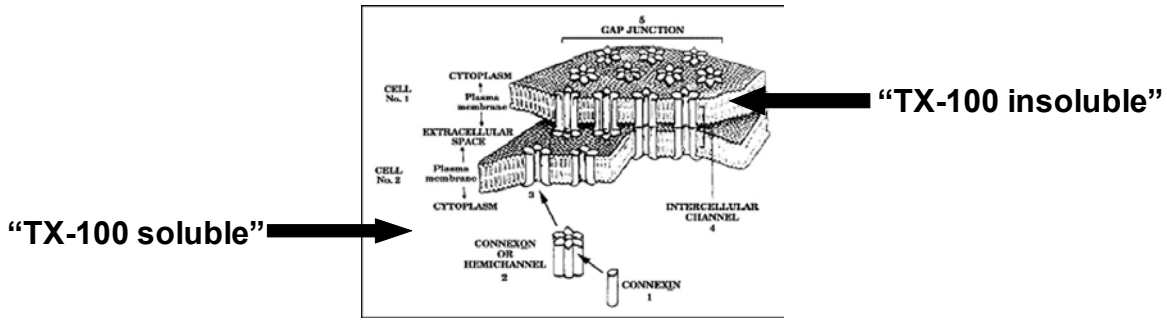

Fig. 4-1 Schematic drawing of gap junction oligomerisation and TX-100 solubility characteristics. Newly synthesised and oligomerised connexins are soluble in 1% TX-100 at 4°C, whereas membrane integrated hexamers acquire TX-100 insolubility due to post translational modifications of connexin subunits.

First, a plasma membrane fraction was isolated from wild type embryonic extract by applying discontinuous density gradient centrifugation on 20%-60% sucrose step gradients. Plasma membranes were harvested from the interphase between 20-40 % sucrose (Quigley, 1976). To prepare plasma membrane fractions, total membrane fractions, obtained by differential centrifugation of wild type extracts for 90 min at 100000 x *g* were loaded onto the gradient and centrifugation was carried out at 100000 x *g* for 3 h at 4°C. Discrete bands of subcellular membranes were removed from the gradient, diluted with homogenisation medium and washed by centrifugation at 100000 x *g* for 1 h, followed by TX-100 solubilisation. Portions of harvested protein were separated on 6% basic native PAGE gels and innexin2 status was further analysed by Western Blot analysis.

Immunoblotting using an anti-innexin2 antibody (inx2KLRH) revealed a band corresponding to the size of approximately 250 kD in total embryonic extracts and in plasma membrane enriched fractions, corresponding to the size of innexin2 containing hexameric assemblies. The TX-100 soluble fraction prepared from total extracts contained an additional band which presents an oligomeric intermediate containing innexin2.

In summary, TX-100 solubility studies showed, that innexin2 containing hexamers are insoluble in TX-100 at chosen conditions as had been shown before for the vertebrate gap junction protein connexin43 (Fig. 4-2; Musil and Goodenough, 1991). Furthermore, the TX-100 treated fractions and the plasma membrane contained only hexamers, whereas the TX-100 soluble fraction showed an additional band, indicating that only the hexameric structures detected in this approach, acquired insolubility upon membrane integration.

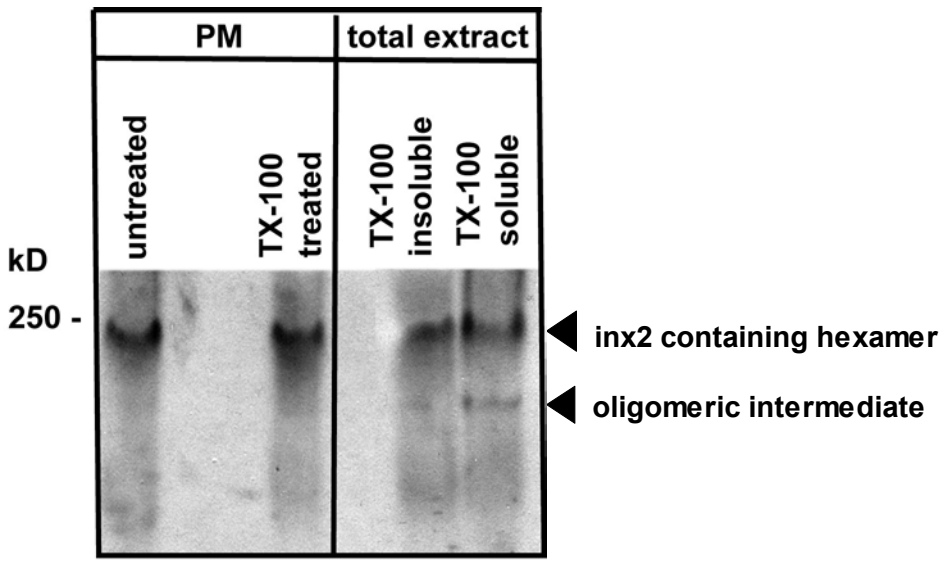

Fig. 4-2 Native PAGE analysis of innexin2 (inx2) containing hemichannels after TX-100 solubilisation. Detection of innexin2 in the PM and in the TX-100 soluble fraction of total extracts reveals one protein band corresponding to the size of a hexameric form of innexin2 in the insoluble fraction, whereas in the soluble fraction an additional band is detected with the innexin2 antibody (oligomeric intermediate).

4.1.2 Modifications of innexin proteins are crucial for the acquirement of TX-100 insolubility

To further characterise TX-100 insolubility of innexin2 containing hexamers, native embryonic extracts solubilised with the non-ionic detergent were also separated under reducing conditions using conventional SDS-PAGE with Laemmli-buffer (Gallagher, 2006). This approach was chosen to figure out whether modifications on innexin2 protein could be detected that distinguish innexin2 insoluble protein from soluble protein.

After TX-100 solubilisation and centrifugation to separate soluble from insoluble proteins, innexin2 was detected again in both, the TX-100 soluble and insoluble fraction. The detected innexin2 protein bands showed differences in their molecular weight. A protein band at 42 kD was detected in the total and the TX-100 soluble fraction, corresponding to the full length size of monomeric innexin2 protein, whereas a protein band of higher molecular weight was detected in the total and the TX-100 insoluble fraction (45 kD). This result indicated modifications are introduced in innexin2 containing hexamers, which might be a general characteristic of TX-100 insolubility (Fig 4-3).

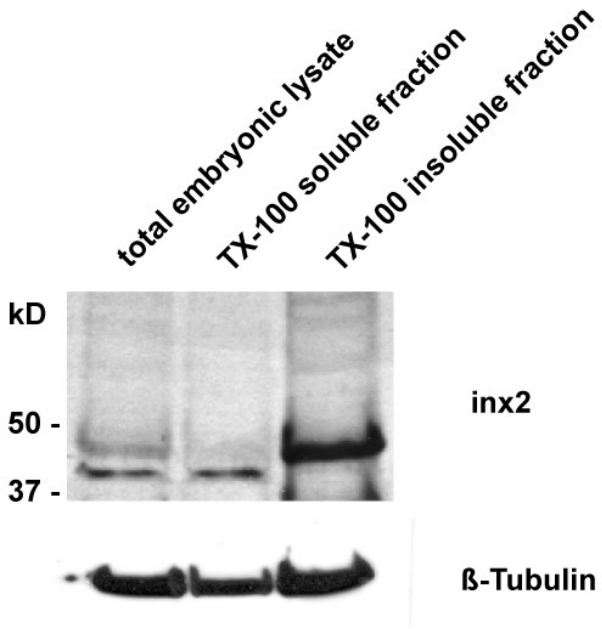

Fig. 4-3 Innexin2-containing hexamers are modified before membrane integration. Innexin2 exhibits two major protein forms in total extracts and in a TX-100 soluble fraction. Only the higher molecular weight form of innexin2 protein is found in the TX-100 insoluble fraction, whereas the lower molecular weight form is absent, pointing to post translational modification of innexin2 upon membrane integration.

In order to evaluate, whether modifications of innexins are a general prerequisite accompanied with TX-100 insolubility and membrane integration, the biochemical behaviour of another innexin isoform was investigated.

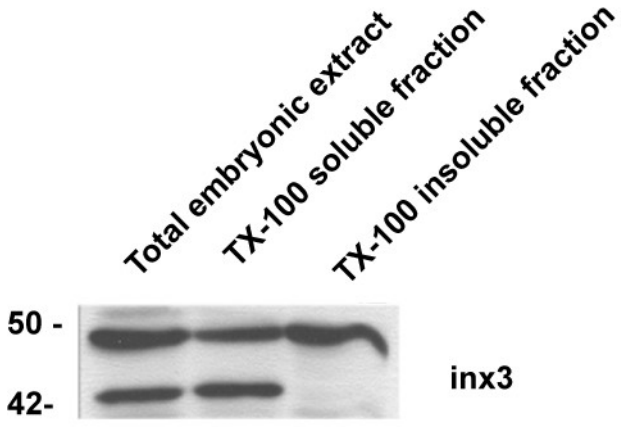

Fig. 4-4 A modification of innexin3 protein is prerequisite for membrane integration. Innexin3 shows two major forms in total extracts and in a TX-100 soluble fraction. Only the higher molecular weight form of innexin3 protein is found in the TX-100 insoluble fraction, whereas the lower molecular weight form is absent. This suggests that post translational modifications of innexins are prerequisite for membrane integration.

Fractionation of TX-100 solubilised embryonic extracts and detection with an anti-innexin3 antibody also showed a higher molecular weight protein band in the insoluble fraction, which

was absent from the TX-100 soluble fraction, indicating that the introduction of modifications in innexin proteins is a necessity for TX-100 insolubility and plasma membrane integration of innexin hexamers (Fig. 4-4).

Investigations, whether phosphorylation, as one possible translational modification, is required for TX-100 insolubility and membrane integration, dephosphorylation reactions were carried out. Dephosphorylation assays of embryonic protein extracts using calf intestine alkaline phosphatase for 30 min at 37°C have been shown to reduce the upper protein band detected with the innexin3 antibody, arguing that phosphorylation is one modification involved in the acquisition of TX-100 insolubility (by B. Loer; Fig. 4-5). Dephosphorylation assays, followed by immunoblot detection of innexin2 did not show this clear effect, indicating that additional modification might play a role in the acquirement of TX-100 insolubility and associated membrane integration.

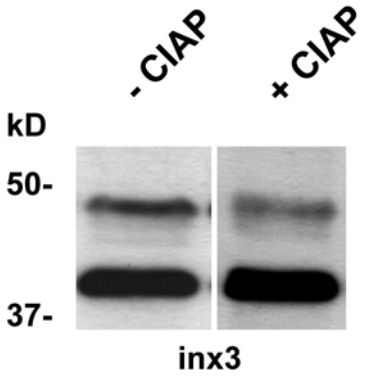

Fig. 4-5 Phosphorylation is one post translational modification of innexin3. Treatment of embryonic extracts with calf intestine alkaline phosphatase (CIAP) leads to a decrease of the higher molecular weight protein band of innexin3 in favour of an increase in intensity of the lower innexin3 protein band.

4.1.3 Innexin2 is detected in different oligomeric forms

A common assay to study oligomerisation of proteins, besides native PAGE analysis used in the first section (4.1.1), is to separate oligomers of different sizes along density gradients following fractionation and SDS-PAGE to analyse the content of those fractions. In this approach a linear 5 - 20% (w/v) sucrose gradient was chosen to separate different oligomeric assemblies of innexin2. To assess the sedimentation of different oligomeric proteins along the gradient, purified marker proteins of different molecular weights, namely ovalbumin (45 kD) and catalase (250 kD) were centrifuged under the same biophysical conditions and their distribution along the sucrose gradient was analysed by Coomassie blue staining.

Figure 4-6 shows that catalase with a molecular weight of 250 kD, corresponding to the size of innexin2 containing hexamers, was detected in fraction between 14 - 19% sucrose, whereas the smaller protein ovalbumin (45 kD) that was used to determine the sedimentation of monomeric innexin2 (42.49 kD), floated between 7 - 11% sucrose.

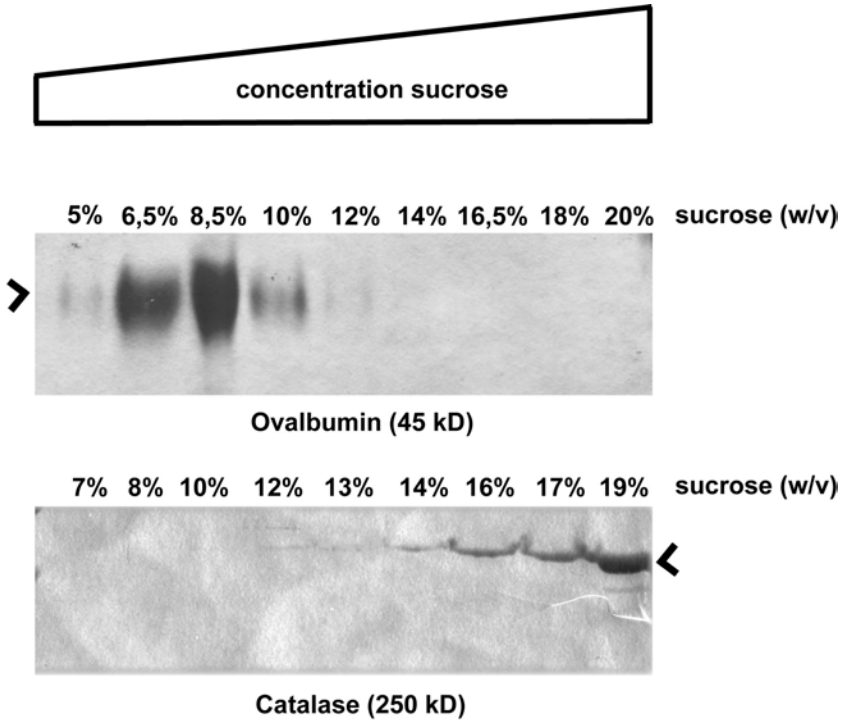

Fig. 4-6 Analysis of sedimentation behaviour of the marker proteins catalase and ovalbumin in sucrose gradients. Coomassie blue-stained SDS-polyacrylamide-gels after density centrifugation of purified catalase, 250 kD and ovalbumin, 45 kD on 5 - 20% sucrose gradients and fractionation. Under chosen conditions, catalase sediments in fractions between 14 - 19% sucrose, whereas ovalbumin is detected in fractions containing 6 - 10% sucrose

Consistently, accumulations of innexin2 protein were detected in fractions between 16 - 19% sucrose (Fig. 4-7), strengthening the evidence for hexameric isoforms that contain innexin2 (section 4.1.1). In addition, an enhanced detection of innexin2 protein was detected also in the 7% sucrose fraction, indicating the presence of monomeric, unassembled protein (Fig. 4-7, upper panel). The detected protein bands in between monomeric and hexameric forms were designated as oligomeric intermediates that have not reached the hexameric status yet. The hexameric form of innexin2-containing oligomers was termed “innexon” in analogy to the hexameric connexon. A control for the oligomerisation assay is to study the behaviour of oligomeric proteins after dissolving non covalent bonds, which mediate adhesiveness of proteins within an oligomer, by the addition of reducing agents. Analyses of such denaturated protein extracts were carried out under the same biochemical conditions that were used for TX-100 solubilised extracts.

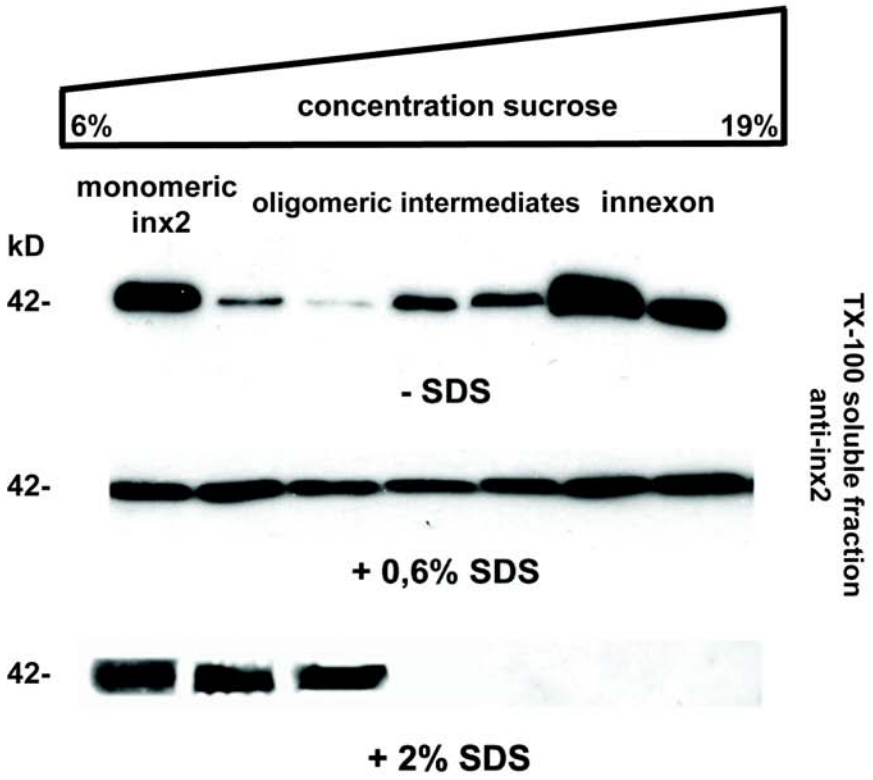

Fig. 4-7 Innexin2 forms hexameric hemichannels and oligomeric intermediates. Addition of different concentrations of SDS (0.6% middle panel, 2% lower panel) to the TX-100 soluble extract before centrifugation leads to the decay of innexin2 containing oligomers as compared to the untreated control (top panel). Analyses were done by continuous density gradient centrifugation of TX-100 solubilised extract on sucrose gradients and fractionation. In untreated controls, monomeric protein (accumulation in low percentage sucrose fractions between 7% - 9%) was separated efficiently from hexameric proteins (detected in fractions between 16% - 19% sucrose).

Applying different concentrations (0.6 and 2%) of SDS, which works by disrupting non-covalent bonds in the proteins, causing the molecules to loose their native shape, to the TX-100 solubilised lysate, resulted in a shift of innexin2 protein distribution to lower sucrose content fractions, indicating that innexin2 containing hexamers resolved into monomers and oligomeric intermediates under denaturating conditions (Fig. 4-7, middle and lower panel).

4.1.4 Innexin2 has the potential to form homomeric hemichannels *in vitro*

The preceding analyses of innexin2 oligomerisation were performed using whole embryonic extracts in the presence of all the other 7 innexin isoforms. In order to test whether innexin2 holds the ability to form hexamers on its own and to exclude the influence of other innexin

proteins on the oligomerisation process, *in vitro* translation of full length *innexin2 m*RNA was carried out in the presence of canine microsomal membranes and the radioactive S^{35}-epitope to label the translated protein. The described approach was commonly used for *in vitro* assembly studies of connexin proteins (Falk, 2000). Using this system and analysing the oligomerisation ability of innexin2 by liquid scintillation counting of integrated S^{35} after separation of the innexin2-oligomeric forms by density gradient centrifugation on 5-20% sucrose gradients followed by fractionation, revealed that innexin2 is to some extend able to assemble into hexameric hemichannels. However, the efficiency of i*n vitr*o translated innexin2 protein in building hexamers was comparatively low. Only 22% of total protein relative to 100% monomers was found in fractions between 18-19% sucrose, which had been shown before to contain only hexameric innexin assemblies (Fig. 4-8). However, most of the protein was detected in fractions from 6-14%, containing innexin2 monomers and oligomeric intermediates.

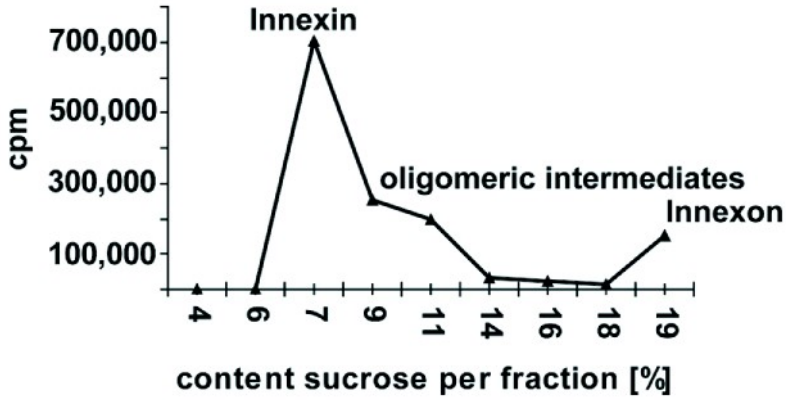

Fig. 4-8 Innexin2 forms homomeric hexamers *in vitro.* Liquid scintillation counting of incorporated S^{35} after *in vitro* oligomerisation of innexin2, density gradient centrifugation and fractionation**.** Only 22% of total protein is found in fractions designated to contain hexameric oligomers. Most of the protein accumulates in fractions between 6-14% sucrose containing monomers and oligomeric intermediates.

In order to evaluate this further, the *in vitro* oligomerisation experiment was repeated and analysed using a different approach. Fractions containing monomeric and oligomeric innexin2 were analysed by SDS-PAGE followed by autoradiography to verify that the signals, obtained by liquid scintillation counting, correspond to *in vitro* translated innexin2 protein and its oligomeric forms.

In fact, detection of a 42 kD protein band in different sucrose fractions corresponded to the size of monomeric innexin2, indicating that the results obtained by liquid scintillation counting, resulted from the investigated protein (Fig. 4-9). Together, these data point to the ability of innexin2 to form homomeric hexamers *in vitro*, however to a quite low extent.

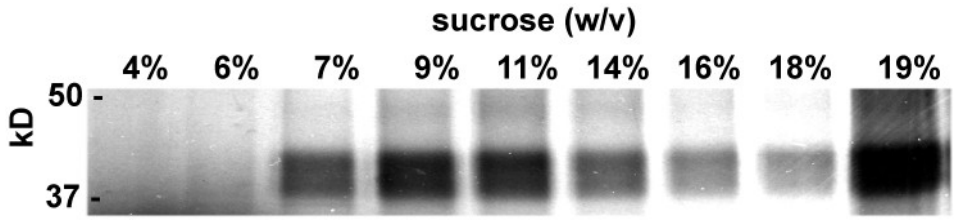

Fig. 4-9 SDS-PAGE and autoradiography of *in vitro* oligomerised innexin2 protein after velocity sedimentation on sucrose gradients. A signal at 42 kD corresponding to the protein size of innexin2 protein is detected in fraction between 7 - 19% sucrose with accumulation of protein in fractions between 7 - 11% (monomers) and 19% sucrose (hexamer containing fraction).

4.1.5 Overexpression of innexin2 in SL2 cells leads to plaque formation among neighbouring cells

Knowing that innexin2 was able to form innexons, which provide on half of gap junction channels, led to investigations of the resulting channels at the plasma membrane between adjacent cells that exhibit a typical plaque like structure in vertebrates.

Cell culture systems are often used to perform trafficking assays and to proof plaque formation ability of gap junction proteins. In this thesis a system was used that enables an inducible overexpression of innexin2 in SL2 cells.

SL2 cells, which are of *Drosophila* embryonic origin, naturally express innexins to a relative low extent. These cells do not show gap junction typical plaque like structures between neighbouring cells, which is detectable by immunofluorescent staining (Bauer et al., 2006). To enhance and to differentiate ectopic from endogenous innexin2 expression in SL2 cells, an epitope-tagged version of innexin2 was introduced in these cells via stable transfection. SL2 cells were co-transfected with an inducible innexin2-myc expression construct (pMTVinx2-myc) and a vector that mediates resistance to the antibiotic hygromycin. Stable cells were selected by hygromycin addition to the medium at a concentration of 300 µg / ml. Overexpression of innexin2-myc protein in these stable cell line, inducible by the addition of copper sulphate, lead to the formation of gap junction typical plaques when cells were in direct contact to each other, even when no *D*E-Cadherin was co-expressed as described previously (Bauer et al., 2006; Fig. 4-10). Plasma membrane expression of innexin2 was verified, applying cell surface biotinylation of extracellularly exposed lysines and pull-down with avidin coated sepharose (Fig 4-11).

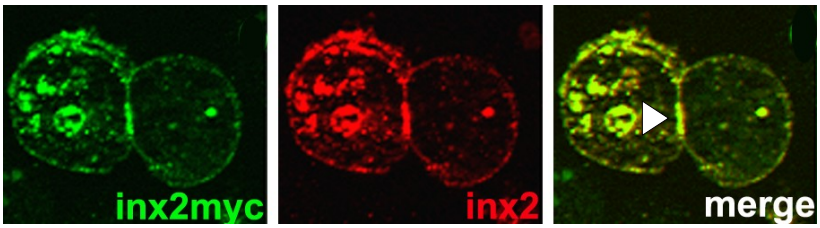

Fig. 4-10 Overexpression of innexin2-myc in stable SL2 cells leads to gap junction plaque formation. Double staining of innexin2-myc (green) and innexin2 (red). Over expression of innexin2-myc results in the formation of plaque like structures between two neighbouring cells (arrow).

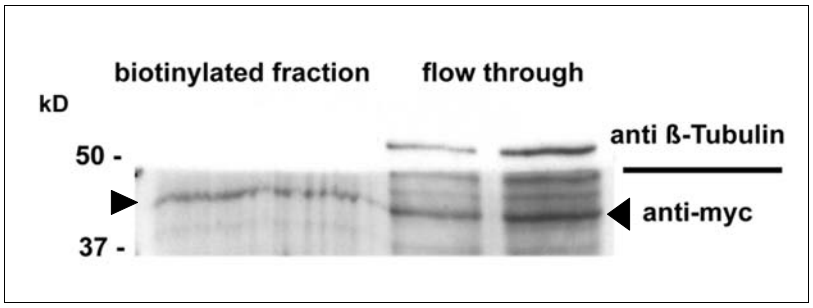

Fig. 4-11 Innexin-2 myc is expressed at the plasma membrane of SL2 cells. Cell surface biotinylation of innexin2-myc. Biotinylation and pull-down of scintillated proteins with avidin coupled sepharose shows innexin2 (arrows) in the biotinylated fraction, whereas ß-tubulin was found only in the flow through, indicating a plasma membrane localisation of over expressed innexin2 protein.

Together, these results showed that the generated SL2 cell line, expressing an epitope tagged variant of innexin2, forms gap junction plaques at the plasma membranes between adjacent cells. The generated cell line was used later on for the trafficking analysing of innexin2 containing gap junction plaques.

4.2 Trafficking of innexin2 to the plasma membrane

After synthesis, transmembrane proteins have to travel to their final destination, namely the plasma membrane taking several routes. The well conserved secretory pathway is one of the major routes transmembrane proteins take to reach the plasma membrane. Different studies addressing exocytosis of vertebrate connexins showed that the secretory pathway is the main trafficking route for connexin oligomers and hemichannels for most of the investigated vertebrate gap junction proteins (Laird, 2006; Martin et al., 2001).

4.2.1 Innexin2 is localised within compartments of the secretory pathway

In a first approach, addressing the issue of innexin2 trafficking, subcellular fractionation experiments were carried out in order to define the subcellular distribution of innexin2 protein within different cellular compartments. Differential centrifugation combined with density gradient centrifugation was used to isolate different membrane compartments of SL2 cells and to analyse them for innexin2 content using established protocols for fractionation of cultured cells (Quigely, 1976; Love et al., 1998).

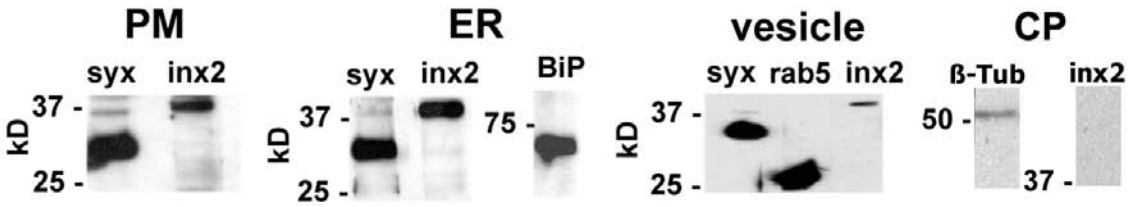

Fig. 4-12 Innexin2 detection in different cellular compartments. Innexin2 is found in all membrane fractions (PM, ER, vesicle fraction) isolated from SL2 cells, whereas the cytoplasmic fraction is devoid of innexin2 protein.

Isolation of plasma membranes from discontinuous sucrose gradients (20 - 60% sucrose) from the 20% to 40% sucrose interphase, followed by SDS-PAGE, Western Blotting and antibody detection of innexin2 as well as the membrane marker syntaxin1A, as total membrane marker, showed that innexin2 was contained in the plasma membrane fraction.

From same gradients a fraction at the interphase between 40-60% sucrose was isolated, designated to a endoplasmic reticulum enriched membrane fraction (Quigely, 1976). As control, BiP/Hsc70-3 protein, which encodes an endoplasmic reticulum located heat shock protein with ATPase activity (Elefant and Palter, 1999), was found to be enriched in this ER enriched membrane fraction. Innexin2 was also found to be present within this fraction, whereas its detection was absent from the isolated cytoplasmic fraction that was obtained by differential pelleting at 100000 x *g* for 90 min. The cytoplasmic fraction was free of contaminating membranes indicated by the absence of the membrane marker syntaxin 1A. As a positive control that protein was present in the isolated fraction, the presence of ß-tubulin as cytoplasmic protein was checked in the same fraction (Fig. 4-12).

Furthermore, a total vesicle fraction was isolated according the protocol of Love and colleagues (Love et al., 1998). Due to their low density, vesicles float up in 10-40% iodixanol gradient and are harvested from the 10% - 25% iodixanol interphase. Analysis of the vesicle fraction revealed an accumulation of rab 5 in this fraction, a marker for early endosomes

(Wucherpfennig et al., 2003). Innexin2 protein was also detected in this isolated vesicle fraction.

In a second approach, fluorescent antibody staining of the epidermis of wild type and transgenic embryos that carry epitope-tagged markers (PDI-GFP; Golgi-CFP) for different organelles was carried out. Innexin2 localisation was analysed using confocal microscopy scanning through different focal planes of the embryonic epidermis.

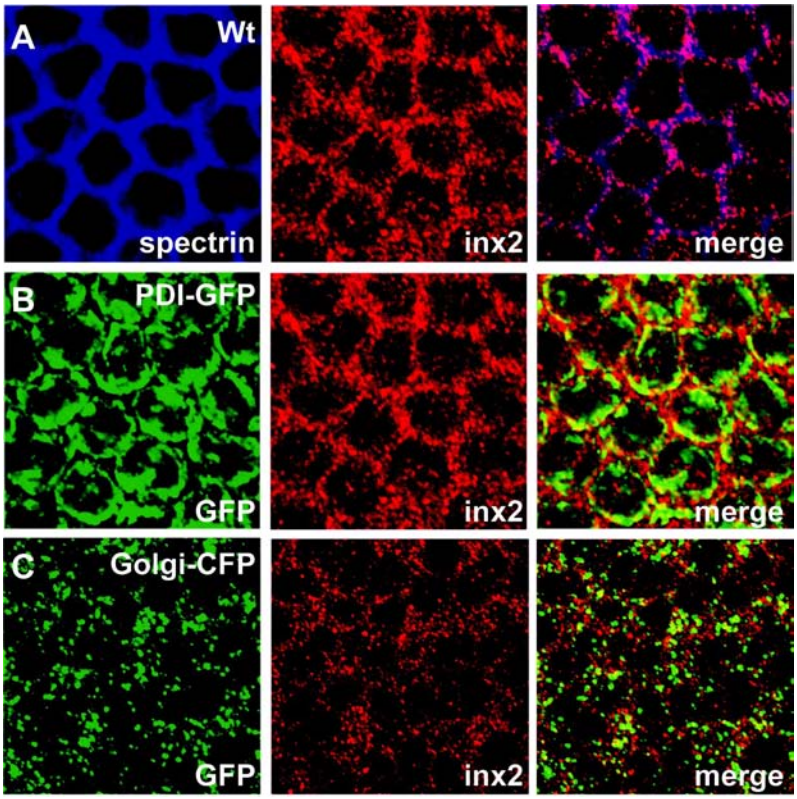

Fig. 4-13 Partial colocalisation of innexin2 and different subcellular markers. Co-immunostaining of innexin2 (red) and the plasma membrane marker spectrin (blue) of wild type embryonic epidermal cells (**A**). Co-immunostaining of PDI-GFP (green) and innexin2 (red) of epidermal cells (**B**) and of Golgi-CFP (green) and innexin2 (**C**) from transgenic embryos (*PDI-GFP* and *Hs::Golgi-CFP*).

As described before, (Lehmann et al., 2006, Bauer et al., 2004) innexin2 expression was found localised at the plasma membranes of epidermal cells (Fig. 4-13 A). Partial overlap with PDI-GFP, a GFP tagged variant of the disulphide isomerase that is ER located, points again to ER localisation of innexin2 (Fig. 4-13 B). Another transgenic line was used to analyse Golgi localisation of innexin2. Only some spots seemed to colocalise with the CFP-tagged Golgi protein galactosyl-tranferase (Fig. 4-13 C). Results from co-immunostainings were consistent with previous finding of subcellular fraction studies, where innexin2 was also found in membrane fractions representing compartments of the secretory pathway.

4.2.2 Brefeldin A treatment blocks endoplasmic reticulum exit of innexin2

To investigate the trafficking route of innnexin2 further and to clarify whether innexin2 transport is indeed dependent on ER to Golgi transport, drug treatment experiments were carried out interfering with the early secretory pathway.

Brefeldin A is known as fungal lactone which interacts with the anterograde transport of proteins from the ER to the Golgi-apparatus (Klausner et al., 1992) by causing a breakdown of the Golgi apparatus and its redistribution into the ER. As a consequence proteins that are transported along the secretory pathway fail to reach their final destination and accumulate in the ER and the cytoplasm of brefeldin A treated cells. This assay was used in SL2inx2-myc cells and follicle cells of the *Drosophila* egg chamber to analyse whether innexin2 membrane trafficking is accomplished via the ER to Golgi trafficking route.

4.2.2.1 Brefeldin A treatment of SL2 cells

In a first approach brefeldin A treatment was carried out in cultured SL2 cells, stably expressing innexin2-myc under an inducible promotor. Applying brefeldin A at concentration of 20 µg / ml for 6 h to 40 h induced cells, resulted in the loss of plaque like structures at the membranes of adjacent cells as compared to the solvent (DMSO) treated controls (Fig. 4-14). Innexin2-myc protein is found strongly colocalised with the ER marker PDI upon brefeldin A treatment, suggesting an ER exit block of innexin2-myc protein.

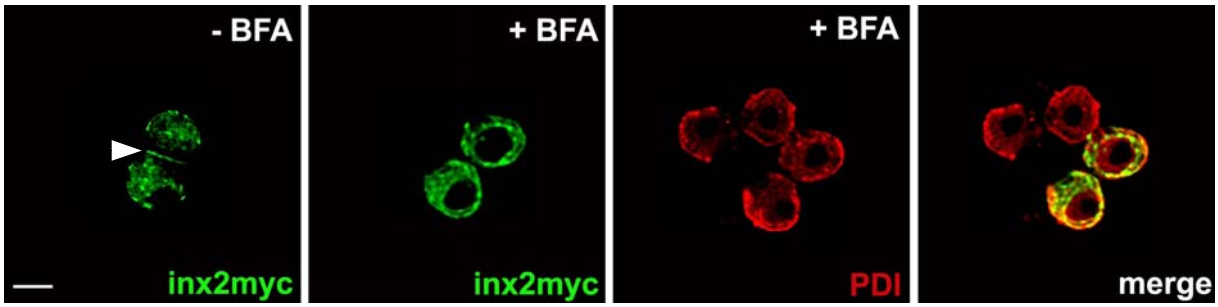

Fig. 4-14 Brefeldin A treatment results in a cytoplasmic accumulation of innexin2-myc in SL2 cells. Mock treated (DMSO) cells show plaque like structures between adjacent cells whereas no plaques are visible after BFA treatment (20 µg / ml) for 6 h. innexin2-myc protein (green) accumulates in the cytoplasm of BFA treated cells, colocalising with the ER marker PDI (red). Scale: 10 µm.

4.2.2.2 Brefeldin A treatment of the follicle cell epithelium of the *Drosophila* egg chamber

The follicle cell epithelium of the *Drosophila* egg chamber serves as and excellent system to study trafficking of epithelial membrane proteins (Fig. 4-15; Horne-Badovinac and Bilder,

2005). These cells provide a highly polar organisation and imaging can be easily accomplished. Localisation and trafficking of various membrane proteins has been investigated successfully within this cellular system (Denef et al., 2008, Tanentzapf et al., 2000). *innexin2 m*RNA expression in the *Drosophila* ovary has already been shown by Stebbings and colleagues, being expressed in both, the germ line and follicle cells (Stebbings et al., 2002)

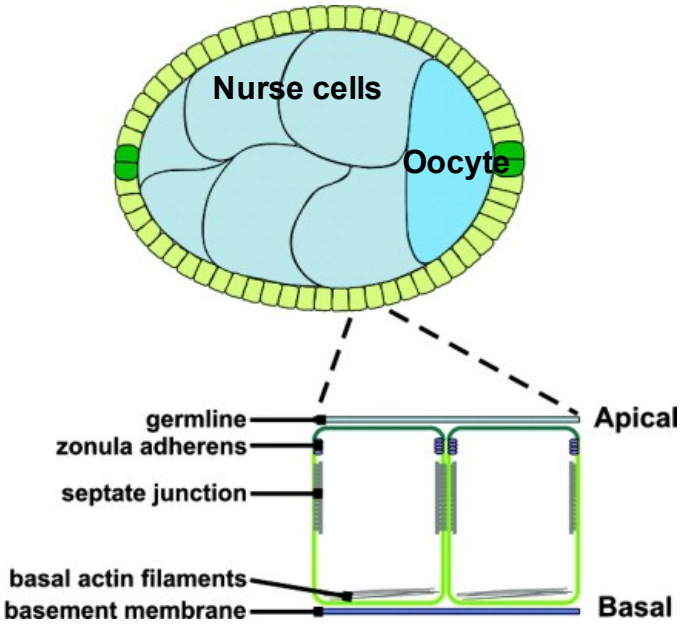

Fig. 4-15 Apico-basal polarity in the follicle cell epithelium. The drawing shows a stage 8 egg chamber with a magnified view of two follicle cells and their polarity showing the localisation of adherens and septate junctions along the apico-basal axis.

To determine the protein localisation of innexin2 in the follicle cell epithelium, co-immunostaining experiments were carried out with an anti-innexin2 antibody and an antibody recognising *D*E-cadherin, a *Drosophila* adherens junction core component, which marks the apico-lateral membranes. Detection of labelled innexin2 protein by confocal microscopy resulted in the observation of a highly ordered expression pattern along the baso-lateral membrane (Fig. 4-16) of the follicle cell epithelium. *D*E-cadherin as adherens junction marker was found accumulating at the apico-lateral domain and with a weaker expression also at the lateral membranes of follicle cells. This highly ordered pattern made it possible to detect changes in the localisation of innexin2 easily.

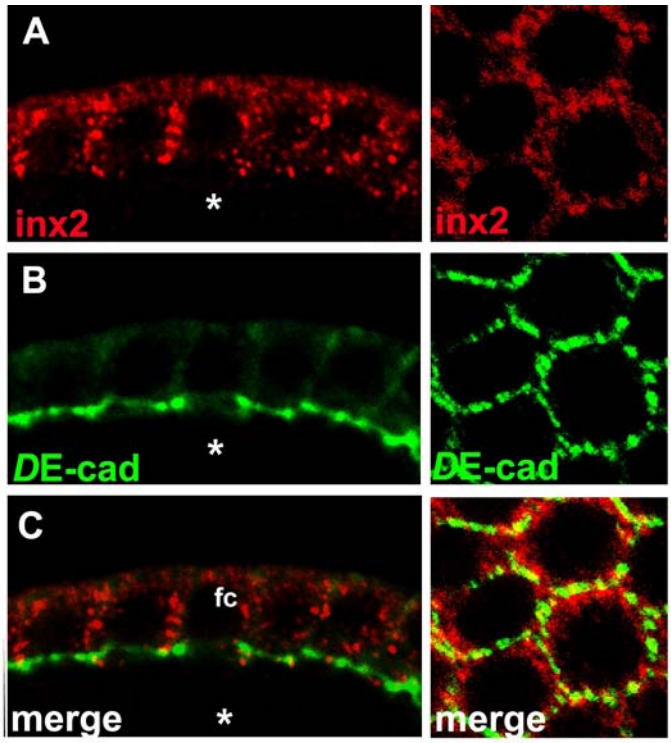

Fig. 4-16 Baso-lateral localisation of innexin2 at the PM of follicle cells. Innexin2 (red) localisation at the baso-lateral membrane of follicle cells (fc) of the egg chamber, lateral view (left), top view (right) (A). *D*E-cadherin (green) was co-stained as a marker for the apico-lateral domains of the follicle cells epithelium. Lateral view (left), top view (right) (**B**). Merged pictures of *D*E-cadherin and innexin2 stainings in (**C**). Asterisks (*) mark the localisation of the oocyte.

Because of the clear expression pattern of innexin2 enriched at the baso-lateral membranes in follicle cells, this system was used as an ex *vivo* model to study brefeldin A dependent changes of innexin2 localisation.

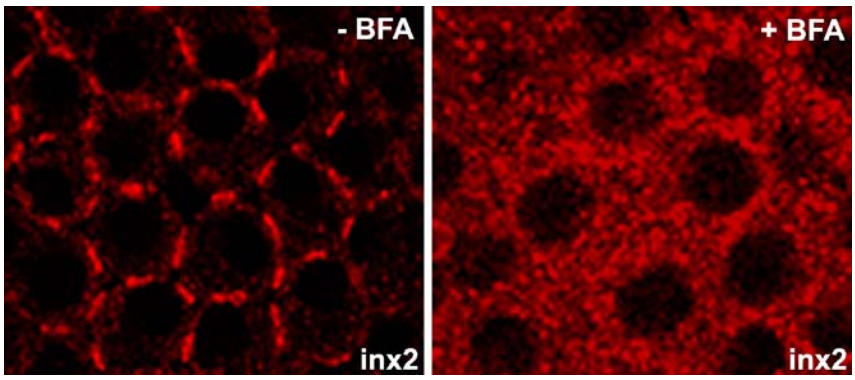

Fig. 4-17 Brefeldin A treatment causes innexin2 accumulation in the cytoplasm of follicle cells. Follicle cells of Brefeldin A (BFA) treated (right panel) and untreated ovaries (left panel). Whereas innexin2 was localised at the plasma membrane of solvent treated control ovaries, localisation was shifted to the cytoplasm in BFA treated cells.

Treatment of freshly isolated ovaries with brefeldin A at a concentration of 20 µg / ml for 4 h at RT resulted in an accumulation of innexin2 protein in the cytoplasm of follicle cells in contrast to the solvent (DMSO) treated control ovaries, where innexin2 localisation was enriched at the plasma membrane, further indicating that the Golgi apparatus is an essential component on the trafficking route of innexin2 to the membrane (Fig. 4-17).

4.2.3 Innexin2 colocalises with ß-tubulin in the follicle cell epithelium

Gap junction membrane trafficking has been shown to be accomplished via microtubule dependent trafficking in the vertebrate cells (Shaw et al., 2007, Guo et al., 2003, Giepmans et al., 2001). To check whether *Drosophila* gap junction proteins do also have the potential to interact with microtubules during trafficking and membrane integration, co-immunostainings of ß-tubulin and innexin2 were carried out in the follicle cell epithelium of the ovary. Localisation of the fluorescently labelled proteins pointed to a spatial overlap of both proteins (Fig. 4-18).

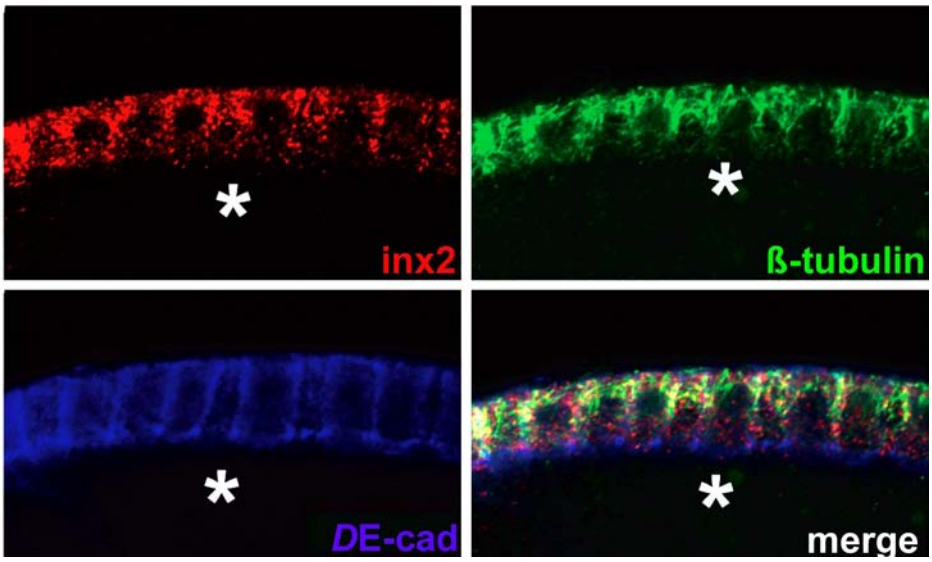

Fig. 4-18 Innexin2, ß-tubulin and *D*E-Cadherin distribution in the follicle cell epithelium of *Drosophila* egg chambers. *D*E-cadherin (blue) was used as a membrane marker. innexin2 (red) and β-Tubulin (green) colocalise in the cytoplasm and predominately at lateral membranes. Asterisk (*) marks the oocyte.

4.2.4 Innexin2 interacts with ß-tubulin

Proteins showing a close spatial vicinity within a cell, may interact with each other directly or may be a part of a protein complex with other proteins. Therefore, the interaction potential of

innexin2 and ß-tubulin was investigated by co-immunoprecipitation experiments using whole embryonic extracts, where colocalisation of both proteins was also detected in the epidermis by co-immunostaining of innexin2 and ß-tubulin (Fig. 4-19). Embryonic extracts were used for the co-immunoprecipitation experiment for the reason that the preparation procedure of whole embryonic extract was much easier compared to the collection of extracts from pure ovaries.

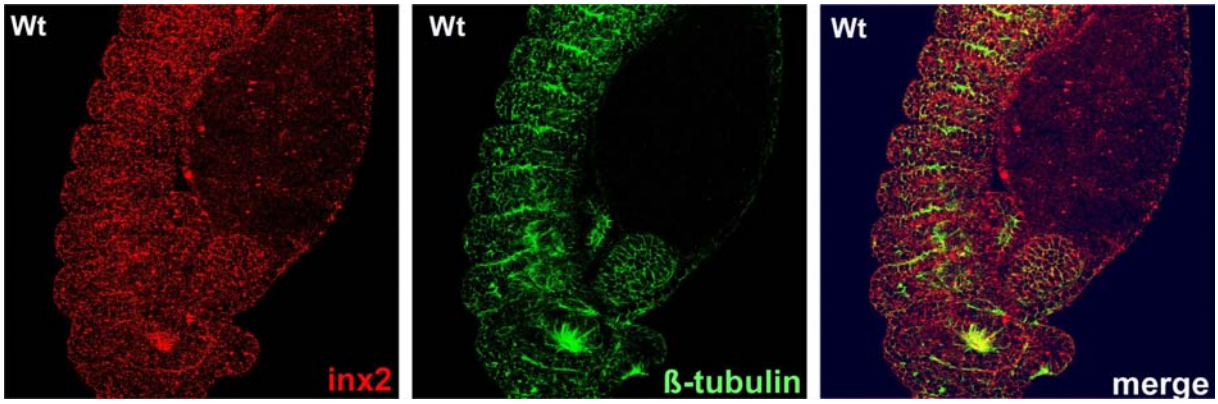

Fig. 4-19 Innexin2 and ß-tubulin colocalise in the epidermis of wild type embryos. Antibody staining of innexin2 (red) and ß-tubulin (green) showed a partial colocalisation especially at the segment boundaries and the anal pads (merge).

Precipitation was carried out on the one hand with an anti-ß-tubulin antibody and an unspecific mouse IgG antibody in the control reaction, followed by immunoblotting with an anti-innexin2 antibody. On the other hand immunoprecipitation reactions were carried out using an anti-innexin2 antibody and an unspecific rabbit IgG control reaction, followed by immunoblotting with an ß-tubulin antibody. The different approaches resulted in the co-immunoprecipitation of both proteins, indicating that both proteins are contained within the same complex (Fig. 4-20).

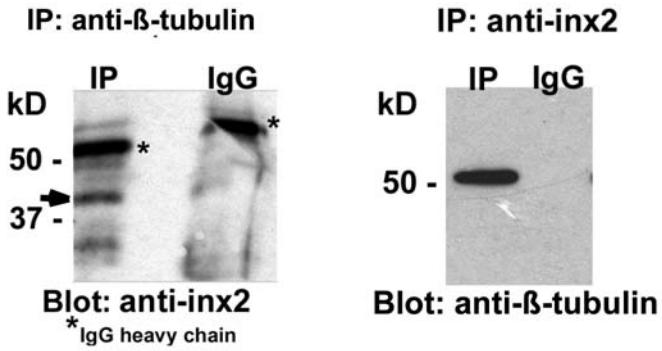

Fig. 4-20 Innexin2 and ß-tubulin interaction. ß-tubulin was able to pull down innexin2 and vice versa, arguing for the existence of both proteins in a complex. IP with an anti-innexin2 antibody as precipitating antibody was done by crosslinking of the antibody to the sepharose beads to avoid the presence of IgG heavy chains in the immunoblot (*), which have a similar size (52 kD) to ß-tubulin (55 kD).

4.2.5 Transport of innexin2 containing hemichannels to the plasma membrane is dependent on microtubules

Co-immunostainings and co-immunoprecipitation experiments point to an interaction of innexin2 and ß-tubulin. To investigate this interaction in respect to innexin2 trafficking further, a series of drug treatment experiments was performed. In a first approach freshly dissected ovaries from fertilised wild type females were incubated for 1 h at RT in Schneiders Medium drugged with colchicine (20 µg / ml). Colchicine inhibits the polymerisation of microtubules by binding to α- or β- tubulin subunits, which are the core constituents of the microtubules. Control ovaries were incubated with medium containing the solvent ethanol. Co-immunostainings of colchicine treated and solvent treated control ovaries were done with anti-innexin2 and anti-disc large antibodies. Disc large, a protein of the septate junction family, has been shown to be not affected upon treatment with tubulin depolymerising drugs (Iizuka-Kogo et al., 2004) and was therefore co-stained as a control. Imaging of the distributions of both proteins in the follicle cell epithelium by confocal microscopy, exhibited a clear delocalisation of innexin2 from the plasma membrane to the cytoplasm upon colchicine treatment, whereas the localisation of disc large was not affected (Fig. 4-21) compared to the solvent treated control (ethanol). This observation indicates that the microtubule network provides the route for innexin2 containing oligomers to the plasma membrane and / or stabilises innexin2 localisation at the membrane.

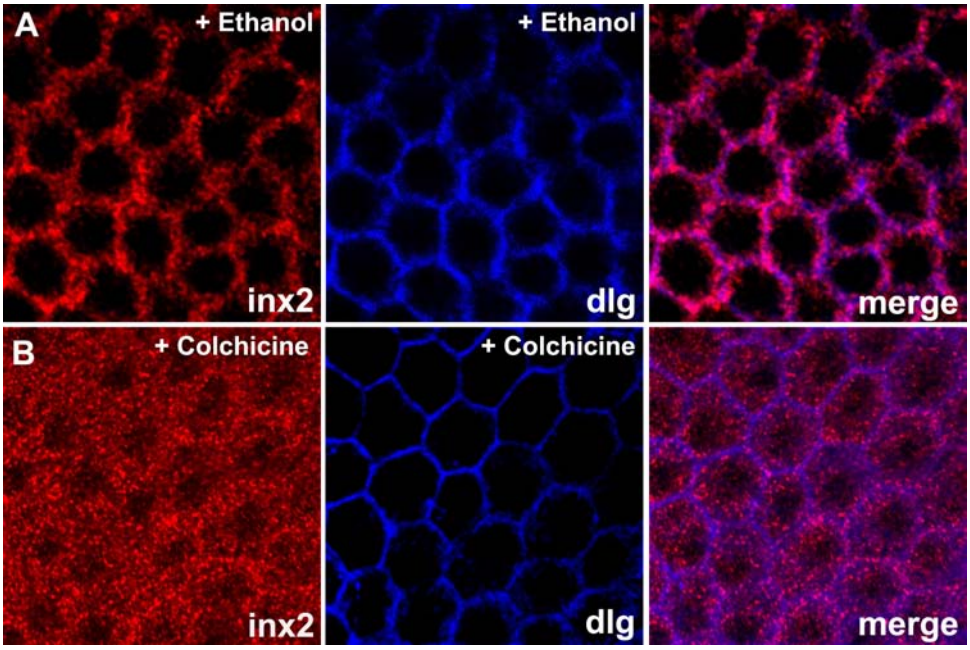

Fig. 4-21 Microtubule disruption affects innexin2 membrane localisation. Treatment with colchicine (**B**) alters the localisation of innexin2 (red), whereas the plasma membrane localisation of disc large (dlg; blue) is unchanged. Ethanol treated control cells show innexin2 localised at the PM of the follicle cell epithelium (**A**).

In a second approach SL2-cells that stably express innexin2 fused to a myc epitope-tag were analysed to support the data obtained from ovary treatments with colchicine. In this approach nocodazole, as another microtubule polymerisation interfering agent was used. After induction of innexin2-myc expression with copper sulphate for 40 h, nocodazole (5 µg / ml) was added to the cells. DMSO was added to control cells in parallel. After 1 and 2 hours incubation, cells were fixed and innexin2-myc expression was detected. Imaging of the treated cells revealed an increasing loss of innexin2 expression at the cell membrane in favour of an accumulation of innexin2 within the cytoplasmic part of cell over the time (Fig. 4-22).

This result proved the latter observations from colchicine treatments of dissected ovaries and indicates a turn over rate of gap junction plaques of 1 - 2 h in SL2 cells.

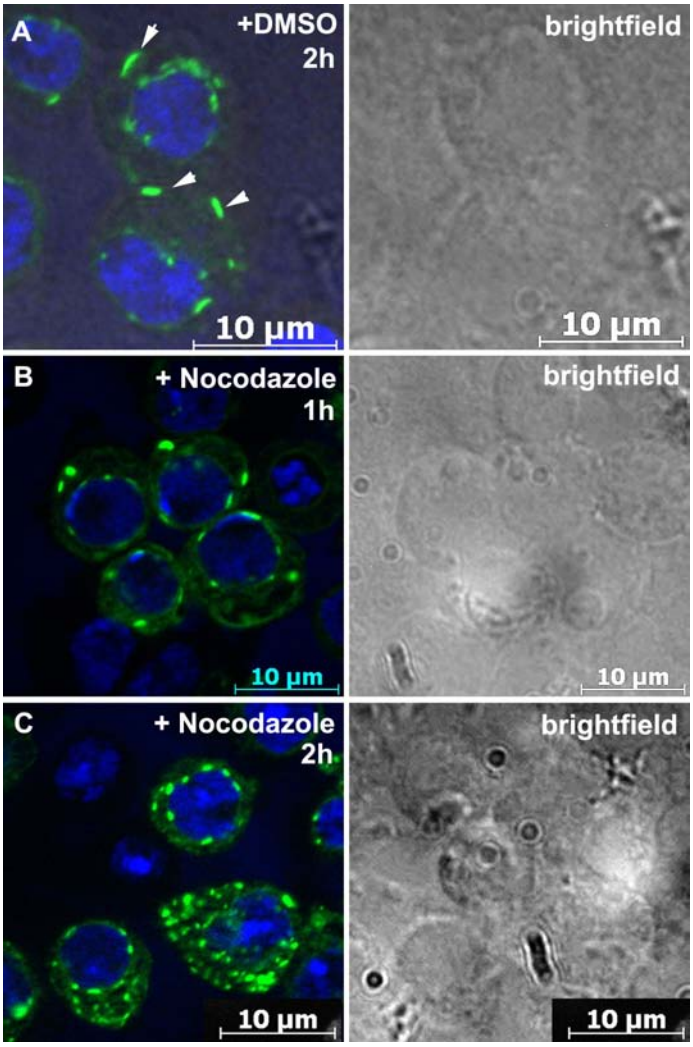

Fig. 4-22 Nocodazole treatment affects gap junction plaque assembly in SL2 cells. Treatment of induced Sl2 cells expressing innexin2-myc (green) with nocodazole for 1 h (**B**) or 2 h (**C**) leads to a time dependent loss of gap junction plaques at the plasma membrane in comparison to the solvent (DMSO) treated control (**A**). Nuclei were stained with DAPI (blue).

4.3 The exocyst complex is involved in innexin2 hemichannel membrane targeting

The exocyst complex has been investigated in *Drosophila* and mammalian cells extensively in recent years. It serves as a platform that enables vesicle fusion at the plasma membrane by binding to secretory vesicles that deliver membrane proteins. Different studies showed an involvement of members of the exocyst complex in membrane trafficking. One example is that the introduction of antibodies against the exocyst subunit sec8 into oligodendrocytes, MDCK (Madin–Darby canine kidney) and acinar cells has been found to inhibit plasma membrane protein transport and plasma membrane addition (Anitei et al., 2006) and that sec8 antibodies inhibit delivery of LDL receptor to the baso-lateral membrane (Grindstaff et al., 1998). Another example is that knockdown of exocyst subunits sec6, sec8 and exo70 resulted in a decreased level of type 4 glucose-transporter at the plasma membrane in adipocytes (Inoue et al., 2006).

Knowing that members of the exocyst complex have such a strong impact on targeting of plasma membrane designated proteins, various approaches were undertaken to gather information whether membrane targeting of innexin2-containing gap junction hemichannels is mediated by members of the exocyst complex.

4.3.1 Innexin2 and sec6 are detected in close vicinity at the cellular cortex of epidermal cells

Vesicle fusion at the plasma membrane takes place just beneath the plasma membrane in the cortical region of a cell. To investigate whether innexin2 localisation can be detected in this region, co-immunostaining experiments of innexin2 and sec6, one crucial component of the exocyst complex, were carried out (Fig.4-23).

Immunofluorescent stainings of embryonic epidermal cells point to a partial colocalisation of both proteins in embryonic epidermal cells in the cortical region (Fig. 4-23 A). To define the place of colocalisation within the the cell, the plasma membrane marker spectrin was co-stained and localisation of sec6 and innexin2 relative to the membrane marker assayed. Whereas innexin2 colocalised mainly with the plasma membrane, a significant amount of protein was detected also at the cellular cortex beneath the plasma membrane (Fig. 4-23 C), sec6 protein expression was found accumulated at the cellular cortex in the cytoplasm (Fig.4-23 B).

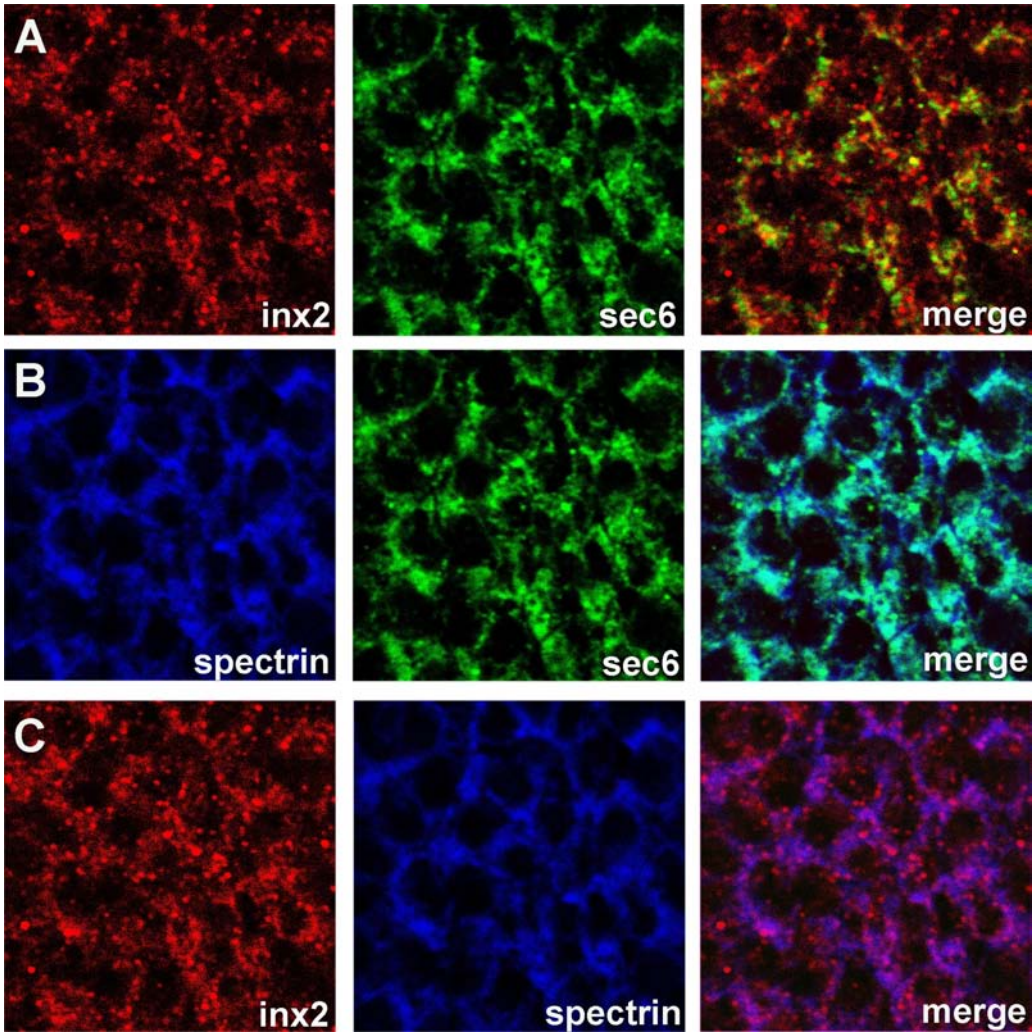

Fig. 4-23 Innexin2 and sec6 are localised in close vicinity at the cellular cortex of epidermal cells. Innexin2 (red) and sec6 (green) show a partial overlap in cells of the embryonic epidermis (**A**). To assess the precise region of overlap, co-staining with the membrane marker spectrin was done, revealing a cortical accumulation of sec6 relative to the membrane marker (**B**). Innexin2 was found localised to the plasma membrane of epidermal cells and was also detected at the cellular cortex, shown in (**C**).

Partial colocalisation of innexin2 and the exocyst component sec6 near the plasma membrane was a first evidence for the involvement of sec6 in inx2 plasma membrane targeting. To follow this evidence, gain and loss of function experiments were carried out in embryos and SL2 cell culture.

4.3.2 Overexpression of sec6 recruits innexin2 into vesicles and the plasma membrane

In a first approach gain of function studies were carried out in embryos. Overexpression of sec6 was accomplished in *Drosophila* embryos and innexin2 distribution was monitored by

subcellular fractionation experiments of plasma membranes and total vesicle fractions using the protocols for cell fractionation presented before. For the overexpression experiment a heat shock inducible Gal4-driver line was crossed to an UAS-*sec6* effector line and embryos were collected for subcellular fractionation of plasma membranes and a total vesicle fraction. As controls, the heat shock inducible driver line was crossed to wild type flies that do not contain the UAS responsive element. The heat shock to activate overexpression of sec6 was applied for 2 h at 37°C on 0-6 h old embryos of both crossings, following 4 h incubation at RT and subsequent homogenisation of the specimen.

Subcellular fractionation and Western blot analysis of the plasma membrane fraction and the total vesicle fractions from embryos that overexpressed sec6 and control embryos showed that the innexin2 protein content was increased in fractions deriving from the se6 overexpressing embryos in comparison to the control sample (Fig. 4-24). As a loading control the membrane marker syntaxin 1A was used. Interestingly, the vesicle fraction contained innexin2 protein in two forms that are described in section 4.1.1, whereas the plasma membrane fraction only contained the higher molecular weight form of innexin2 protein.

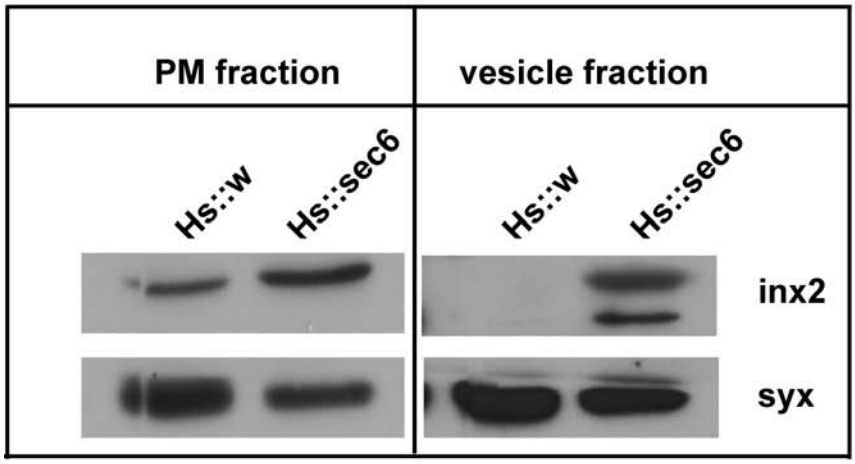

Fig. 4-24 Overexpression of sec6 recruits innexin2 into vesicles and the plasma membrane. Plasma membrane fractions of wild type control extracts were compared to the equivalent fraction isolated from embryonic extracts, in which sec6 had been overexpressed. innexin2 shows an enhanced expression in the sec6 overexpressed sample (compared to syntaxin (syx) as loading control, left panel). The same result was obtained analysing differences of innexin2 expression intensity in vesicle fractions (compared to the membrane marker syx, right panel).

Loss of function experiments carried out in embryos did not show clear results. Therefore, additional RNAi approaches on different components of the exocyst were performed in SL2 cells, stably expressing innexin2-myc. As shown before, gap junction plaque assembly at the plasma membrane of adjacent cells takes place in those cells. The formation of innexin2 positive plaque-like structures was taken as a readout system to study exocyst involvement

in innexin2 membrane targeting.

One advantage of this loss of function approach is that several components of the exocyst complex could be investigated in parallel approaches. First, double stranded RNA was generated against the exocyst components sec5, sec6 and sec15 by *in vitro* transcription. The purified double strand RNA was applied afterwards and incubated on SL2inx2-myc cells for three consecutive days. Innexin2 expression in the SL2 cells was induced at the second day of RNAi treatment with copper sulphate followed by an incubation for 40 h. After that, cells were analysed by immunhistochemistry of inx2-myc. The knock down efficiencies of the different double stranded RNAs were determined in parallel by quantitative real-time PCR analysis.

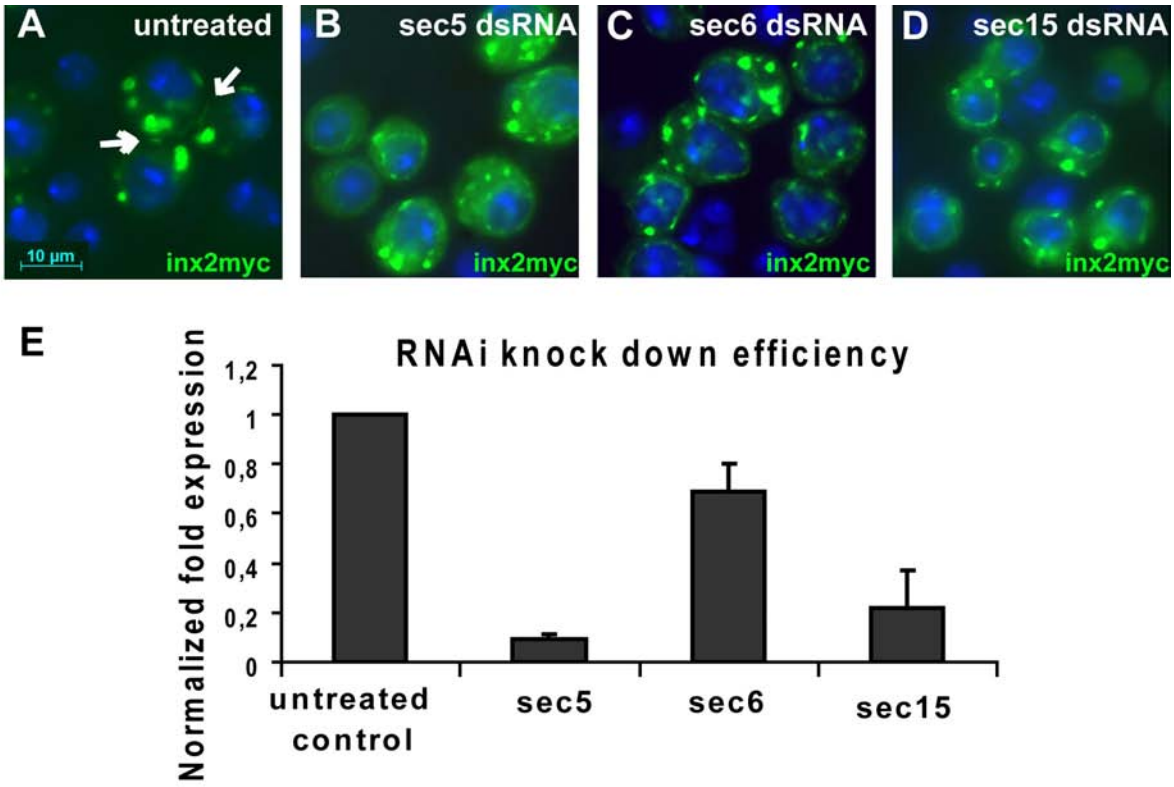

Fig. 4-25 Knock down of exocyst components affects innexin2 plaque formation in SL2 cells. Knock down of *m*RNA levels of various exocyst components by dsRNA treatment results in a decreased detection of innexin2-myc positive plaques (**B-D**) in contrast to the untreated control (**A**), where innexin2 positive plaques are clearly visible between neighbouring cells (arrows). The knock down efficiency of applied dsRNA was monitored using qRT-PCR analysis from cells of same sample in parallel (**E**).

Upon an RNAi mediated knock down of *m*RNA expression of various exocyst (sec5, se6, sec15) components, transport of innexin2 proteins to the plasma membrane was diminished, as assayed by observation of a decreased number of gap junction plaque like structures at the plasma membrane between adjacent cells, as shown in Fig. 4-25.

Together, these data provide first evidence for the importance of sec6 and other members of exocyst complex in membrane targeting of innexin2 containing hemichannels.

4.4 Expression of innexins in vertebrate cells

In order to establish another cellular system for the biochemical analysis of *Drosophila* innexin gap junction hemichannel formation and transport on the one hand, and to proof the functionality of resulting innexin2 gap junction channels by dye-coupling experiments on the other hand, mammalian HeLa cells were chosen and innexin expression tested in those cells. An advantage of this mammalian cell line the possibility to express *Drosophila* gap junction proteins in an otherwise innexin free background. In addition, this cell line had been used successfully in the past to investigate trafficking of the vertebrate gap junction proteins and protocols for various approaches are established (Falk et al., 2001; Thomas et al., 2005).

Evidence, that vertebrate cells have the potential to be used as a testing system for the expression of invertebrate gap junction proteins, came from studies in coupled *Xenopus* oocytes that have been used successfully in the past for the expression and analysis of connexins, pannexins and innexins (Bahima et al., 2006; Bruzzone et al., 2003; Stebbings et al., 2000) with regards to study and proof their ability to form functional gap junction channels between adjacent cells. One of the mentioned studies showed that *Drosophila* innexin2 and innexin3 were able to form functional gap junction when co-expressed in *Xenopus* oocytes and that expression of the innexin2 isoform alone lead to homomeric channel formation (Stebbings et al., 2000).

4.4.1 Analysis of innexin2 expression in HeLa cells

HeLa cells, which are commonly used to study vertebrate gap junction assembly and coupling assays (Elfgang et al., 1995), were transfected with different constructs containing *innexin2* cDNA. The vertebrate Kozak-core (*CCACC*) sequence was cloned 5`-prime of the start codon in the pMJgreen vector to enhance the translation efficiency. Cloning of the optimal vertebrate Kozak-sequence in front of the open reading frame was carried out because expression efficiencies of constructs just containing the cDNA sequence were in general very low. Aim of these expression studies was to analyse innexin2 behaviour in vertebrate cells in regards to “plaque”-formation in those cells.

To determine best conditions for the transfection of HeLa cells with *Drosophila* innexin2 constructs, cells were transfected with various ratios of DNA to Lipofectamine. Transfectants were harvested and analysed 24 - 30 h later. At this time, cells begun to round up and to loose their matrix adhesion finally ending in up in cell death. The obtained transfection efficiencies of innexin2 constructs, were in general much lower (approx. 10-20%) as compared to transfection controls. For control transfections the same plasmid lacking innexin2 cDNA, but containing an open reading frame for GFP expression was used which resulted in 90% of the cells expressing the reporter (pMJgreen; empty). The low transfection efficiency using innexin constructs made the analyses of large scale approaches difficult. Best transfection rates were obtained using a ratio of 1 : 2 ratio of DNA to Lipofectamine.

However, expression analysis of a innexin2-myc construct shows both, cytoplasmic and also membrane localisation of innexin2, observed by double immunostaining with the anti-innexin2 and the epitope-tag antibody myc to verify fusion-protein expression (Fig. 4-26). Innexin2-myc protein expression of was also confirmed by Western blot analysis, detecting innexin2-myc only in the transfected sample (Fig. 4-27).

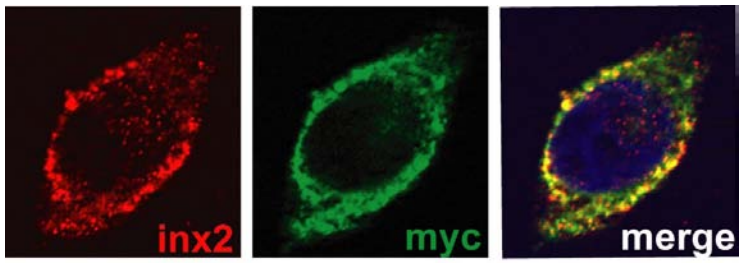

Fig. 4-26 Expression of innexin2-myc in HeLa cells. Double immunostaining of innexin2 (red) and myc (green) showed innexin2-myc expression in the cytoplasm and presumably at the plasma membrane.

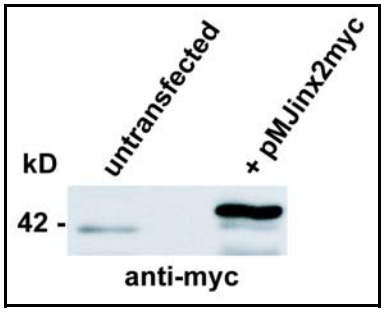

Fig. 4-27 Western Blot analysis of HeLa cells transfected with innexin2-myc. Detection of innexin2 protein expression from lysates of transfected cells and untransfected control cells revealed the detection of a clear protein band at 42 kD, corresponding to the size of innexin2-myc.

Several transfection approaches using an innexin2-myc construct, lead to the formation of gap junction typical plaque-like structures between plasma membranes of adjacent cells, observed 26 - 28 h after transfection (Fig. 4-28 A). The same result was obtained using an innexin2 construct without a tag fusion (Fig. 4-28 B).

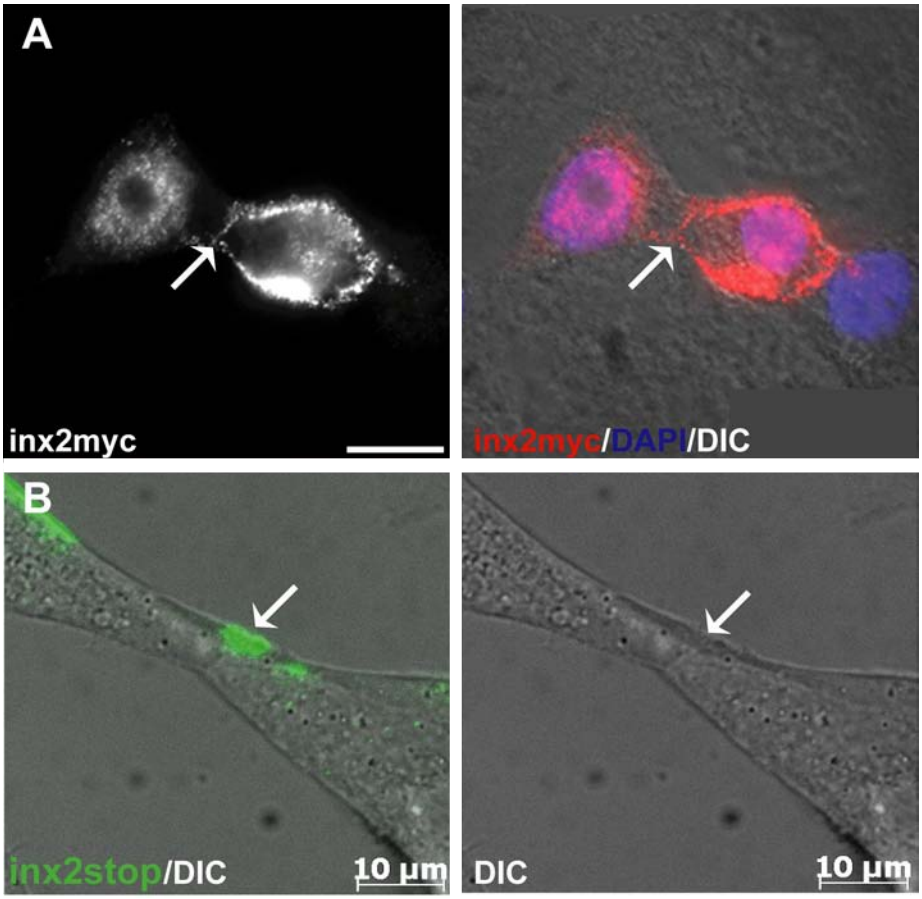

Fig. 4-28 Localisation of innexin2-myc and inx2stop in gap junctional plaque like structures at the plasma membrane of adjacent HeLa cells. Innexin2 expression is detected in a gap junction typical plaque-like structure at the membranes of two adjacent HeLa cells. Ectopic expression of innexin2-myc is shown in (**A**), expression of an untagged innexin2 variant is shown in (**B**). DIC was used to assess membrane-localisation. Scale in (**A**) 20µm.

In addition to plaque formation between two adjacent cells, a distinct membrane localisation of innexin2 became also visible at membranes of cells that do not have direct contacts to a neighbouring cell (Fig. 4-29), arguing for the existence of hemichannel accumulations in addition.

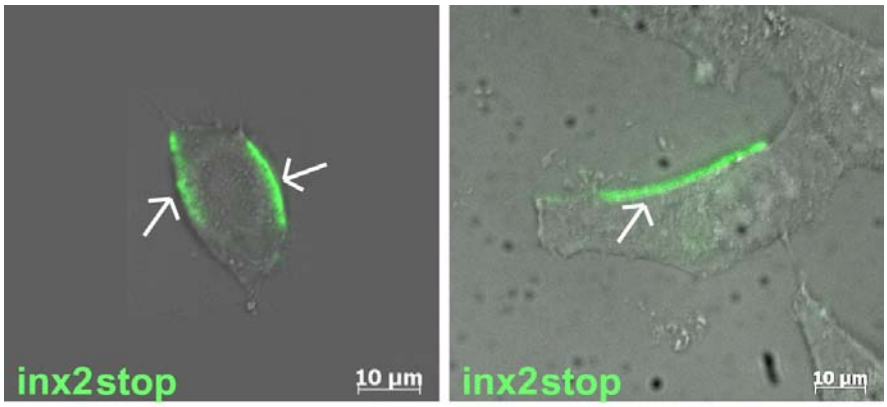

Fig. 4-29 Expression of inx2stop in HeLa cells results plaque like structures at plasma membrane of single cells. Cells were transfected with pMJinx2stop and fixed 26 h later following immunofluorescent staining of innexin2 (green). Membrane localisation of innexin2 arranged as plaque like structure in single cells is a frequent finding. DIC was used to assess membrane-localisation.

Together, expression analyses of innexin2 in HeLa cells indicate, that innexin2 forms gap junction typical plaque like structures between neighbouring cells to a low extent. These findings suggest the formation of homomeric, homotypic gap junctions and in vertebrate cells. In addition, observations of innexin2 localisation of at membranes of single cells, point to the formation of unopposed hemichannels in HeLa cells.

4.4.2 Innexin2 is integrated in plasma membranes of transfected HeLa cells

Various experiments using immunofluorescent staining combined to differential interference contrast (DIC) microscopy point to the localisation of innexin2 positive gap junction plaques at plasma membranes of transiently transfected HeLa cells. To further confirm the membrane integration of innexin2, a different approach was used to study membrane localisation of proteins.

The plasma membrane sheet assay is a unique tool for studies of the organisation and function of membrane proteins using microscopic methods (Lang et al., 2003). An additional advantage of this method is the fact that the amount of transfected cells needed for analysis is very low in comparison to the amount needed for subcellular fractionation approaches and that it can be carried out quickly.

With the help of a short ultrasound pulse cells, cultured on coverslips, can be “unroofed”, meaning, only the basal membranes remain on the coverslip that can be fixed and stained with antibodies against the protein of interest (Fig. 4-30; Lang, 2003). The generated

membrane sheets are co-stained with a probe against lipids of the inner plasma membrane leaflet (TMA/DPH).

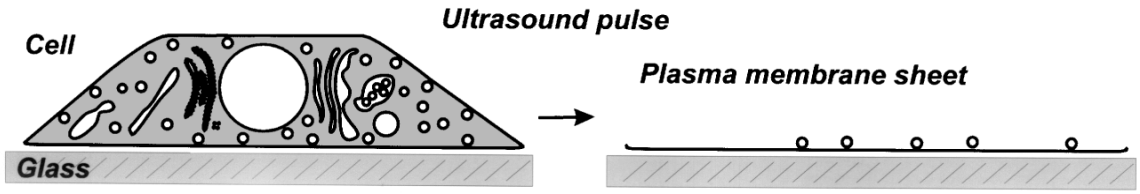

Fig. 4-30 Scheme of plasma membrane sheet preparations from cultured cells. (Modified after Lang, 2003).

Analysis of membrane sheets produced from innexin2 and innexin3 transfected HeLa cells (Fig. 4-31 A-C) verified the observation of former experiments that innexins are inserted in the plasma membrane of those cells whereas control stainings of untransfected cells did not show a signal (Fig. 4-31 D).

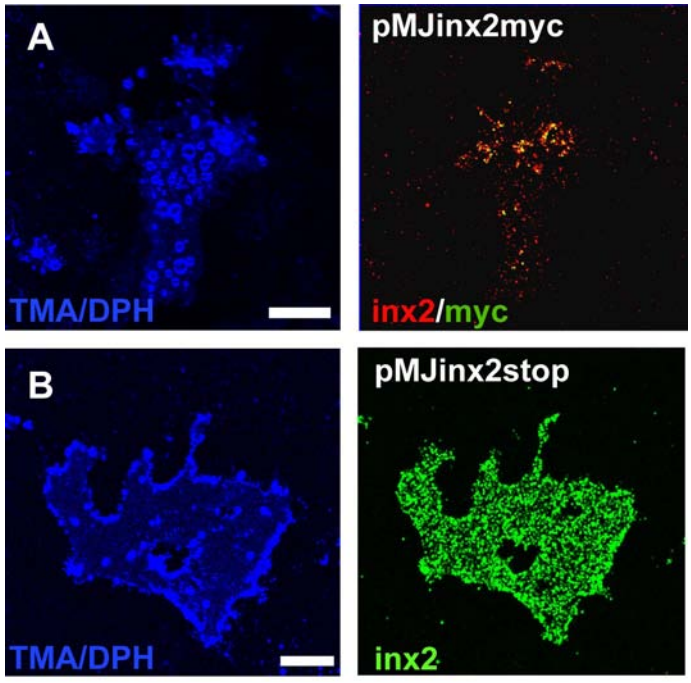

Fig. 4-31a Detection of innexin2 in plasma membrane sheets of transfected HeLa cells 28 h post transfection. Detection of innexin2 (red) and myc (green) showed co-localisation of both antibodies after transfection of pMJinx2myc (**A**), detection of innexin2 (green) after transfection of pMJinx2stop (**B**).

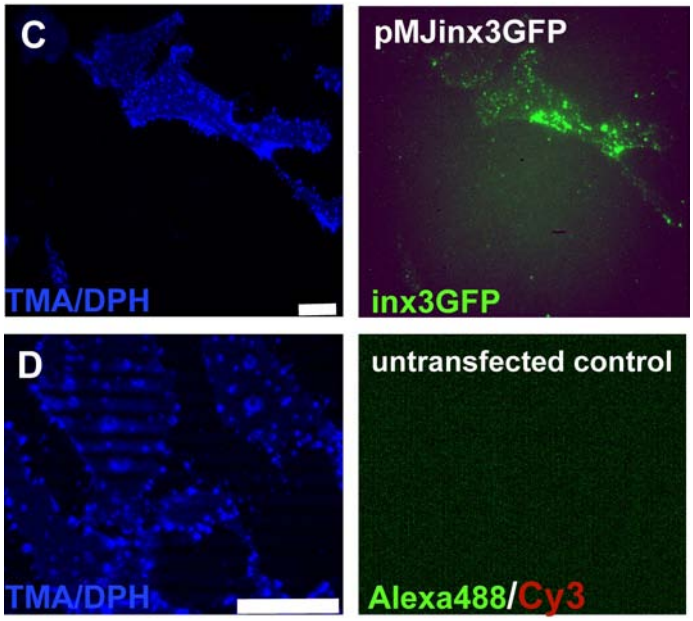

Fig. 4-31b Detection of innexin3 in plasma membrane sheets of transfected HeLa cells 28 h post transfection. Detection of inx3GFP with an anti-GFP antibody in membrane sheets (**C**), untransfected controls stained with secondary antibodies used in A-C showed no unspecific signals (**D**), scale: 10 µm.

Together, these data provide evidence for membrane insertion and plaque formation of invertebrate innexins in vertebrate cells, which do not express connexins, indicating a conserved mechanism of plaque formation between adjacent cells between analogous gap junction proteins.

4.4.3 Oligomerisation of innexin2 in HeLa cells

Assembled innexin2 hemichannels acquire TX-1000 insolubility upon plasma membrane integration and plaque formation in *Drosophila* as shown in section 4.1. The observation of innexin2 plaque formation in transfected HeLa cells therefore also lead to the biochemical investigation of innexin2 in extracts of transfected HeLa cells with regards to oligomerisation and the acquirement of TX-100 insolubility.

TX-100 solubilisation was carried out with extracts from transfected HeLa cells, to determine whether innexin2 is found in the TX-100 insoluble fraction upon plasma membrane integration. Fig. 4-32 shows that a significant amount of innexin2 protein was detected in the TX-100 insoluble fraction, revealing a faint band of higher molecular weight in contrast to the total lysate and the TX-100 soluble fraction, where both forms are detected.

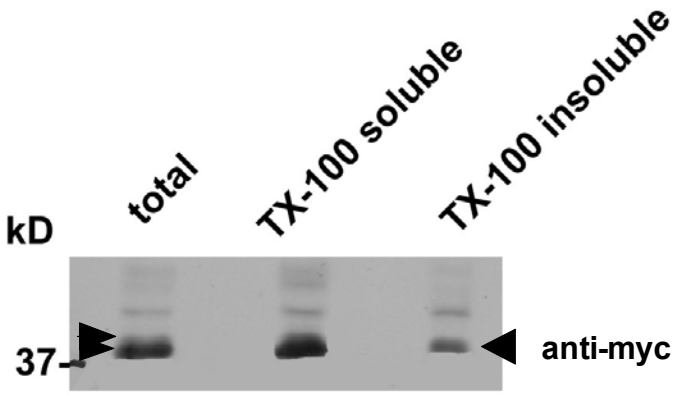

Fig. 4-32 Innexin2-myc acquires TX-100 insolubility in HeLa cells. TX-100 solubilisation of extracts from of HeLa cells transfected with innexin2-myc, results in the detection of innexin2-myc in the TX-100 insoluble fraction.

To determine whether innexin2 oligomerisation occurs in innexin2-myc transfected HeLa cells, velocity sedimentation of TX-100 soluble extracts of innexin2-myc transfected cells was performed. Fractions of 5 - 20% sucrose gradient were analysed in the same way as done for the analysis of oligomerisation in embryos in section 4.1.3.

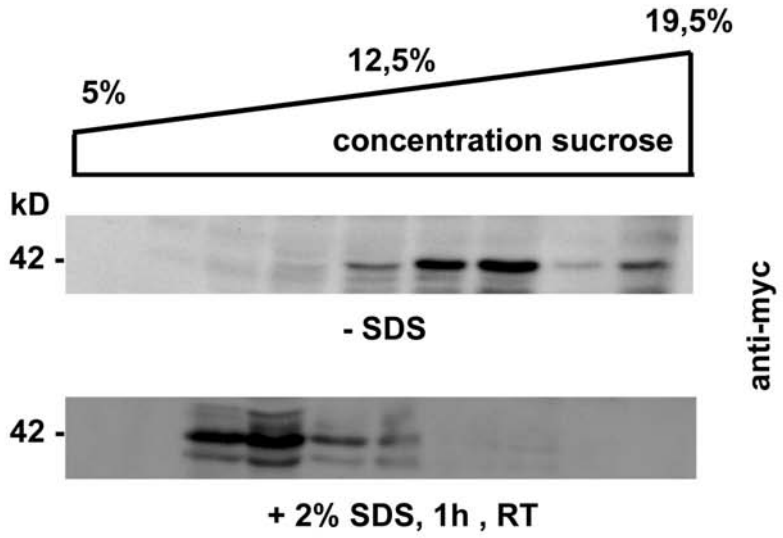

Fig. 4-33 Innexin2 oligomerises in HeLa cells. The status of oligomerisation of innexin2 in vertebrate cells was detrmined by velocity sedimentation on 5 - 20% (w/v) sucrose gradients, resulting in the detection of innexin2 protein in high percentage sucrose fractions. Addition of SDS prior velocity sedimentation shifts innexin2 detection to low percentage sucrose fractions, indicating the decay of oligomeric assemblies.

Figure 4-33 shows that innexin2 was detected within fractions that had been designated to contain hexameric proteins after fractionation of TX-100 soluble extracts from innexin2-myc

transfected cells by continuous sucrose gradients and Western blot analysis. Treatment of TX-100 solubilised extracts with 2% SDS prior velocity sedimentation, led to a shift of innexin2 distribution to lower percent sucrose fractions, suggesting that innexin2 oligomerised in HeLa cells to some extent. It is noteworthy, that under non-denaturing conditions (- SDS) most of the protein is detected in higher percentage sucrose fractions from 12.5-19.5% sucrose, indicating that monomers seem to be directly assembled into oligomers in HeLa cells.

Together, data collected from expression analyses by immunohistochemical stainings of innexin2 and innexin3 in transfected HeLa cells revealed that innexins are able to traffic to the plasma membrane of HeLa cells and to form gap junction typical plaque like structures between adjacent cells. Initial biochemical approaches also point to the ability of innexin2 to oligomerise and to integrate into the plasma membrane, which mediates TX-100 insolubility.

4.5 Cross regulation of innexin2 and major signalling components during organogenesis of the posterior foregut

Investigations on the assembly and transport of *Drosophila* innexin2 containing gap junction hemichannels revealed that oligomerisation of hexameric innexons, which are assembled and transported to the plasma membrane along the secretory pathway via microtubules, is a crucial process for gap junction plaque formation.

The functional role of thus assembled gap junctions during organogenesis was addressed in the second part of this thesis. Analyses on the physiological impact of innexin2 containing gap junctions during development concentrated on the posterior foregut of *Drosophila* embryos. The posterior foregut constitutes in general a center of cell signalling and morphogenetic movements (Grapin-Botton and Melton, 2000), where cellular boundaries are created, resulting in the development of gut accessory organs (Ramalho-Santo et al., 2000). The creation of cellular boundaries in this compartment of the gut primordium enables the morphogenesis of gut accessory organs. The accessory organ that is derived from the posterior foregut in *Drosophila* is the proventriculus, a valve like structure that serves as a regulator for the food passage from the fore-into the midgut in larvae and adults. It develops during early embryogenesis at the junction of the ectodermal foregut and the endodermal anterior midgut primordia (Bauer et al., 2004).

The proventriculus organ is formed by subsequent foldings of ecto- and endodermal tissue layers resulting in a cardia shaped organ in the end of embryogenesis at stage 17. It starts

with an evagination (at stage 11) and constriction (at stage 13) of the ectodermal tissue layer followed by an inward movement of the ectoderm into the endoderm in stage 15 (Fig. 4-34). The establishment of two rows of cells, the anterior and posterior boundary cells have been found to be crucial for the morphogenetic endo- and ectodermal movements (Fuss et al., 2004).

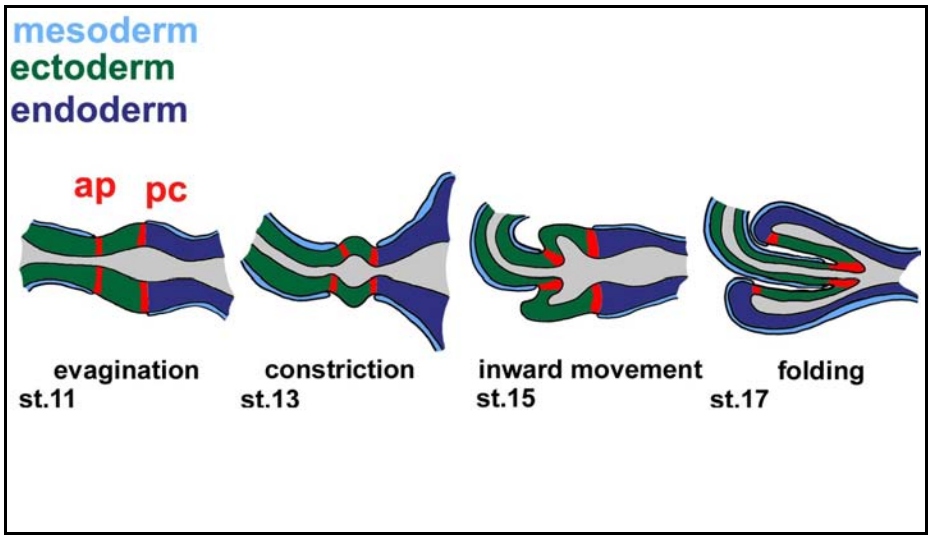

Fig. 4-34 Scheme of proventriculus morphogenesis. The proventriculus is formed by subsequent foldings of ecto- (green) and endodermal (violet) tissue layers resulting in a cardia shaped organ in the end of embryogenesis (st. 17) starting with evagination (at st. 11) and constriction (at st. 13) of the ectodermal tissue layer following inward movement of the ectoderm into the endoderm (st. 15). The anterior (ac) and posterior cells (pc) are labelled in red. (Modified after Lechner et al., 2007)

Development of the proventriculus has been studied extensively in our laboratory over the last years. Various studies identified different signalling pathways that take part in the morphogenetic movements during proventricular development. All mutants of different signalling proteins isolated, revealed a similar phenotype. It manifests itself by the failure of inward movement and folding of the ectodermal proventricular cells (Lechner et al., 2007; Fuss et al., 1998, 2004; Josten et al., 2004; Pankratz and Hoch, 1995).

In the context of morphogenetic movements, the importance of the above mentioned two rows of cells in the ectodermal tissue layer, the anterior and posterior boundary cells, were studied. It could be shown that the specification of both cell rows is dependent on the activity of the juxtacrine Notch signalling pathway, which is activated by its ligands Delta or serrate, in cooperation with the JAK/STAT signal transduction cascade (Fuss et al., 2004). The interplay of both pathways was shown to be crucial for the expression of the cytoskeleton crosslinking protein short stop, a member of the spectraplakin protein family. (Gergory and Brown 1998; Röper, 2002). Short stop stabilises the cytoskeleton in the posterior boundary

cells to provide a stiffness function essential for the invagination of the anterior cells to invaginate. (Fuss et al., 2004; Josten et al., 2004).

Furthermore, the expression of wingless, as the activator of the paracrine signalling Wnt/wingless pathway was shown to be functionally required for cell migration of proventricular cells. Wingless protein was shown to be initially expressed at the site of ectodermal constriction at stage 13. Later on, wingless expression is detected in two more defined domains, in the anterior and posterior boundary cells (Pankratz and Hoch, 1995, Fuss and Hoch, 1998, Bauer et al., 2004)

Another study revealed that hedgehog expression, ligand of the well conserved hedgehog signalling pathway, is required for the expression of Notch and wingless in the anterior boundary cells (Lechner et al., 2007; Josten, PhD thesis). It could be shown in this thesis that hedgehog protein is expressed in wild type from early to late embryonic stages in a broad expression domain in the posterior foregut. Hedgehog expression covers cells of the developing esophagus and all the ectodermal cells of the proventriculus primordium, which invaginate during formation of the multi layered organ (Fig. 4-35).

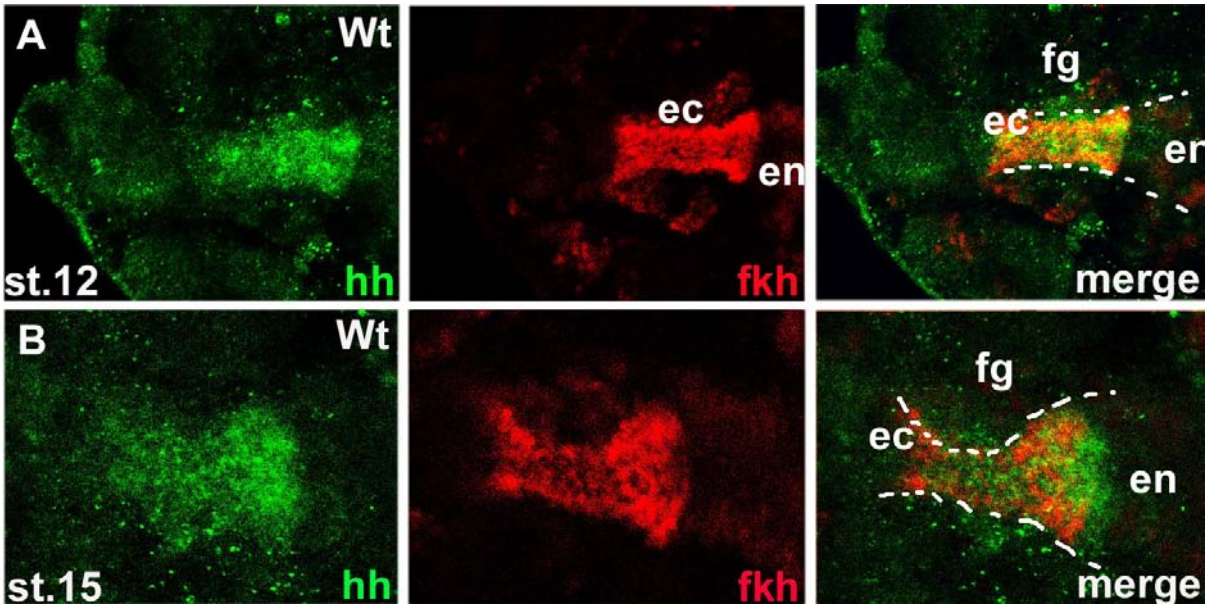

Fig. 4-35 Hedgehog is expressed in ectodermal cells of the embryonic foregut. Hedgehog protein staining (green) overlaps with forkhead (red), an ectodermal marker, of *Drosophila* in early (**A**) and late (**B**) stages of proventriculus development. (ec, ectoderm; en, endoderm; fg, foregut). (Modified after Lechner et al., 2007).

Analyses of *hedgehog* mutants revealed a specific loss of wingless expression in the anterior boundary cells, whereas the posterior wingless domain was not affected (Lechner et al., 2007; Josten, PhD thesis). This is consistent with previous findings that temperature sensitive *wingless* mutants show an invagination defect of the ectodermal proventricular cells

(Pankratz and Hoch, 1995), which is very similar to the phenotype observed in *hedgehog* mutants.

Recently, a mutant of the gap junction forming protein innexin2 was identified that also showed severe defects in proventriculus organogenesis (Bauer et al., 2004). In the *innexin2* mutant it was observed that food could not be transported into the midgut, resulting in an engorged oesophagus. Therefore, the innexin2 mutant was named "*krop*f".

The fact that *innexin2* was shown to be a direct target gene of wingless signalling (Bauer et al., 2004) and that its expression was missing in *hedgehog* mutants (Josten, PhD thesis), suggested a dependency of gap junctional communication, paracrine and juxtacrine signalling pathways. This dependency was analysed in *kropf* mutants to understand the impact of gap junctional communication during proventriculus development.

Altogether, accumulating evidence points to the existence of a complex signalling and cell communication network that is involved in programming the morphogenetic movements during proventriculus development (Fig. 4-36).

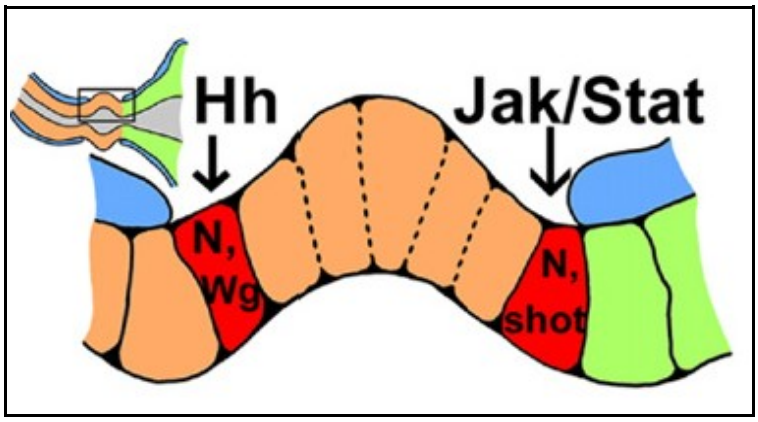

Fig. 4-36 Schematic representation of the hedgehog and JAK/STAT pathways controlling ac and pc allocation and proventriculus morphogenesis. Hedgehog is required for the expression of Notch target genes and of wingless in the anterior boundary cells, whereas JAK/STAT signalling induces the expression of Notch target genes such as short stop in the posterior boundary cells. (after Lechner et al., 2007)

4.5.1 Innexin2 is expressed in the ecto- and endodermal part of the developing proventriculus primordium

The observation that *kropf* mutants showed proventricular defects, prompted us to have a closer look at innexin2 expression in the proventriculus and to determine the subcellular distribution of innexin2 in the different tissue layers that build the folded organ.

Using fluorescent *in situ* hybridisation and antibody staining, *innexin2 m*RNA and protein expression was monitored in the developing proventriculus to assess the distribution of

innexin2 within the two different tissue layers that are involved in folding processes of the proventriculus organ. Detection of *innexin2 m*RNA with an *innexin2* specific antisense probe showed expression in both, the ectodermal and endodermal tissue layer. Co-immunostaining with anti-forkhead antibody marks the ectodermal tissue layer (Fig. 4-37 A). Protein co-staining with the fasciclin II as membrane marker also pointed to ubiquitous expression of innexin2 protein in the two germ layers (Fig. 4-37 B).

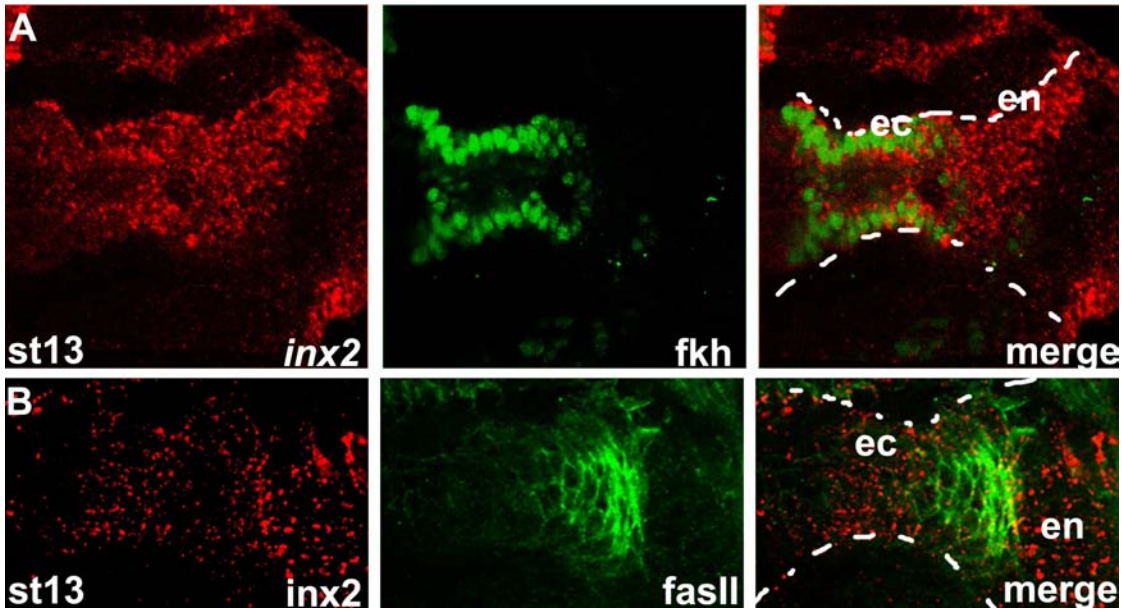

Fig. 4-37 *Innexin2 m*RNA and protein is expressed in both the ectodermal and endodermal tissue layers of the proventriculus. Fluorescent *in situ* hybridisation combined with antibody staining of st. 13 proventriculi showed that *innexin2 m*RNA (**A**), (red), is expressed in both the ectodermal and endodermal tissue layer co-stained with the ectodermal marker forkhead (green). Innexin2 protein was also found in both tissue layers (**B**), co-stained with fasciclin II (green) as membrane marker (**en**, endoderm **ec**, ectoderm).

Together, these results indicate that innexin2 expression might be crucial for intercellular communication within the endo- and ectodermal tissue layer of the proventriculus primordium.

Earlier findings revealed that *hedgehog* mutants lack, in addition to their invagination defect, wingless and innexin2 expression in the proventricular primordium. In *hedgehog* mutants, innexin2 expression is specifically lost in the proventriculus whereas it is still present in the salivary glands of the embryo (Lechner et al., 2007; F.Josten, PhD thesis). In addition, it was found that *innexin2* is a direct target gene of the wingless signalling pathway (Bauer et al., 2004). Together, previous results pointed to direct dependency of wingless and innexin2 expression on hedgehog expression. To proof this findings, a rescue experiment was performed to investigate the observed cross regulatory effects. In this experiment, the expression of *innexin2* should be reestablished by the over expression of wingless protein,

activating the wingless signalling cascade that regulates *innexin2* expression.

In fact, expression of *innexin2* transcripts could be rescued by overexpression of wingless, using the Gal4/UAS system in the *hedgehog* mutant background. Wingless protein expression was monitored by an anti-hemaglutinin-tag (HA) antibody recognising the overexpressed wingless-HA fusion protein. On the one hand, the obtained result argues for innexin2 being a downstream target of wingless and hedgehog signalling. On the other hand, it revealed that expression of wingless and *innexin2* in the *hedgehog* mutant background abolished in addition the invagination phenotype of *hedgehog* mutants (Fig. 4-38), resulting in a properly folded organ in these embryos (inset in Fig. 4-38). The above data clearly implicate that hedgehog activates wingless, which in turn regulates innexin2 expression.

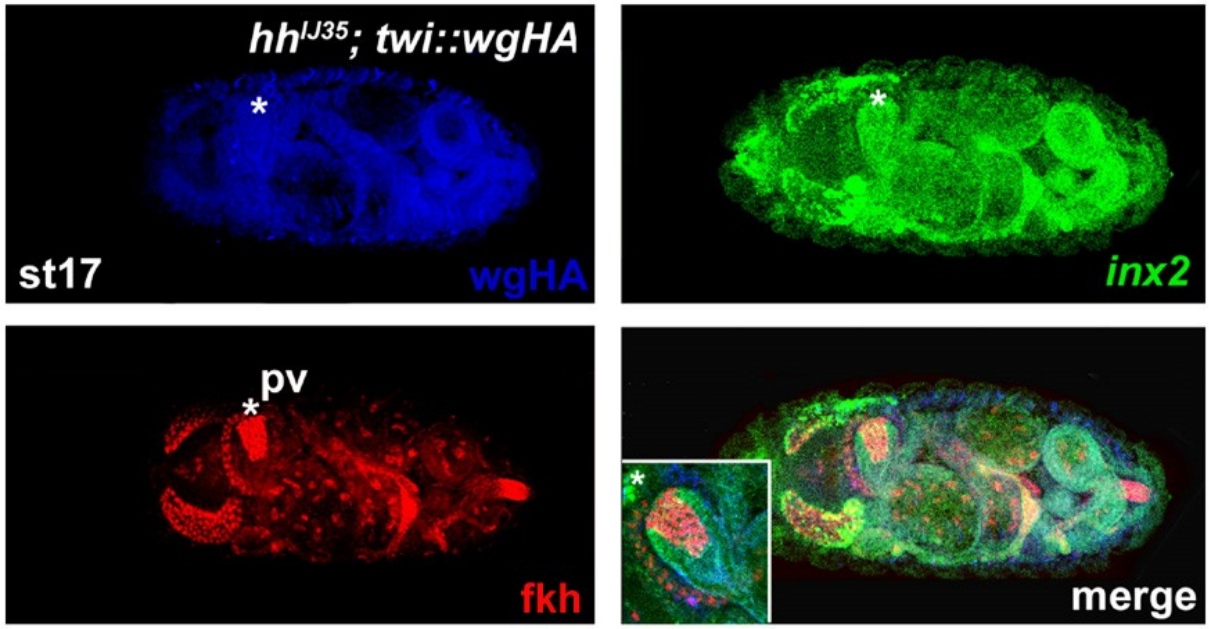

Fig. 4-38 *Innexin2 m*RNA expression is rescued by overexpression of wingless protein in *hedgehog* mutants. Fluorescence *in situ* hybridisation of *innexin2 m*RNA (green) combined with antibody staining against wgHA (blue) and Fkh (red). Inset in merged picture shows magnification of the invaginated proventriculus. The asterisk (*) marks the proventriculus.

4.5.2 *Kropf and hedgehog* mutants show reduced cell communication between proventricular cells

Cell-cell communication is a prerequisite for the spatial and temporal coordination of patterning and morphogenesis. Gap junctions play an important role here, enabling the direct communication between adjacent cells within a tissue or organ. The analysis of coupling between cells of an organ or tissue is a key experiment to assay gap junctional communication. Injection of the fluorescent dye Lucifer yellow into cells that express gap

junctions has become a versatile tool to study intercellular communication between coupled cells (Weir et al., 1982; Huang et al., 2005). In *hedgehog* mutants, innexin2 expression was specifically lost in the proventriculus, however it was still detectable in the salivary glands of the embryo. Therefore, we analysed whether innexin2 dependent gap junction communication was affected in *hedgehog* mutants by using the described coupling assay. Consistent with the above data, which showed a clear dependency of wingless and innexin2 on hedgehog expression, dye diffusion was reduced between cells of the proventriculus primordium of *kropf and hedgehog* mutants (F. Josten, PhD thesis). This pointed to a defective communication between cells (Fig. 4-38; Lechner et al., 2007), suggesting that gap junctional communication is disturbed in the absence of innexin2 protein. In summary, these data provide evidence that hedgehog activates *wingless* and *innexin2* expression and affects thereby also the innexin2 dependent gap junction activity. These data are also in good agreement with the fact that *hedgehog, wingless* or *innexin2* mutants display very similar invagination defects.

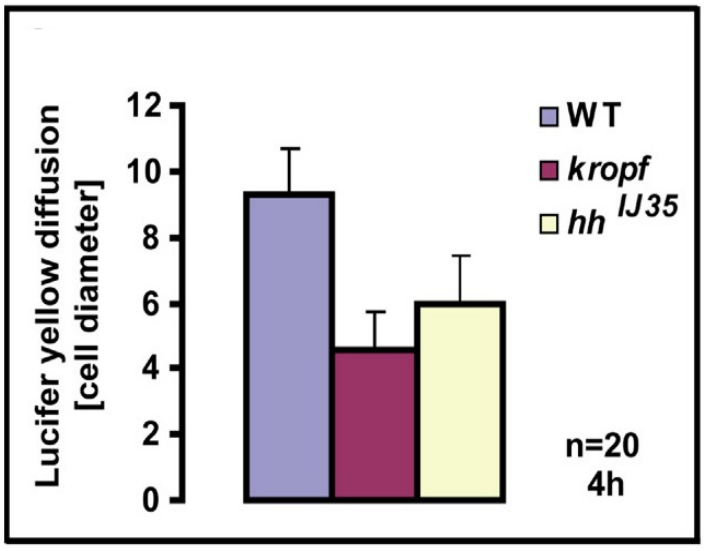

Fig. 4-39 Statistic of reduced dye coupling between proventricular cells of wild type a *kropf* and *hedgehog* mutants. Lucifer yellow (LY) diffusion through wild-type proventricular (blue bar) cells compared to diffusion through proventricular cells of *kropf* mutants (red bar) and *hedgehog* mutants (yellow bar) 4 h after injection. Dye diffusion was strongly decreased in proventriculi of both mutants. (After Lechner et al., 2007).

4.5.3 Innexin2-dependent alterations of *hedgehog*, *wingless,* and *Delta* transcription in the proventriculus primordium

Next, we wanted to understand whether innexin2 gap junctional communication is, in turn, crucial for the expression of major signalling molecules involved in proventriculus

morphogenesis. A series of loss and gain of function experiments using innexin2 were performed and the *m*RNA expression levels of *hedgehog*, *wingless* and *Delta*, encoding the ligand for the Notch receptor, were investigated by *in situ* hybridisation and quantitative real time PCR analyses. In this context, previously performed immunofluorescent stainings and *m*RNA *in situ* hybridisation *in kropf* mutants and in embryos overexpressing innexin2 have shown changes in protein or *m*RNA expression levels of *wingless*, *Delta*, and *hedgehog*. These was already first evidence for an innexin2 dependent regulation of important signalling molecules (Lechner et al., 2007, PhD thesis F. Josten).

For quantitative real time PCR (*q*RT-PCR) analyses, *m*RNA from stage 13 embryos, was isolated. At this stage of embryogenesis the invagination of ectodermal tissue occurs (compare to figure 4-34). *q*RT-PCR analyses and normalisation of the obtained values to the housekeeping gene expressions of *actin* and *ribosomal protein*, revealed that upon loss of innexin2 expression in *kropf* mutants, *m*RNA levels of *Delta (Dl)*, *hedgehog (hh)* and *wingless (wg)* dropped to various extents compared to the wild type control (Fig. 4-40 A).

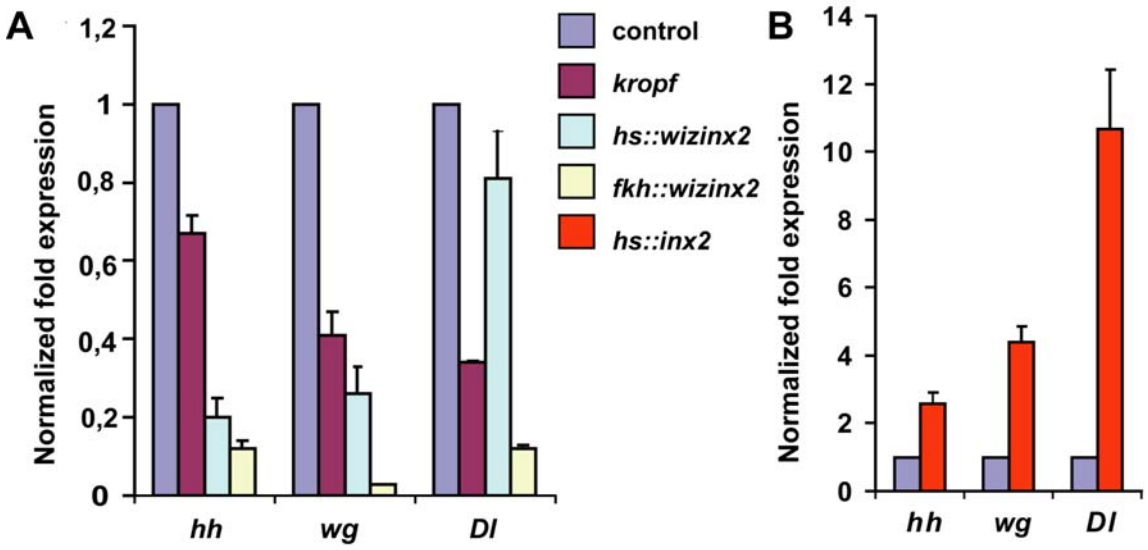

Fig. 4-40 H*edgehog*, *wingless and Delta m*RNA levels are altered upon innexin2 gain and loss of function experiments. Quantitative real-time PCR demonstrating the transcriptional regulation of *hedgehog* (*hh*), wingless (*wg*) and Delta (*Dl*) in response to innexin2 activity (**A**). Decreased expression of *hh*, *wg* and *Dl m*RNA levels is observed in *kropf* mutants as well as in innexin2 RNAi knock downs using the UAS-*WIZinx2* in combination with *hs*-Gal4 or *fkh*-Gal4 driver lines. In contrast, overexpression of innexin2 by using UAS-*innexin2* in combination with *hs*-Gal4 results in enhanced *Dl*, *wg* and *hh m*RNA levels, as compared to the control (**B**).

This result was confirmed by innexin2 RNAi knock down experiments. Down regulation of *innexin2* transcripts was accomplished by crossing a innexin2 RNAi fly line (UAS-*WIZinx2)* to

a *heat shock*-inducible Gal4 driver line (*hs*-Gal). The heat shock was applied for 30 min at 37°C, thereby activating innexin2 dsRNA expression that targets innexin2 expression. The following analysis of *m*RNA expression levels 2.5 h after the heat shock resulted again in a severe knock down of *hedgehog* (5 - fold reduction) and *wingless* (4 - fold reduction) *m*RNA expression, whereas *Delta* expression was only reduced 1.25 - fold. Usage of a *fkh*-Gal4 driver line, which drives the RNAi mediated knock down of *innexin2* constitutively in most of the embryonic tissues, showed an even more dramatic effect on all three genes. In contrast, overexpression of innexin2 using a heat shock driver line, resulted in increased levels of all three transcripts (Fig. 4-40 B). These experiments indicate that innexin2 expression is crucial for the expression of major signalling components showing phenotypes, similar to *kropf* mutants and validate previous findings which showed an innexin2 dependent regulation of gene expression. As controls wild type flies were crossed to the appropriate driver lines that were exposed to identical experimental procedures.

Consistently with these strong read outs from real time PCR analyses, whole mount *in situ* hybridisations of *hedgehog* *m*RNA in *kropf* mutants showed an overall reduction of transcripts as compared to control embryos. The expression of *orthopedia* (otp), which was used as intestinal staining control was not altered (Fig. 4-41).

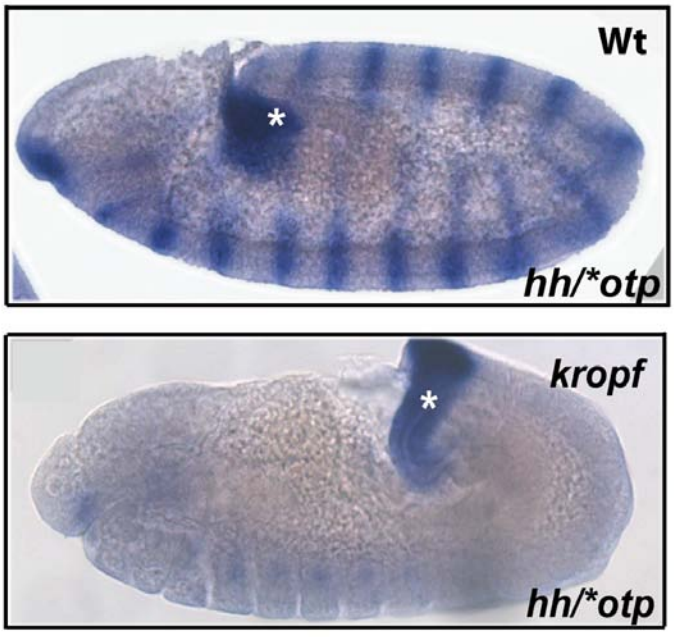

Fig. 4-41 *Kropf* mutant embryos show a reduced expression of *hedgehog* expression. *In situ* hybridisation of wild type and *kropf* mutant embryos using antisense probes against *hh* and the hindgut marker *otp*. *Otp*, marked with asterisk (*), served as a staining control. A significant reduction of *hh* expression in *kropf* mutants is visible.

4.5.4 Importance of the innexin2 C-terminus for the transcriptional regulation of *wingless*, *hedgehog*, and *Delta* transcripts

A next approach aimed on understanding whether a special domain of the innexin2 protein might be involved in the observed effects of innexin2 on *hedgehog*, *wingless* and *Delta* *m*RNA expression (Fig. 4-42). Evidence for the importance of the C-terminal domain of innexin2 in transcriptional regulation derive from motif-predictions *in silico*, where a nuclear receptor box motif is predicted to be contained within the terminal domain (Fig. 4-42). Proteins that exhibit this motif in their amino acid sequence have been shown to bind nuclear receptors, which in turn regulate gene expression (Savkur et al.,. 2004, Mahajan and Samuels, 2005).

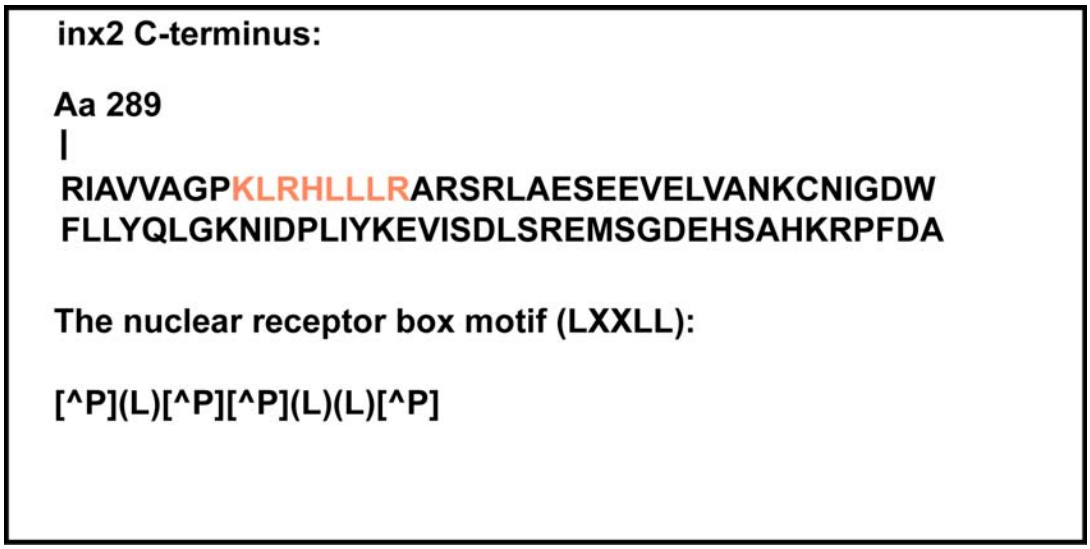

Fig. 4-42 The innexin2 C-terminus contains a nuclear receptor box motif. The nuclear receptor box motif (LXXLL) confers binding to nuclear receptors, which modulate gene expression. Prediction made by http://elm.eu.org/.

This prediction lead to the overexpression of a transgene that contain a innexin2 C-terminal deletion (see appendix) with a heat shock inducible driver line. The truncated transgene misses amino acids 301-367 of the innexin2 protein. The result of this experiment was a similar downregulation of all three transcript levels as shown for the *kropf* mutant in figure 4-40. This indicates the necessity of the full length protein expression or the C-terminal part of innexin2 itself for proper target gene expression.

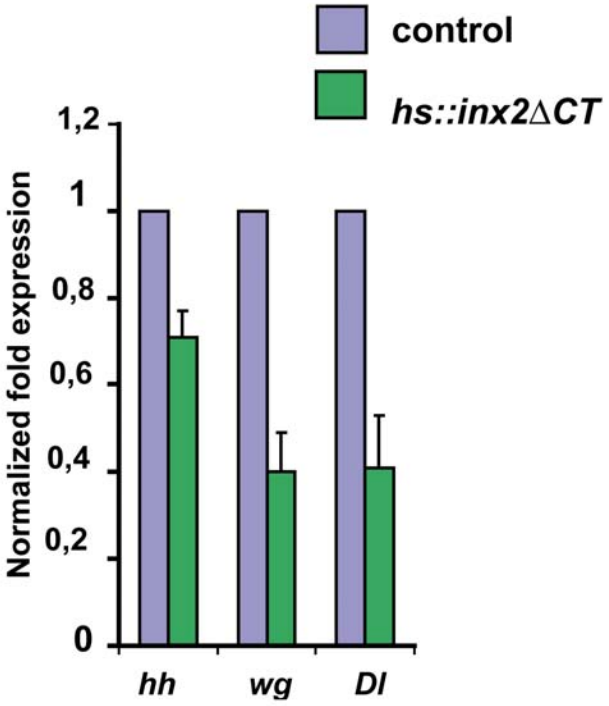

Fig. 4-43 Transcript levels of *hh*, *wg*, and *Dl* drop upon overexpression of an innexin2 C-terminal truncated transgene. Overexpression of innexin2ΔCT containing a C-terminal deletion (innexin2 aa 301–367) with a *hs*-Gal4 driver line results in a similar reduction of *hh*, *wg* and *Dl* *m*RNAs, as observed in *kropf* mutants (compare to Fig. 4-26).

4.5.5 Evidence for the existence of an innexin2 C-terminal fragment that is directly or indirectly involved gene expression

Observations in cell culture point to the existence of an innexin2 C-terminal fragment in addition to the full length protein that might be involved in the regulation of transcription. Co-immunoprecipitation experiments and Western blotting analyses in cell culture using SL2-cells, where overexpression of C-terminal GFP tagged innexin2 resulted in a second product which corresponds to the size of a C-terminal fragment fused to GFP (Fig. 4-44).

The detected fragment exhibits a molecular weight of 37 kD, indicating that the innexin2 C-terminal fragment has a size of approximately 10 kD, whereas GFP contributes with a size of 27 kD. The innexin2 cytoplasmic C-terminus has a predicted molecular weight of 9 kD, indicating that a part of the fourth transmembrane domain must be contained in the fragment in addition.

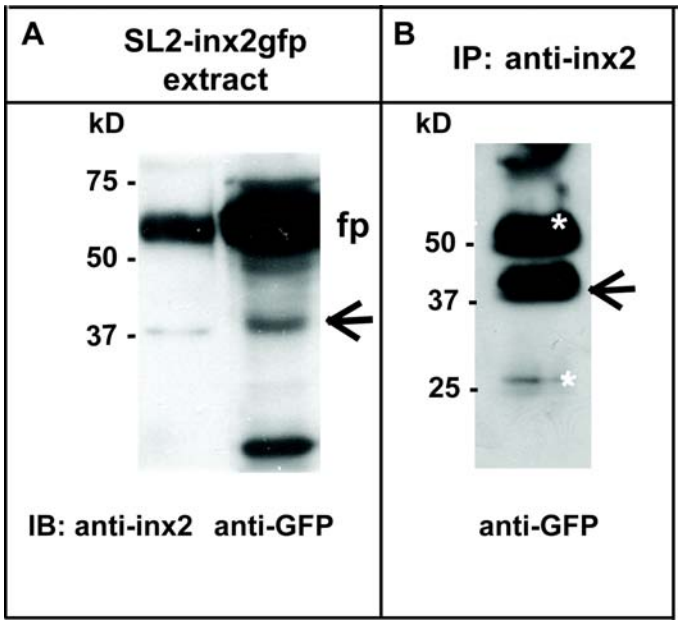

Fig. 4-44 Detection of a C-terminal fragment of innexin2 in SL2 cells. Western Blot analysis of extracts from SL2 cells, stably expressing inx2gfp fusion protein (fp) resulted in the detection of an additional protein fragment that is fused to GFP with a size of 37 kD (**A**). The observed fragment was also precipitated with the innexin2 antibody and detected with the anti-GFP antibody. IgG chains are marked by asterisk (*; **B**).

This finding led to the hypothesis that the C-terminal domain of innexin2 might be directly or indirectly involved in the transcriptional regulation of the mentioned target genes.

5 Discussion

5.1 Analogous gap junction proteins show common features

Vertebrate gap junction channels are formed by two opposing hemichannels, each consisting of six connexin protein subunits. One hemichannel can be either formed by six connexin proteins of the same isoform or by connexin proteins of different isoforms. Hemichannels are termed homomeric when they are made up by one isoform only, heteromeric when more then one connexin isoform is involved in the composition of one half channel. The existence of 20 connexin isoform in mouse and 21 isoforms in humans opens the possibility for a variety of resulting hemichannel assemblies. This diversity is limited by different expression patterns of connexin isoforms and their different abilities to oligomerise with each other. Whereas connexin43 is the most abundant connexin in mice and its expression is widely distributed throughout the organism, the expression of other connexins like mouse connexin 46 is limited to the lens (Willecke at al., 2002).

Pannexins, a second group of gap channel forming proteins, that have been isolated initially from mice several years ago, are found to assemble also into hexameric hemichannels as shown by Boassa and colleagues (Boassa et al., 2007), despite of lacking sequence homology to the connexins. To date, this family consists of three members in rodents and two in humans (Litvin et al., 2006). The potential of pannexins in forming intercellular gap junction channels was shown by Bruzzone and colleagues, who co-expressed pannexin 1 and 2 in paired oocytes derived from *Xenopus* and found that they form functional gap junction channels (Bruzzone et al., 2003). However, a functional gap junction channel was not formed between pannexin1 and pannexin3 as investigated by Penuela and coworkers (Penuela et al., 2007). In fact, the finding that pannexins become glycosylated could argue for an additional function of those proteins, namely a function in the construction of functional hemichannels at the plasma membrane from cells. The existence of functional unopposed hemichannels became a highly debated topic in both connexin and pannexin research. Meanwhile a number of studies claim the existence of functional hemichannels that have additional functions to their conventional role as one half channel the formation of intercellular channels (Spray et al., 2006).

A third group of gap junction proteins are the invertebrate innexins. An interesting feature of innexins is that parts of their amino acid sequence are conserved to the sequence of vertebrate pannexins. The region of strongest similarity between vertebrate pannexin proteins and invertebrate innexin proteins includes the first two transmembrane domains and

the intervening stretch of amino acids (Baranova et al., 2004).

In *Drosophila* eight members of the innexin protein family, sharing the same protein topology despite the lack of sequence homology to connexins, are known to form gap junctions. Their expression has been found in overlapping patterns in various tissues and organs. Furthermore, on the genetic level, some of the *Drosophila* innexin encoding genes are found organised in clusters on one chromosomal region, which may indicate a common expression control. The phenomenon of chromosomal clustering has been also shown for connexins resulting in overlapping expression patterns of the clustered isoforms (Fig. 5-1; Bauer et al., 2005; Willecke et al., 2002).

Despite of the initial identification of gap junctional structures in invertebrates, no biochemical data existed to date about the composition and nature of gap junction channel subcomponents. So far, evidence of a conserved protein topology among innexins, connexins and pannexins led to the assumption, that independently of species related differences on the sequence levels, the construction mechanism of gap junction hemichannels is the same.

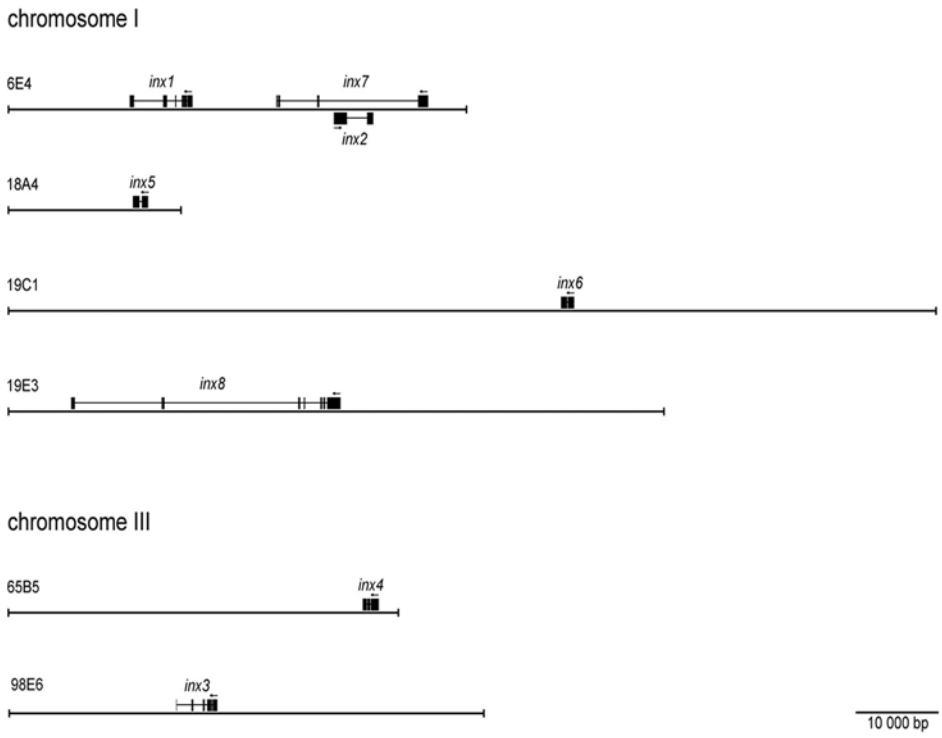

Fig. 5-1 Overview of the clustered organisation of innexin genes in the *Drosophila* genome.

A common feature of genes that encode for gap junction proteins is a clustered genomic organisation on different chromosomes. Genes encoding for *Drosophila* gap junction proteins inx1, inx2 and inx7 are arranged as a cluster on the chromosomal region 6E4 of chromosome I, whereas inx5, inx6 and inx8 are all located on chromosome I, but with a greater distance to each other. The remaining innexin isoforms inx3 and inx4 are located on chromosome III (65B5-98E6). (After Bauer et al., 2005).

5.2 Innexin2 is part of hexameric innexons

As already mentioned in the previous paragraph, is the predicted overall protein structure of innexin proteins comparable to the structures of connexins and pannexins. All three protein families exhibit four transmembrane domains, two extracellular loops with conserved cysteine residues and three cytoplasmic located domains C-and N-termini as well as a cytoplasmic loop. In this thesis hemichannel assembly of innexin2 containing hemichannels was analysed using different biochemical approaches.

The oligomeric structure of innexin2 containing hemichannels was studied, first by analyses of native protein extracts from embryos (section 4.1.1). Basic native PAGE was carried out to investigate the size of innexin hemichannels after TX-100 solubilisation. This method is used to separate oligomeric proteins with an isoelectric point (pI) < 7.0. The mobility of proteins in native gels depends on both, the protein charge and its hydrodynamic size. (Lebendiker et al., 2000).

Separation of embryonic protein lysates by basic native PAGE revealed the presence one major signal at around 250 kD as determined by the molecular marker catalase having the size of 250 kD (Fig. 4-2). The size of the detected oligomer was in line with the size of hexameric innexin2 containing structures and was termed innexon according to the hexameric hemichannel of vertebrates, the connexon. This first result, addressing the oligomeric composition of *Drosophila* innexin hemichannels, led to the conclusion that the largest oligomeric assembly containing innexin2 detected in 6% polyacrylamide gels displays the size of a hexamer (all innexin proteins exhibit a molecular weight in a range between 42 and 55 kD, with 42.49 kD for innexin2 as the smallest innexin isoform) This is in accordance to earlier studies of gap junction channels in crayfish done by Perrachia showing an electron-microsocopic picture of gap junction plaques detected in giant fibers (Perrachia, 1976) that clearly displays an hexagonal arrangement of gap junctions at the plasma membrane.

The question about the quality of the intermediate protein oligomers that are formed before the hexameric innexon status is reached, is unclear. Only chemical crosslinking experiments performed before (H. Lechner, diploma thesis) pointed to the existence of dimers as the smallest oligomeric subunit, suggesting a mechanism for the assembly of hexameric innexons that proceeds from monomers to dimers, tetramers and finally to hexamers. The issue of the oligomeric intermediate formation of connexins was addressed by several groups. Using *in vitro* oligomerisation studies they found dimers and tetramers as the most preferred intermediates (Ahmad et al., 2001). Other studies claimed the existence of trimeric and pentameric intermediates in addition (Diez et al., 1999). All observations concerning this question rely on results from cross-linking studies using different agents. Due to the ambiguity of these results the issue of intermediate formation was not addressed further and

is only mentioned here for sake of completeness.

Further experiments, for the separation of different innexin2 containing oligomers along continuous sucrose gradients using protocols by VanSlyke and Musil (VanSlyke and Musil, 2000), confirmed the existence of hexameric proteins that co-sedimented in fractions together with the molecular weight marker catalase, that has a size of 250 kD. In addition, the sedimentation behaviour of innexin2 in linear sucrose gradients, that exhibits a similar protein size to connexin43, was also related to hexameric connexin43 protein, sedimenting in 14% - 17% sucrose fractions, whereas monomers sedimented between 7-9% sucrose at chosen centrifugation conditions. Oligomerisation of innexin2 containing hemichannels was further verified by SDS treatments of TX-100 soluble fractions prior velocity sedimentation, an experiment that has already been performed before to validate the existence of connexin oligomers (Diez et al., 1999).

Treatments with different concentrations of SDS led to a clear decay of innexin2 containing hexameric assemblies in favor of an increased detection of monomeric innexin2 protein and intermediate oligomeric forms (Fig. 4-7).

Comparison of the oligomerisation results of innexin2 and connexin43, reveal only slight differences in the sedimentation behavior. These may result from experimental setup fluctuations such as the usage of different rotors where centrifugation speed had to be adjusted or temperature fluctuations during measurements of the sucrose concentration of the different fractions by refractometry.

Nevertheless, data obtained on the oligomerisation of innexin2 containing hemichannels point to comparable biochemical characteristics of *Drosophila* innexin2 and connexin43 that show similar molecular weights of 42.49 kD (innexin2) and 43 kD (connexin43).

Together, findings that innexin2 is part of a hexameric innexon as shown by usage of combined methods to study oligomeric proteins, suggest that the hexameric hemichannel structure of gap junction subunits is conserved among species despite the lack of sequence homology.

In addition to the biochemical investigation on the oligomerisation process of innexin2 containing hemichannels, further studies aimed on understanding the requirements for membrane integration of assembled innexons.

The finding that innexin2 as well as innexin3 need to undergo post translational modifications before acquirement of TX-100 insolubility and plasma membrane integration, is in good agreement with investigations of connexin43 and its acquirement of TX-100 insolubility (Musil and Goodenough, 1991). Phosphorylation had been shown to be the prerequisite for membrane integration of connexin43 and insolubility in 1% TX-100 at 4°C.

Studies on the post translational modification of innexin3 showed that the higher molecular weight protein band, which was detected as the only form of innexin3 in the TX-100 insoluble

fraction, could be diminished by treatment with the calf intestine alkaline phosphatase in favour of a slight increase of the lower innexin3 protein band. Such a clear result was not obtained for innexin2. Nonetheless, both proteins exhibit several putative phosphorylation sites, containing sites for serine, tyrosine and threonine (section 7.3) that might be crucial for membrane integration of the hexamer.

An additional post translational modification that could lead to the biochemical characteristic of insolubility of innexins in non-ionic detergents at chosen conditions might be also be the attachment of carbohydrate chains to the hexamer in the Golgi network. Another explanation for TX-100 insolubility could be in addition, the integration of hexamers into detergent resistant membranes, which are defined as microdomains, known commonly as lipid “rafts”. They are characterised by their resistance to solubilisation in cold nonionic detergents or to cold sodium carbonate extraction at high alkaline pH (Locke at al., 2005). Since rafts also selectively include and exclude specific proteins, rafts may also have functional relevance with respect to protein sorting of innexin hemichannels.

5.2.1 Innexin2 forms homomeric and heteromeric hemichannels

The existence of eight innexin isoforms in *Drosophila* as well *as* the occurrence of overlapping expression patterns of some family members point to the existence of various gap junction hemichannel assemblies.

The fact that innexin2 and innexin3 could be co-immunoprecipitated from whole oligomeric and dimeric fractions (11-13% sucrose) in addition, point to the existence of heteromeric gap junction hemichannels. This is in accordance with their overlapping expression patterns in *Drosophila* embryos, GST-pull downs and the finding that the usage of innexin2 specific aptamers inhibited innexin2 and inx3 C-terminal interactions (Lehmann et al., 2005; Knieps et al., 2007; Fig. 5-2). Whether innexin2 can form additional heteromeric gap junction channels has not been investigated yet. However, co-localisation studies in *Drosophila* embryos as well as co-immunoprecipitation experiments performed in transfected SL2 cells (J. Martini, PhD thesis), to analyse the interaction potential of innexin2 and innexin1, point to the existence of other heteromeric hemichannel combinations containing innexin2 protein.

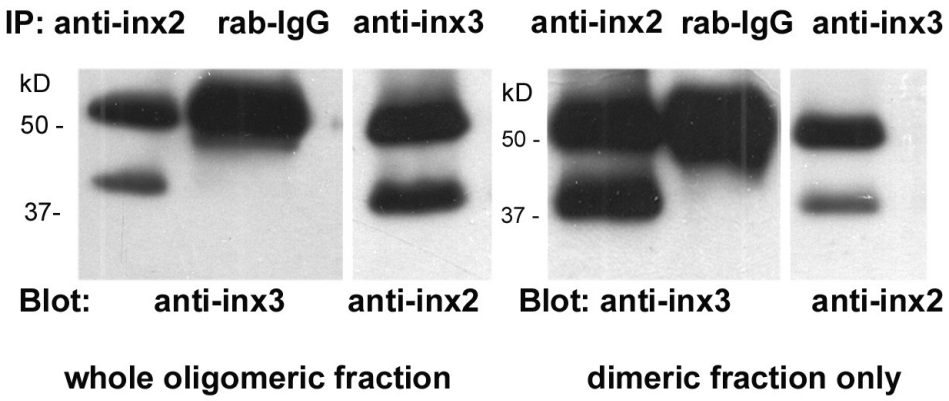

Fig. 5-2 Co-immunoprecipitation of innexin2 and innexin3 from oligomeric fractions. Oligomeric fractions from TX-100 soluble embryonic lysates were pooled and co-immunoprecipitation was carried out. For co-immunoprecipitation from dimeric fractions lysates fractions between 11-13% sucrose were pooled. Both experiments confirmed an interaction of innexin2 and innexin3.

Moreover, innexin2 is able to form homomeric hexamers, too. Both, cell free expression and oligomerisation experiments (section 4.1.4), as well as the observation of plaque like structures after transfection of HeLa cells with innexin2 (section 4.4.1) provide strong evidence that innexin2 is able to form homomeric hemichannels as well as homomeric, homotypic plaques.

The inefficient oligomerisation process that was observed when analysing innexin2 homomerisation *in vitro* (Fig. 4-8) *w*as also described for the *in vitro* assembly of connexin proteins. *In vitro* oligomerisation of connexin proteins has been conducted various times, indicating that oligomerisation can be mimicked in a cell free system that is only supplemented with microsomal membranes, which resemble core components of the endoplasmic reticulum (Ahmad et al., 2001, 2002; Falk, 2000). Several reports discuss the low efficiency of the oligomerisation process to form hexamers. Most of the protein translated, remained in its monomeric status and is not oligomerised.

This inefficiency can be explained by the fact that the used microsomal membranes are missing crucial components that are provided *in vivo,* for example by the proteins residing in the Golgi compartment. According to this assumption Ahmad and co-workers showed that the efficiency of oligomerisation could be improved for connexin32 by the addition of isolated Golgi membranes to the system (Ahmad et al., 1999).

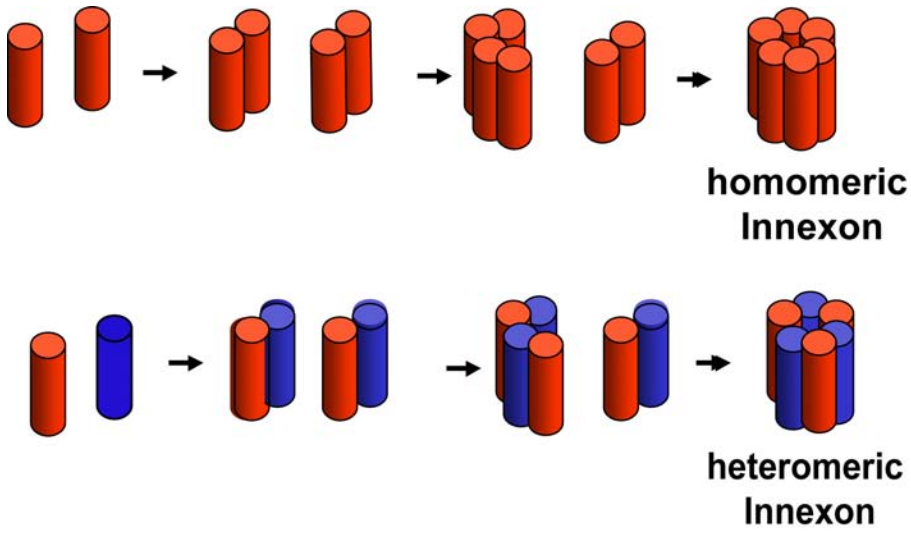

Fig. 5-3 Innexin2 forms homomeric and heteromeric innexons. Schematic drawing of homomeric and heteromeric hemichannel formation by innexin2 proteins alone or with innexin3. Dimers are the smallest oligomeric subunit.

However, the finding that innexin2 is able to form homomeric hemichannels and homotypic gap junctions is also supported by previous coupling experiments in paired *Xenopus* oocytes. Expression of *Drosophila innexin m*RNAs resulted in the measurable induction of gap junctional communication when expressing innexin2 *m*RNA only (Stebbings et al., 2000). However, the reliability to induce of gap junctional communication was greater in oocytes that co-expressed innexin2 and innexin3. In contrast, injection of innexin3 *m*RNA alone and expression of innexin3 protein did not lead to the induction measurable currents between membranes of patch-clamped oocytes. This recent findings point to the fact that all innexin proteins are able to form functional homomeric gap junction channels.

5.3 Trafficking of innexin2 along the secretory pathway is dependent on microtubules and the exocyst complex

Another part of this work aimed on the elucidation of trafficking of innexin2 containing hemichannels.

The secretory pathway is the major trafficking route of transmembrane proteins after their translation in the endoplasmic reticulum.

Subcellular fraction studies combined with drug treatments experiments and antibody stainings of embryos, ovaries and cultured cells led to the conclusion that innexin2 containing hemichannels are transported along the secretory pathway to their final destination, the plasma membrane. Evidence for that conclusion was obtained first from findings that

innexin2 was found enriched in different membrane fractions from organelles, namely plasma membrane, endoplasmic reticulum and vesicles. The dependency of innexin2 containing hemichannels on ER to Golgi apparatus trafficking was further confirmed by brefeldin A treatments, which are classically conducted for the analysis of exocytosis of transmembrane proteins (Klausner et al., 1992). Brefeldin A treatments of ovaries and SL2 cells, stably expressing inx2myc, resulted in a failure in delivery of newly synthesised hemichannels to the plasma membrane. Simultaneously, an accumulation of innexin2 was observed at the endoplasmic reticulum, as shown by co-staining with the ER marker PDI in cultured cells in section 4.2.2.1. The observations are line with data obtained from rat tumor cell line that showed a redistribution of transfected connexin 26 and 43 from the plasma membrane to the ER (Thomas et al., 2005) upon brefeldin A treatment.

5.3.1 Microtubule dependent transport of innexons

Microtubules provide one main trafficking road for newly synthesised proteins within cells. With the help of microtubule based motor proteins a directive transport of proteins is enabled in both directions along the tubules. Whereas kinesin ensures thetransport of cargo to the plus end direction of microtubules towards the cell periphery, dynamin takes over transport processes to the minus end of microtubules.

Previous investigations of connexin hemichannel dependent transport showed the dependency on microtubules. As a first evidence for possible connexin and microtubule interactions, Giepmans and coworkers showed the direct interaction of connexin43 with both, α– and β–tubulin subunits *in vitro* (Giepmans et al., 2001, 2003). In GST-pull down experiments a tubulin binding site in the C-terminal region of connexin43 was identified, that showed no conservation within other connexin isoforms.

Publications on a microtubule dependent connexin trafficking also argue for the existence of microtubule independent trafficking routes. For instance, treatment of the connexin isoform cx26 with nocodazole did not have impact on the plasma membrane integration of cx26 positive plaques in normal rat kidney cells, whereas it affected membrane integration of connexin43 (Thomas et al., 2005). These findings suggest an isoform dependent regulation of trafficking, indicating that specific analyses on single isoforms are necessary and that all gap junction proteins do not obligatory exhibit the same characteristics. None such studies have been conducted to analyse innexin2 transport.

To address this question a combination of various *in vivo* and cell culture experiments were conducted in this work. Co-immunoprecipitation (Fig. 4-20) as well as co-immunostainings of wild type embryos (Fig. 4-19) and dissected ovaries (Fig. 4-18), resulted in the finding that

innexin2 is part of a complex with ß-tubulin, one of the two subunits that gives rise to the microtubule architecture. The identification of a tubulin binding motif was not possible due to the variability of potential binding site sequences among gap junction proteins (Giepmans et al., 2001).

Evidence for the importance of microtubules on the transport of innexin2 containing hemichannels was provided by the application of microtubule depolymerising agents, such as colchicine and nocodazole to cultured cells and *Drosophila* ovaries (Fig. 4-21; 4-22). Whereas the localisation of other membranes proteins such as the septate junction protein disc large was still intact upon treatment, innexin2 became redistributed to the cytoplasm of follicle cells. The effect of innexin2 redistribution to the cytoplasm was also obtained in SL2 cell culture, where nocodazole as a second microtubule depolymerising agent was applied. These data argue for the importance of the microtubular cytoskeleton in trafficking and/or stabilising of innexin2 containing gap junctions.

Shaw and colleagues showed in addition, that connexin gap junction plasma membrane trafficking is dependent on the microtubule associated plus end binding protein EB1 and on the formation of adherens junctions (Shaw et al., 2007). EB1 was identified as microtubule associated protein that binds to microtubule plus ends, regulating microtubule dynamics and perhaps cortical attachment. It was first identified as a binding partner of the human tumor suppressor APC, which plays distinct roles in Wnt signalling and cytoskeletal regulation (Grevengoed and Peifer, 2003).
Several studies in our group also pointed to an adherens junction based localisation of innexin2 to the plasma membrane. One example is the proven interaction between *D*E-cadherin, as a core component of adherens junctions, and innexin2 in embryos and SL2 cells. When *D*E-cadherin is overexpressed in SL2 cells enhanced gap junction plaque formation is detected between adjacent cells (Bauer et al., 2006).
Interestingly, first double immunostainings of embryos, overexpressing EB1gfp ubiquitously, using antibodies against innexin2 and GFP revealed partial overlapping regions of both proteins near the plasma membrane with innexin2 accumulating at the apico-lateral domain of epidermal cells (Fig. 5-4).
However, co-immunoprecipitation experiments, which were carried out subsequently to this finding, did not point to a direct interaction of both proteins. The negative result obtained from co-immunoprecipitation may result from the fact that the GFP tagged variant of EB1 is unable to bind innexin2 due to steric hindrances. An alternative approach would have been co-immunoprecipitation using an EB1 antibody. This could not be done due to the unavailability of an *Drosophila* EB1 antibody working in immunoblot analysis.

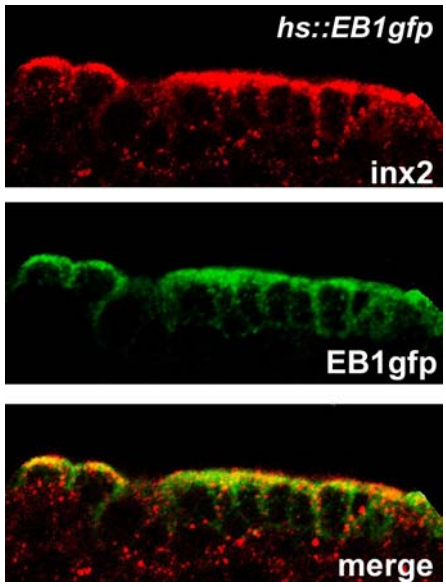

Fig. 5-4 Overexpression of the microtubule plus end binding protein EB1gfp resulted in an accumulated localisation of innexin2 at apico-lateral membranes of embryonic epidermal cells. Co-immunostaining of inx2 (red) and EB1gfp (green) are detected in overlapping expression patterns**.**

In summary, it could be shown that innexin2 is transported via the secretory pathway to the plasma membrane and that innexin2 containing hemichannel transport is mediated by microtubules. Figure 5-5 summarises again the different approaches that were undertaken to clarify innexin2 containing hemichannel assembly and trafficking of those to the plasma membrane.

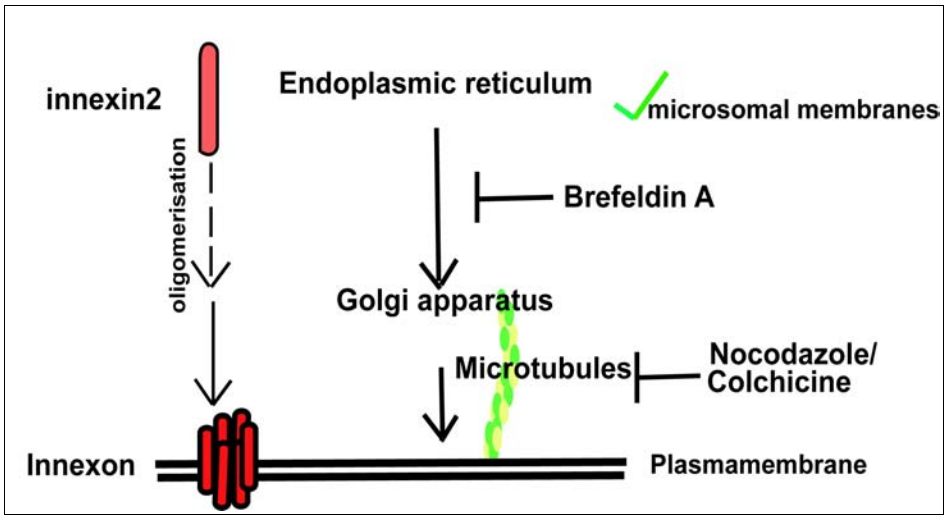

Fig. 5-5 Summary of undertaken approaches providing evidence for a microtubule dependent trafficking of innexin2 hemichannels along the secretory pathway. I*n vitro* oligomerisation approaches that used canine microsomal membranes resulted in the formation of hexamers indicating that endoplasmic reticulum membranes are sufficient for innexin2 hexamer assembly. Transport of innexin2 containing hemichannels from the endoplasmic reticulum to the golgi apparatus was abolished by brefeldin A treatment. Finally, interference with microtubule depolymerising drugs indicate a microtubule dependent trafficking of innexin2 hemichannels to the plasma membrane.

5.3.2 Evidence for an exocyst dependent targeting of innexons

Targeting of transmembrane proteins to specific domains at the cell membrane is a widely used mechanism for the establishment of cell polarity. The spatial specificity of vesicle trafficking is thought to occur at a late step in this process through the tethering of exocytic vesicles at defined membrane sites by the eight-subunit exocyst complex (Blankenship et al., 2007). The exocyst complex was initially identified in a screen for major regulators of exocytosis in yeast. Ongoing studies on the exocytosis in polarised cells of metazoens revealed the existence of such a complex also in higher eukaryotes and also in *Drosophila*. Members of the exocyst complex show a high sequence homology between investigated species, indicating an ancient mechanism that is involved in transport of membrane proteins to the plasma membrane throughout the animal kingdom. In addition, recent studies point to a role of the exocyst complex in endocytic events within a polarised cell. The exocyst subunits sec6, sec8, and exo70 were localised to early endosomes, transferrin-positive common recycling endosomes, and rab11a-positive apical recycling endosomes of polarised MDCK cells, indicated that it may be involved in a broader range of trafficking events than originally proposed (Oztan et al., 2007).

Previous studies of the exocyst complex in *Drosophila* enabled the access to a variety of tools, which allowed to start the analysis of exocyst mediated trafficking of innexin2. First hints that innexin2 trafficking might be influenced by members of the exocyst complex came from co-immunostainings with an anti-sec6 antibody. Co-immunostaining using this antibody in combination with an antibody against innexin2, revealed a clear overlap of the innexin2 and sec6 expression patterns in the cortical region of cell in the embryonic epidermis (Fig. 4-23). Overexpression analyses *in vivo* and double stranded RNAi treatments of various members of the exocyst complex, performed in insect cell culture, point to the exocyst dependent delivery of innexin2 containing hemichannels to the plasma membrane. A preliminary result for a direct dependency of innexin2 on sec6 comes from clonal analysis of sec6 negative cells. Innexin2 is found highly accumulated in the cytoplasm of follicle cells of the *Drosophila* ovary devoid of sec6 expression, whereas sec6 expressing cells showed the normal innexin2 pattern with a prominent staining at cellular membranes of follicle cells.

Ongoing genetic analyses using a recombinant inducible RNAi fly-line in combination with the eye specific driver line eyes absent-Gal4 that knocks down *innexin2 m*RNA efficiently, revealed a small eye phenotype. This small eye-phenotype was enhanced when crossing an an sec6 RNAi line to the recombinant small eyed flies. Progeny of such crossings showed the total lack of one eye or even more drastically, the complete absence of the head structures, finally resulting in pupal cell death.

All together, the hypothesis that the exocyst complex might be involved innexin2 containing gap junction trafficking is strengthened by different findings and should be investigated further.
This could also contribute to elucidate an exocyst dependent trafficking of vertebrate connexins and pannexins.

5.4 Implications on conservation

Studies on the oligomerisation and trafficking of innexin2-containing hemichannels to the plasma membrane revealed that the procedures of both, hemichannels assembly and trafficking, is highly comparable to the assembly and trafficking data available for vertebrate connexin43.
The next question was whether the similarities found for oligomerisation and trafficking of connexins and innexins, would allow to express innexins in vertebrate HeLa cells and whether the expressed innexin2 protein would be transported to the plasma membrane in this heterologous cellular system.
It was possible to detect plaque like structures between some of the transfected cells and first biochemical approaches also point to the potential of innexin oligomerisation in vertebrate cultured cells (Fig. 4-32). Membrane integration of innexin2 was proven by analyses of plasma membrane sheet preparations from transfected HeLa cells (Fig. 4-31). This indicates that innexin2 is integrated in the plasma membrane of vertebrate cells that do not express connexins. In addition, immunofluorescent stainings show that innexin2 able to form plaque like structures between membranes of two neighboring cells, but to very inefficient level (Fig. 4-28). Various attempts to gain high levels of innexin expression in these cells failed, and transfection of innexin2 (and innexin3) resulted in increased cell death occurring soon after transfection. These circumstance made statements on the potential of innexin2 to form homomeric and homotypic plaques difficult.

Due to the low efficiency of plaque formation and the observation of high cell lethality, this system could not be used for functional studies, namely dye-tracer injection experiments, which should have been used to show the functionality of generated plaques.
However, altogether evidence was obtained for a conserved procedure of gap junction hemichannel formation and trafficking to the plasma membrane.

5.5 Cross regulation between gap junctions and major signalling pathways

A number of signalling cascades and communication mechanisms are implicated in the formation of shaped tissues and organs during embryogenesis. In this work the effect of innexin2 mediated gap junction communication was studied using the proventriculus as a model for organ formation. The proventriculus develops at the junctions of posterior foregut and midgut. It is known that morphogenesis of the posterior foregut and midgut is under the control of regulatory networks involving hedgehog, wingless and Notch signalling. Mutants encoding genes of signalling components show similar phenotypes, namely a failure in the correct folding ectodermal and endodermal tissue layers, which normally results in a valve like structure that serves as a regulator for the food passage from the fore into the midgut (Fig. 5-6).

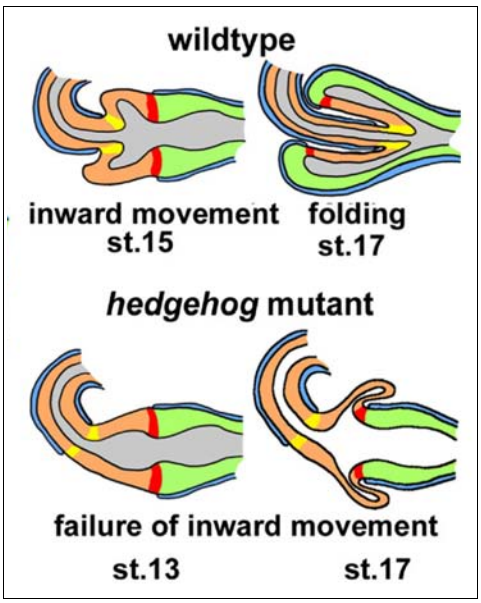

Fig. 5-6 Schematic drawing of the proventriculus formation in wild type and *hedgehog* mutants during embryogenesis. Whereas proventriculi of wild type embryos construct a valve like structure at stage 17 of embryogenesis, a failure of inward movement of ectodermal tissue layer is observed in *hedgehog* mutants.(Modified after Lechner et al., 2007)

Recent studies revealed that two groups of cells, the anterior and posterior boundary cells play an important role during proventriculus development. It has been shown that the inward movement of the ectodermal proventricular cells is controlled by the anterior boundary cells, in which the Notch signalling pathway is activated (Fuss et al., 2004; Josten et al., 2004). Furthermore, hedgehog signalling is involved in the invagination process of the ectodermal tissue layer and is crucial for the allocation of anterior boundary specification. Evidence for this finding is that Notch signalling activity is missing in the anterior boundary cells of

hedgehog mutants. Interestingly, wingless expression is lost in the same row of cells in hedgehog mutants (Lechner et., 2007). Moreover, it could be shown in our laboratory recently, that innexin2 is a direct target of wingless signalling (Bauer et al., 2004). This led to the question how paracrine signals and gap junctional communication cooperate to regulate the coordinated behaviour of cells during patterning and morphogenesis, especially of the proventriculus. Analyses on *innexin2 m*RNA and protein expression, resulted in the detection of innexin2 expression in both, the ecto- and the endodermal tissue layer, arguing for the existence of innexin2-containing gap junction channels in both tissue layers (Fig. 4-37).
Interestingly, innexin2 protein expression was lost in proventriculi of *hedgehog* mutants (Lechner et al., 2007), which is in good agreement with innexin2 being a target gene of wingless, as wingless expression is also lost in *hedgehog* mutants. Finally, this loss of innexin2 expression in *hedgehog* mutants resulted in a reduced dye coupling between cells of *hedgehog* mutant proventriculi (Fig. 4-38; Lechner et al., 2007). The observation of a reduced dye transfer to an even stronger extent was also obtained in proventriculi of *kropf* mutants. Therefore, dye tracer injection experiments suggest, that the direct coupling of cells via innexin2-containing gap junctions, which are induced in response to hedgehog and wingless activities, is important for the coordinated movement of the ectodermal cell layer. It is known from extensive studies in mammals that the coupling of cells and tissues via gap junctions enables the diffusion of second messengers, such as Ca2+, inositol-trisphosphate (IP3) or cyclic nucleotides to allow the rapid coordination of cellular behavior during morphogenetic processes such as cell migration and growth control (Chen et al., 1995; Wei et al., 2004). These results suggest that wingless and Notch signalling in the anterior boundary cells depend on hedgehog expression. This hypothesis was verified *in vivo* by a rescue experiment resupplying wingless expression with the *twist*-Gal4 driver line in *hedgehog* mutants. As a result, *innexin2 m*RNA expression, as direct target gene of wingless signalling, was restored in *hedgehog* mutants (Fig. 4-39), pointing to the interconnection of major signalling cascades in the posterior foregut. Additionally, the invagination phenotype that can be observed in *hedgehog* mutants was rescued (Fig. 5-6).
Finally, the similarity of proventricular defects, which can be seen in *hedgehog*, *wingless* and in the innexin2 *kropf* mutants are in good agreement with the idea that hedgehog acts on wingless thereby regulating innexin2 dependent gap junction activity required for the invagination of ectodermal foregut cells.

In addition, further studies revealed that innexin2 itself is indispensable for the precise expression of components of the signalling cascades mentioned above. Innexin2 loss and gain of function analyses point to clear cross regulatory effects on the *m*RNA expression levels of major regulatory components involved in proventriculus organogenesis as found out

by *q*RT-PCR analyses. Innexin2 loss of function experiments resulted in a severe reduction of *m*RNA expression levels fo*r hedgehog, wingless* and *Delta* transcripts, whereas the overexpression of innexin2 led to elevated levels for all three transcripts (Fig. 4-40). These findings support observations of fluorescent antibody stainings and *in situ* hybridisations, which showed innexin2 dependent alterations in expression levels of all three *m*RNAs or proteins (Lechner et al., 2007; Josten, PhD thesis).

Together, the collected data point towards an essential requirement of gap junction communication for the transcriptional activation of morphogen-encoding genes activating evolutionary conserved signalling cascades essential for patterning in animals (Lechner et al., 2007; Serrano and O'Farrell, 1997). The question, in which way innexin2 mediates transcriptional control remains unclear. Several experiments in cell culture point to a innexin2 C-terminus dependent mechanism. Quantitative real time PCR analyses on *m*RNA from embryos, where a truncated form the innexin2 full length protein was overexpressed, resulted in a comparable reduction of *hedgehog*, *wingless*, and *Delta* transcripts as was obtained when analysing transcript levels in *kropf* mutants (Fig.4 -40).

One hypothesis that was followed up to explain this result, is a potential involvement of the innexin2 C-terminal domain in the activation of transcription. *In silico* predictions point to the existence of a nuclear receptor binding site in the C-terminal part of the innexin2 amino acid sequence (Fig. 4-42). Nuclear receptors are known to mediate regulation of transcription. The regulation of gene expression by nuclear receptors only happens in the presence of a ligand, a molecule, which affects the behaviour of the receptor. More specifically, ligand binding to a nuclear receptor results in a conformational change of the receptor leading to its activation and up-regulation of gene expression. The C-terminal innexin2 domain, which contains a predicted nuclear receptor motif, may serve as such a ligand for a nuclear receptor that is involved in the activation of target gene expression because it contains a predicted nuclear receptor binding motif (Fig. 4-43).

Further evidence for the existence of such a mechanism, derives from biochemical experiments in Schneider cell culture. Overexpression of inx2-gfp resulted in the observation of an additional C-terminal fragment that could be immunoprecipitated with an anti-innexin2 and an anti-GFP antibody (Fig. 4-44). The detection of an additional innexin2 protein fragment also implicates the existence of a mechanism, which is responsible for the generation of the C-terminal innexin2 fragment. One possibility might be a C-terminal cleavage event that takes place upon innexin2 overexpression within the fourth transmembrane domain. Another possibility is the existence of an additional translation start codon, an internal ribosomal entry site (IRES), resulting in a truncated C-terminal innexin2 fragment. The existence of IRES-sites could be shown the in different connexin *m*RNAs. For

example, the zebrafish *connexin55.5 m*RNA produces a C-terminal fragment, that was also found in nuclei of transected NIH3T3 cells. It was shown that the generation of this C-terminal fragment is IRES mediated. IRES sites were also found for connexins43, 32 and 26 (Ul-Hussain et al., 2008). The impact of IRES mediated translation and the generation of additional connexin protein fragments is only poorly understood.
The existence of a an additional C-terminal fragment was also described for connexin43 in different cellular systems. The group around Steven Taffet identified a C-terminal connexin43 fragment with a size of 20 kD in chinese hamster kidney cells (Joshi-Mukherjee et al., 2007). Another study reported the observation that a truncated C-terminal fragment of connexin43. This fragment was localised in the nucleus of HeLa cells and led to a reduced proliferation of cells expressing this C-terminal Cx43 protein fragment (Dang et al., 2003).

The direct association of a transcription factor with gap junctions has been recently proposed for the mouse homologue of ZO-1-associated nucleic acid-binding protein (ZONAB). This transcription factor binds to ZO-1, which is associated with oligodendrocyte, astrocyte and retina gap junctions (Penes et al., 2005; Ciolofan et al., 2006). It is possible that innexin2-dependent transcriptional regulation may involve a similar type of mechanism: A still unknown transcriptional regulator associated with the C-terminus of innexin2-containing gap junctions could be released upon modulation of gap junction composition thereby modulating the transcription of innexin2-dependent target genes (Lechner et al., 2007).

Another explanation for the oberserved modulation of transcription by innexin2 could be a gap junction mediated signalling via second messengers that modulate the transcription of target genes in response to gap junction mediated intercellular communication. This assumption is supported by a study from Stains and colleagues who found a dependency of transcriptional activities of different osteoblast genes on gap junction expression. In Cx43 loss and gain of function experiments an altered recruitment of ubiquitously expressed Sp1/Sp3 transcription factors to the promoters of these genes was observed. This might represent a potential general mechanism for transcriptional control of target genes by signals passing through gap junctions (Stains et al., 2003).
It was found in the laboratory that upon loss of innexin2 expression in the proventriculus, the coexpressed innexins 1 and 3 are also down regulated on the transcriptional level (Martini, PhD thesis). This results in a severe loss of gap junction formation associated with a loss of direct communication via heteromeric gap junction channels. Loss of direct cell communication via second messengers that are normally transported through gap junction channels and control transcriptional control, argues also for the assumption of a modulated gene expression via an altered exchange rate of second messengers.

5.6 Outlook

In this thesis, methods for the analysis of oligomerisation and trafficking of gap junction proteins were established that led to the identification that innexin2 is transported to the plasma membrane via the secretory pathway. These methods can be used in the laboratory to analyse oligomerisation and trafficking of other *Drosophila* gap junction isoforms.

Further studies on the potential of innexins in the formation of homo- or heteromeric gap junction channels will clarify whether innexin2 is able to form other types of heteromeric hemichannels with the remaining members of the gap junction family or whether there is only a limited number of interaction partners as outlined for the connexins.

Another question that should be addressed, is whether innexin2 hemichannels can function besides their involvement as gap junction constituents as autonomous channels by itself. Indication for the existence of unopposed hemichannels come from immunohistochemical stainings cells, where innexin2 was overexpressed in various cell culture systems and the fact that members of the pannexin and connexin family were also implicated in hemichannel function.

Concerning trafficking, it would be very interesting to follow evidences for the involvement of members of the exocyst complex in plasma membrane trafficking of innexin2-containing hemichannels. An expansion of analyses concerning an exocyst dependent targeting also to the connexin field, where transport mechanisms between TGN sorting and plasma membrane integration are also unclear, would be an interesting topic.

Finally, further studies on the mechanism by which the gap junction protein innexin2 controls the transcription of major signalling proteins is an interesting issue that also might contribute to the understanding of the phenomenon of C-terminal fragments of connexins in nuclei that alter gene expression levels.

Altogether, findings of conserved gap junction hemichannel structures and trafficking routes to the plasma membrane open the possibility to screen for new interaction partners that are crucial for the formation and function of gap junction proteins for all three families of gap junction proteins.

6 Summary

Gap junctions channels serve as mediators for direct cell-to cell communication between cells of different tissue and organs by the exchange of small metabolites and signalling molecules. They are formed by analogous protein families in vertebrates and invertebrates. The docking of two hemichannels leads to gap junction channel formation at the plasma membrane of two adjacent cells, resulting in so called “plaque like” structures that consist of accumulations of gap junction channels at contact sites.
Whereas the biogenesis and functions of vertebrate gap junction channels consisting of connexins have been analysed in some detail, biochemical studies on innexin gap junction assembly and trafficking are lacking for any innexin known to date.

The formation and trafficking of innexin2 containing gap junction hemichannels to the plasma membrane was analysed in *Drosophila melanogaster* and cultured cells in this thesis. Analysis of innexin2 oligomerisation by biochemical approaches like velocity sedimentation of different oligomers in density gradients combined to cell-free transcription/translation assays revealed the existence of hexameric innexin2 containing hemichannels that were termed innexons. It could be shown that the identified innexons formed by innexin2 can be either homomeric, meaning that they are composed of innexin2 subunits only, or heteromeric meaning that other innexin isoforms are part of one hemichannel in addition. Immunohistochemical analysis of innexin2 expression in *Drosophila* ovaries, invertebrate and mammalian cell culture as well as biochemical fractionation experiments indicate that innexin2-containing oligomers are transported along the secretory pathway to the plasma membrane. Moreover, by the combination co-immunoprecipitation and drug treatment experiments it could be demonstrated that innexin2-containing hemichannels are transported along the microtubule cytoskeleton to the plasma membrane with an involvement of the exocyst complex taking part in the anterograde transport of gap junction hemichannels.

These findings provide the first biochemical evidence that innexins form hexameric innexon hemichannels and suggest that the oligomerisation and trafficking of connexins and innexins may rely on a common mechanism despite lacking of sequence similarity between both protein families.

Investigation of the innexin2 function during the development of the proventriculus, an accessory organ of the *Drosophila* gastrointestinal tract that is formed during *Drosophila* embryogenesis, pointed in addition to an innexin2 dependent gap junctional cross regulation of major signalling molecules like hedgehog, Delta and wingless which are crucial for the formation of shaped organs.

7 Literature

Ahmad, S., Diez, J.A., George C.H., Evans, W.H. (1999). Synthesis and assembly of connexins in vitro into homomeric and heteromeric functional gap junction hemichannels. Biochem. J. 339: 247-53.

Ahmad, S., Martin, P.E., Evans, W.H. (2001). Assembly of gap junction channels: mechanism, effects of calmodulin antagonists and identification of connexin oligomerization determinants. Eur. J. Biochem. 268: 4544-4552.

Ai, Z., Fischer, A., Spray, D.C., Brown, A.M., Fishman, G.I. (2000). Wnt-1 regulation of connexin43 in cardiac myocytes. J. Clin. Invest. 105: 161-171 .

Alberts, B., Bray, D., Lewis, J., Raff, M., Roberts, K., Watson, J. (2004). Molekularbiologie der Zelle. VCH Verlagsgesellschaft mbH, Weinheim.

Anitei, M., Ifrim, M., Ewart, M.A., Cowan, A.E., Carson, J.H., Bansal, R. and Pfeiffer, S.E. (2006). A role for Sec8 in oligodendrocyte morphological differentiation. J. Cell Sci. 119: 807–818.

Antonny, B. (2006). Membrane deformation by protein coats. Curr. Opin. Cell Biol. 18: 386–394.

Bahima, L., Aleu, J., Elias, M., Martín-Satué, M., Muhaisen, A., Blasi, J., Marsal, J., Solsona, C. (2006). Endogenous hemichannels play a role in the release of ATP from Xenopus oocytes. J. Cell Physiol. 206: 95-102.

Baranova, A., Ivanov, D., Petrash, N., Pestova, A., Skoblov,, M., Kelmanson, I., Shagin, D., Nazarenko, S., Geraymovych, E., Litvin, O., Tiunova, A., Born, T.L., Usman, N., Staroverov, D., Lukyanov, S., Panchin, Y. (2004). The mammalian pannexin family is homologous to the invertebrate innexin gap junction proteins. Genomics 83: 706-716.

Bauer, R., Lehmann, C., Fuss, B., Eckardt, F., and Hoch, M. (2002). The Drosophila gap junction channel gene innexin 2 controls foregut development in response to Wingless signalling. J. Cell Sci. 115: 1859-1867.

Bauer, R., Lehmann, C., Martini, J., Eckardt, F., and Hoch, M. (2004). Gap junction channel protein innexin 2 is essential for epithelial morphogenesis in the Drosophila embryo Mol. Biol. Cell 15: 2992-3004.

Bauer, R., Löer, B., Ostrowski, K., Martini, J., Weimbs, A., Lechner, H., Hoch, M. (2005). Intercellular communication: the Drosophila innexin multiprotein family of gap junction proteins. Chem. Biol. 12: 515-526.

Blankenship, J.T., Fuller, M.T., Zallen, J.A. (2007). The *Drosophila* homolog of the Exo84 exocyst subunit promotes apical epithelial identity. J. Cell Sci. 120: 3099-3110.

Blount, P., and Merlie, J.P. (1988). Native folding of an acetylcholine receptor alpha subunit expressed in the absence of other receptor subunits. J. Cell Biol. 263: 1072-1080.

Bobinnec, Y., Marcaillou, C., Morin, X., Debec A. (2003). Dynamics of the endoplasmic reticulum during early development of Drosophila melanogaster. Cell Motil. Cytoskeleton 54: 217-225.

Bruzzone, R., Hormuzdi, S.G., Barbe, M.T., Herb, A., Monyer, H. (2003). Pannexins, a family of gap junction proteins expressed in brain. Proc. Natl. Acad. Sci. 100: 13644-13649.

Bryant, D.M., Mostov, K.E. (2008). From cells to oragns: building polarized tissues. Nat. Rev. Mol. Cell Biol. 9: 887-901.

Campbell, N.A., Reece, J. B. and Mitchell, L.G. (1999). Biology. Addison Wesley Longman, Inc.

Chuang, C.F., Vanhoven, M.K., Fetter, R.D, Verselis, V.K., Bargmann, C.I. (2007). An innexin-dependent cell network establishes left-right neuronal asymmetry in C. elegans. Cell 129: 787-799.

Ciolofan, C., Li, X.B., Olson, C., Kamasawa, N., Gebhardt, B.R., Yasumura, T., Morita, M., Rash, J.E., Nagy, I.J. (2006). Association of connexin36 and zonula occludens-1 with zonula occludens-2 and the transcription factor zonula occludens-1-associated nucleic acid-binding protein at neuronal gap junctions in rodent retina. Neuroscience 140: 433–451.

Dang, X., Doble, B.W., Kardami, E. (2003). The carboxy-tail of connexin-43 localizes to the nucleus and inhibits cell growth.Mol. Cell Biochem. 242: 35-38.

De Matteis, M.A., Godi, A. (2004). Protein–lipid interactions in membrane traffcking at the Golgi complex. Biochim. Biophys. Acta 1666: 264–274.

Denef, N., Chen, Y., Weeks, S.D., Barcelo, G., Schüpbach, T. (2008). Crag regulates epithelial architecture and polarized deposition of basement membrane proteins in Drosophila. Dev Cell. 14: 354-364.

Desai, A., Mitchison, T.J. (1997). Microtubule polymerization dynamics. Annu. Rev. Cell Dev. Biol. 13: 83-117.

Dodd, R.B., Drickamer, K. (2001). Lectin-like proteins in model organisms: implications for evolution of carbohydrate-binding activity. Glycobiology 11: 71-79.

Elefant, F., Palter, K.B. (1999). Tissue-specific expression of dominant negative mutant Drosophila HSC70 causes developmental defects and lethality. Mol. Biol. Cell 10: 2101-2117.

Elfgang, C., Eckert, R., Lichtenberg-Fraté, H., Butterweck, A., Traub, O., Klein, R.A., Hülser, D.F., Willecke, K. (1995). Specific permeability and selective formation of gap junction channels in connexin-transfected HeLa cells. J Cell Biol.129: 805-817.

Ellis, M.A., Potter, B.A., Cresawn, K.O., Weisz, O,A. (2006). Polarized biosynthetic traffic in renal epithelial cells: sorting, sorting, everywhere. Am. J. Physiol. Renal Physiol. 291: 707-713.

Falk, M.M., Lauf, U. (2001). High resolution, fluorescence deconvolution microscopy and tagging with the autofluorescent tracers CFP, GFP, and YFP to study the structural composition of gap junctions in living cells. Microsc. Res. Tech. 52: 251-262.

Fölsch, H. (2005).The building blocks for basolateral vesicles in polarized epithelial cells. Trends Cell Biol.15: 222-228.

Fölsch, H. (2008). Regulation of membrane trafficking in polarized epithelial cells. Curr Opin. Cell Biol. 20: 208-213.

Fuss, B., Becker, T., Zinke, I., Hoch, M. (2006). The cytohesin Steppke is essential for insulin signalling in Drosophila. Nature 444: 945–948.

Fuss, B., Josten, F., Feix, M., Hoch, M. (2004). Cell movements controlled by the Notch signalling cascade during foregut development in Drosophila. Development 131: 1587–1595.

Gallagher, S.R. (2006). One-dimensional SDS gel electrophoresis of proteins. Curr.. Protoc. Immunol. Chapter 8: Unit 8.4.

Giepmans, B.N, Verlaan, I., Moolenaar, W.H. (2001). Connexin-43 interactions with ZO-1 and alpha- and beta-tubulin. Cell Commun. Adhes. 8: 219-223.

Giepmans, B.N., van Ijzendoorn, S.C. (2008). Epithelial cell-cell junctions and plasma membrane domains. Biochim. Biophys. Acta. Jul 28. [Epub ahead of print]

Giepmans, B.N., Verlaan, I., Hengeveld, T., Janssen, H., Calafat, J., Falk, M.M., Moolenaar. W.H. (2001). Gap junction protein connexin-43 interacts directly with microtubules. Curr. Biol.11: 1364-1368.

Goode, B.L., Drubin, D.G., Barnes, G. (2000). Functional cooperation between the microtubule and actin cytoskeletons. Curr. Opin. Cell Biol.12: 63-71.

Grapin-Botton, A., Melton, D.A. (2000). Endoderm development: from patterning to organogenesis. Trends Genet. 16: 124-130.

Grevengoed, E.E., Peifer, M. (2003). Cytoskeletal connections: building strong cells in new ways. Curr. Biol. 13: R568-570.

Grindstaff, K.K., Yeaman, C., Anandasabapathy, N., Hsu, S.C., Rodriguez-Boulan, E., Scheller, R.H., Nelson, W.J. (1998). Sec6/8 complex is recruited to cell-cell contacts and specifies transport vesicle delivery to the basal-lateral membrane in epithelial cells. Cell 93: 731–740.

Halpain, S., Dehmelt, L. (2006). The MAP1 family of microtubule-associated proteins. Genome Biol. 7: 224.

Harris, AL. (2007). Connexin channel permeability to cytoplasmic molecules. Prog. Biophys. Mol. Biol. 94: 120-143.

Hartenstein, V. (1993). Atlas of *Drosophila* Development. Cold Spring Harbor Laboratory Press,U.S.

Hebrok, K., Kim, S.K., St Jacques, B., McMahon, A.P., Melton, D.A. (2000). Regulation of pancreas development by hedgehog signaling. Development 127: 4905–4913.

Horne-Badovinac, S., Bilder, D. (2005). Mass transit: epithelial morphogenesis in the Drosophila egg chamber. Dev. Dyn. 232: 559-574.

Huang, T.Y, Cherkas, P.S., Rosenthal, D.W., Hanani, M. (2005). Dye coupling among satellite glial cells in mammalian dorsal root ganglia. Brain Res.1036: 42-49.

Iizuka-Kogo, A., Shimomura, A., Senda, T. (2004). Colocalization of APC and DLG at the tips of cellular protrusions in cultured epithelial cells and its dependency on cytoskeletons. Histochem. Cell Biol. 123: 67-73.

Inoue, M., Chiang, S.H., Chang, L., Chen, X.W. and Saltiel, A.R. (2006). Compartmentalization of the exocyst complex in lipid rafts controls Glut4 vesicle tethering. Mol. Biol. Cell 17: 2303–2231.

Joshi-Mukherjee, R., Coombs, W,. Burrer, C., de Mora, I.A., Delmar, M., Taffet, S.M. (2007). Evidence for the presence of a free C-terminal fragment of connexin43 in cultured cells. Cell Commun. Adhes. 14: 75-84.

Josten, F. (2005). Charakterisierung der epithelialen Morphogenese im Proventrikulus von *Drosophila melanogaster*. PhD thesis, Universität Bonn.

Josten, F., Fuss, B., Feix, M., Meissner, T., Hoch, M. (2004). Cooperation of JAK/STAT and Notch signaling in the Drosophila foregut. Dev. Biol. 267: 181–189.

Kiefer, J.C. (2003). Molecular mechanisms of early gut organogenesis: a primer on development of the digestive tract. Dev. Dyn. 228: 287–291.

Knieps, M., Herrmann, S., Lehmann, C., Löer, B., Hoch, M., Famulok, M. (2007). Anti-innexin 2 aptamers specifically inhibit the heterologous interaction of the innexin 2 and innexin 3 carboxyl-termini in vitro. Biol. Chem. 388: 561-568.

Krendel, M., Mooseker, M.S. (2005). Myosins: tails (and heads) of functional diversity. Physiology (Bethesda). 20: 239-251.

Lang, T. (2003). Imaging SNAREs at work in 'unroofed' cells--approaches that may be of general interest for functional studies on membrane proteins. Biochem. Soc. Trans. 31: 861-864.

Langford, G.M. (1995). Actin- and microtubule-dependent organelle motors: interrelationships between the two motility systems. Curr. Opin. Cell Biol. 7: 82-88.

Lebendiker, M. (2000). Effects on Additives on Reversibility of Thermal unfolding. Well Characterized Biological Pharmaceuticals Meeting, San Francisco. Http:// wolfson.huji.ac.il/ purification/Protocols/PAGE_Basic.html

Lechner, H. (2004). Biochemische und molekulare Funktionsanalyse von Innexin2 in *Drosophila melanogaster*. Diploma thesis, Universität Bonn.

Lechner, H., Josten, F., Fuss, B., Bauer, R., Hoch, M. (2007). Cross regulation of intercellular gap junction communication and paracrine signaling pathways during organogenesis in Drosophila. Dev Biol. 310: 23-34.

Lehmann, C., Lechner, H., Löer, B., Knieps, M., Herrmann, S., Famulok, M., Bauer, R., and Hoch, M. (2006). Heteromerization of innexin gap junction proteins regulates epithelial tissue organization in Drosophila. Mol. Cell Biol. 17: 1676–1685.

Leithe, E., Rivedal, E. (2007). Ubiquitination of gap junction proteins. J. Membr. Biol. 217: 43-51.

Litvin, O., Tiunova, A., Connell-Alberts, Y., Panchin, Y., Baranova, A. (2006). What is hidden in the pannexin treasure trove: the sneak peek and the guesswork. J. Cell Mol. Med.10: 613-634.

Locke, D., Liu, J., Harris, A.L. (2005). Lipid rafts prepared by different methods contain different connexin channels, but gap junctions are not lipid rafts.Biochemistry 44: 13027-13042.

Lodish, H., Berk, A., Zipursky, S.L., Matsudaira, P., Baltimore, D., Darnell, J. (2000). Molecular Cell Biology. 4th Edition WH Freeman & Company, New York.

Love, H.D., Lin, C-C., Short, C.S. and Ostermann, J. (1998). Isolation of functional Golgi-derived vesicles with a possible role in retrograde transport. J. Cell Biol. 147: 1457-1472.

Luini, A., Mironov, A.A., Polishchuk, E.V., and Polishchuk, R.S. (2008). Morphogenesis of post-Golgi transport carriers. Histochem. Cell Biol. 129: 153–161.

Mahajan, M.A., Samuels, H.H. (2005). Nuclear hormone receptor coregulator: role in hormone action, metabolism, growth, and development. Endocr. Rev. 26: 583-597.

Margolis RL, Wilson L. (1998). Microtubule treadmilling: what goes around comes around. Bioessays. 20: 830-836.

Martini, J. (2007). Die Funktion des Gap junction Proteins Innexin 2 im larvalen Proventrikulusvon Drosophila melanogaster. PhD thesis, Universität Bonn.

Meier, C., Dermiezel, R. (2006). Electrical synapses-gap junctions in the brain. Results Prob. Cell Differ. 43: 99-128.

Meşe, G., Richard, G., White, T.W. (2007). Gap junctions: basic structure and function. J. Invest Dermatol. 127: 2516-2524.

Murthy, M., Schwarz, T.L. (2004). The exocyst component Sec5 is required for membrane traffic and polarity in the Drosophila ovary. Development 131: 377-388.

Musil, L.S., Goodenough, D.A. (1993). Multisubunit assembly of an integral plasma membrane channel protein, gap junction connexin43, occurs after exit from the ER. Cell 74: 1065-1077.

Niessen, C.M. (2007). Tight junctions/adherens junctions: basic structure and function. J. Invest. Dermatol.127: 2525-2532.

Novick, P., Field, C. and Schekman, R. (1980). Identification of 23 complementation groups required for post-translational events in the yeast secretory pathway. Cell 21: 205-215.

Ohno, H., Tomemori, T., Nakatsu, F., Okazaki, Y., Aguilar, R.C., Folsch H., Mellman, I., Saito, T., Shirasawa, T., Bonifacino, J.S. (1999). Mu1B, a novel adaptor medium chain expressed in polarized epithelial cells. FEBS Lett. 449: 215-220.

Orci, L. and Perrelet, A. (1975). Freeze-Etch Histology/ Heidelberg: Springer Verlag, 1999 Addison Wesely Longman Inc.

Oztan, A., Silvis, M., Weisz, O.A., Bradbury, N.A., Hsu, S.C., Goldenring, J.R., Yeaman, C., Apodaca, G. (2007). Exocyst requirement for endocytic traffic directed toward the apical and basolateral poles of polarized MDCK cells.Mol. Biol. Cell. 18: 3978-3992.

Panchin, Y.V. (2005). Evolution of gap junction proteins--the pannexin alternative. J. Exp. Biol. 208: 1415-1419.

Pankratz, M.J., Hoch, M. (1995). Control of epithelial morphogenesis by cell signaling and integrin molecules in the Drosophila foregut. Development 121: 1885–1898.

Penes, M.C., Li, X., Nagy, J.I. (2005). Expression of zonula occludens-1 (ZO-1) and the transcription factor ZO-1-associated nucleic acid-binding protein (ZONAB)-MsY3 in glial cells and colocalization at oligodendrocyte andastrocyte gap junctions in mouse brain. Eur. J. Neurosci. 22: 404–418.

Penuela ,S., Bhalla, R., Gong, X.Q., Cowan, K.N., Celetti, S.J., Cowan, B.J., Bai, D., Shao, Q., Laird, D.W. (2007). Pannexin 1 and pannexin 3 are glycoproteins that exhibit many distinct characteristics from the connexin family of gap junction proteins. J. Cell Sci. 20: 3772-3783.

Pepicelli, C.V., Lewis, P.M., McMahon, A.P. (1998). Sonic hedgehog regulates branching morphogenesis in the mammalian lung. Curr. Biol. 8: 1083–1086.

Piehl, M., Lehmann, C., Gumpert, A., Denizot, J.P., Segretain, D., Falk, M.M. (2007). Internalization of large double-membrane intercellular vesicles by a clathrin-dependent endocytic process. Mol. Biol. Cell 18: 337-447.

Quigley, P.J. (1976). Association of a protease (plasminogen activator) with a specific membrane fraction isolated from transformed cells. J. Cell Biol. 71: 472-486.

Ramalho-Santos, M., Melton, D.A., McMahon, A.P. (2000). Hedgehog signals regulate multiple aspects of gastrointestinal development. Development 127: 2763–2772.

Raynaud-Messina, B., Merdes, A. (2007). Gamma-tubulin complexes and microtubule organization. Curr. Opin. Cell Biol. 19: 24-30.

Rogers, S.L. and Gelfand, V.I. (2000). Membrane trafficking, organelle transport, and the cytoskeleton. Curr. Opin. Cell Biol 12: 57–62.

Ross, J.L., Ali, M.Y., Warshaw, D.M. (2008). Cargo transport: molecular motors navigate a complex cytoskeleton. Curr. Opin. Cell Biol. 20: 41-47.

Sanson, B. (2001). Generating patterns from fields of cells. Examples from Drosophila segmentation. EMBO Rep. 2: 1083-1088.

Satoh, A.K., O'Tousa, J.E., Ozaki, K., Ready, D.F. (2005). Rab11 mediates post-Golgi trafficking of rhodopsin to the photosensitive apical membrane of Drosophila photoreceptors. Development 132: 1487-1497.

Savkur, R.S, Burris, T.P. (2004). The coactivator LXXLL nuclear receptor recognition motif. J. Pept. Res. 63: 207-212.

Schroer, T.A., Sheetz, M.P. (1991). Functions of microtubule-based motors. Annu. Rev. Physiol. 53: 629-652.

Serrano, N., O'Farrell, P.H. (1997). Limb morphogenesis: connections between patterning and growth. Curr. Biol. 7: 186–195.

Shaw, R.M., Fay, A.J., Puthenveedu, M.A., von Zastrow, M., Jan, Y.N., Jan, L.Y. (2007). Microtubule plus-end-tracking proteins target gap junctions directly from the cell interior to adherens junctions. Cell 128: 547-560.

Sieber ,J.J., Willig, K.I., Kutzner, C., Gerding-Reimers, C., Harke, B., Donnert, G., Rammner, B., Eggeling, C., Hell, S.W., Grubmüller, H., Lang, T. (2007). Anatomy and dynamics of a supramolecular membrane protein cluster. Science 317: 1072-1076.

Söhl, G., Willecke, K. (2004). Gap junctions and the connexin protein family. Cardiovasc. Res. 62: 228-32.

Spray, D.C., Ye, Z.C., Ransom, B.R. (2006). Functional connexin "hemichannels": a critical appraisal. Glia 54: 758-773.

Stains, J.P., Lecanda, F., Screen, J., Towler, D.A., Civitelli, R. (2003). Gap junctional communication modulates gene transcription by altering the recruitment of Sp1 and Sp3 to connexin-response elements in osteoblast promoters. J. Biol. Chem. 278: 24377-24387.

Stebbings, L.A., Todman, M.G., Phillips, R., Greer, C.E., Tam, J., Phelan, P., Jacobs, K., Bacon, J.P., Davies, J.A. (2002). Gap junctions in Drosophila: developmental expression of the entire innexin gene family. Mech. Dev. 113: 197-205.

Tabata, T., Kornberg, T.B. (1994). Hedgehog is a signaling protein with a key role in patterning Drosophila imaginal discs. Cell 76: 89-102.

Tanentzapf, G., Smith, C., McGlade, J., Tepass, U. (2000). Apical, lateral, and basal polarization cues contribute to the development of the follicular epithelium during Drosophila oogenesis. J. Cell Biol. 151: 891-904.

TerBush, D.R., Maurice, T., Roth, D., Novick, P. (1996). The Exocyst is a multiprotein complex required for exocytosis in Saccharomyces cerevisiae. EMBO J. 15: 6483-6494.

Thomas, T,. Jordan, K., Simek, J., Shao, Q., Jedeszko, C., Walton, P., Laird, D.W. (2005). Mechanisms of connexin43 and Cx26 transport to the plasma membrane and gap junction regeneration. J. Cell Sci.118: 4451-4462.

Ul-Hussain, M., Zoidl, G., Klooster, J., Kamermans, M., Dermietzel R. (2008). IRES-mediated translation of the carboxy-terminal domain of the horizontal cell specific connexin Cx55.5 in vivo and in vitro. BMC Mol. Biol. 9: 52.

van der Heyden, M.A., Rook, M.B., Hermans, M.M., Rijksen, G., Boonstra, J., Defize, L.H., Destrée, O.H. (1998). Identification of connexin43 as a functional target for Wnt signalling. J. Cell Sci. 111: 1741-1749.

Weir, M.P., Lo, C.W. (1982). Gap junctional communication compartments in the Drosophila wing disk. Proc. Natl. Acad. Sci. 79: 3232-3235.

Wessel, D. and Fluegge, U.I. (1984). A method for the quantitative recovery of protein in dilute solution in the presence of detergents and lipids. Anal. Biochem. 138: 141-143.

Willecke, K., Eiberger, J., Degen, J., Eckardt, D., Romualdi, A., Güldenagel, M., Deutsch, U., Söhl, G. (2002). Structural and functional diversity of connexin genes in the mouse and human genome. Biol. Chem. 383: 725-737.

Wucherpfennig, T., Wilsch-Bräuninger, M., González-Gaitán, M.J. (2003). Role of Drosophila Rab5 during endosomal trafficking at the synapse and evoked neurotransmitter release. Cell Biol. 161: 609-624.

Yeaman, C., Grindstaff, K.K., Nelson, W.J. (1999). New perspectives on mechanisms involved in generating epithelial cell polarity. Physiol. Rev. 79: 73–98.

8 Appendix

8.1 Functionality proof of the UAS-inx2ΔCT fly strain

The functionality of the UAS-inx2ΔCT transgene was tested and verified using *in situ* hybridization, detecting *m*RNA levels of the overexpressed transgene (prd-Gal4) with an *inx2*-antisense probe. *inx2* mRNA expression was detected in enhanced stripes of the epidermis.

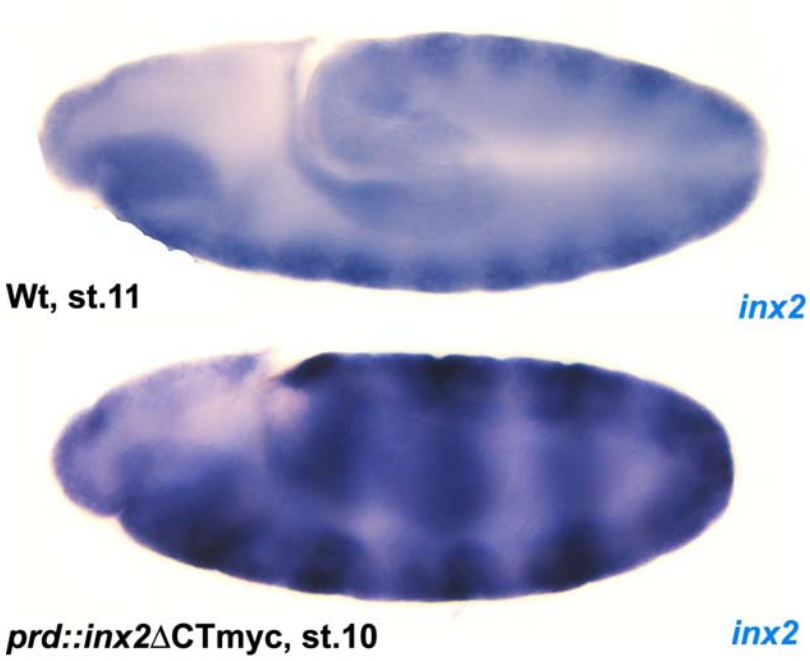

Fig. 8-1 *In situ* hybridisation of *innexin2* mRNA in embryos that overexpress the transgene *inx2ΔCTmyc*.

Amino acid-sequence inx2 full length

MFDVFGSVKGLLKIDQVCIDNNVFRMHYKATVIILIAFSLLVTSRQYIGDPIDCIVDEIPLGVM
DTYCWIYSTFTVPERLTGITGRDVVQPGVGSHVEGEDEVKYHKYYQWVCFVLFFQAILFYV
PRYLWKSWEGGRLKMLVMDLNSPIVNDECKNDRKKILVDYFIGNLNRHNFYAFRFFVCEAL
NFVNVIGQIYFVDFFLDGEFSTYGSDVLKFTELEPDERIDPMARVFPKVTKCTFHKYGPSGS
VQTHDGLCVLPLNIVNEKIYVFLWFWFIILSIMSGISLIYRIAVVAGPKLRHLLLRARSRLAES
EEVELVANKCNIGDWFLLYQLGKNIDPLIYKEVISDLSREMSGDEHSAHKRPFDA

intracellular domain

transmembrane domain

extracellular domain

Amino acid- sequence inx2ΔCT:

MFDVFGSVKGLLKIDQVCIDNNVFRMHYKATVIILIAFSLLVTSRQYIGDPIDCIVDEIPLGVM
DTYCWIYSTFTVPERLTGITGRDVVQPGVGSHVEGEDEVKYHKYYQWVCFVLFFQAILFYV
PRYLWKSWEGGRLKMLVMDLNSPIVNDECKNDRKKILVDYFIGNLNRHNFYAFRFFVCEAL
NFVNVIGQIYFVDFFLDGEFSTYGSDVLKFTELEPDERIDPMARVFPKVTKCTFHKYGPSGS
VQTHDGLCVLPLNIVNEKIYVFLWFWFIILSIMSGISLIY

intracellular domain

transmembrane domain

extracellular domain

8.2 Phosphorylation - site predictions

Predictions were done using the following link:

http://www.cbs.dtu.dk/services/NetPhos/

inx2

MFDVFGSVKGLLKIDQVCIDNNVFRMHYKATVIILIAFSLLVTSRQYIGDPIDCIVDEIPLGVMDTYCWIYSTFTVPERL
TGITGRDVVQPGVGSHVEGEDEVKYHKYYQWVCFVLFFQAILFYVPRYLWKSWEGGRLKMLVMDLNSPIVNDECKNDRKK
ILVDYFIGNLNRHNFYAFRFFVCEALNFVNVIGQIYFVDFFLDGEFSTYGSDVLKFTELEPDERIDPMARVFPKVTKCTF
HKYGPSGSVQTHDGLCVLPLNIVNEKIYVFLWFWFIILSIMSGISLIYRIAVVAGPKLRHLLLRARSRLAESEEVELVAN
KCNIGDWFLLYQLGKNIDPLIYKEVISDLSREMSGDEHSAHKRPFDA

Serine phosophorylation prediction

Threonine phosphorylation prediction

Tyrosine phosphorylation prediction

inx3

MAVFGMVSAVSGFIKIRYLLDKAVIDNMVFRCHYRITTAILFTCCIIVTANNLIGDPISCINDGAIPMHVINTFC
WITYT
YTIPGQQHRQIGTDVAGPGLGNEYGQEKRYHSYYQWVPFVLFFQGLMFYVPHWVWKNMEDGKIRMITDGLRGMVS
VPDDY
RRDRQDRILKYFVNSLNTHNGYSFAYFFCELLNFINVIVNIFMVDKFLGGAFMSYGTDVLKFSNMDQDKRFDPMI
EIFPR
LTKCTFHKFGPSGSVQKHDTLCVLALNILNEKIYIFLWFWFIILATISGVAVLYSLVVIMMPTTRETIIKRSYRS
AQRKE
IAGLVRRLEIGDFLILHFLSQNLSTRSYSDMLQQLCGLLGASRTPSAPSTLEMNRISHPIYPPVETFGGGKETET

Serine phosophorylation prediction

Threonine phosophorylation prediction

Tyrosine phosphorylation prediction

8.3 Development of the *Drosophila* embryo

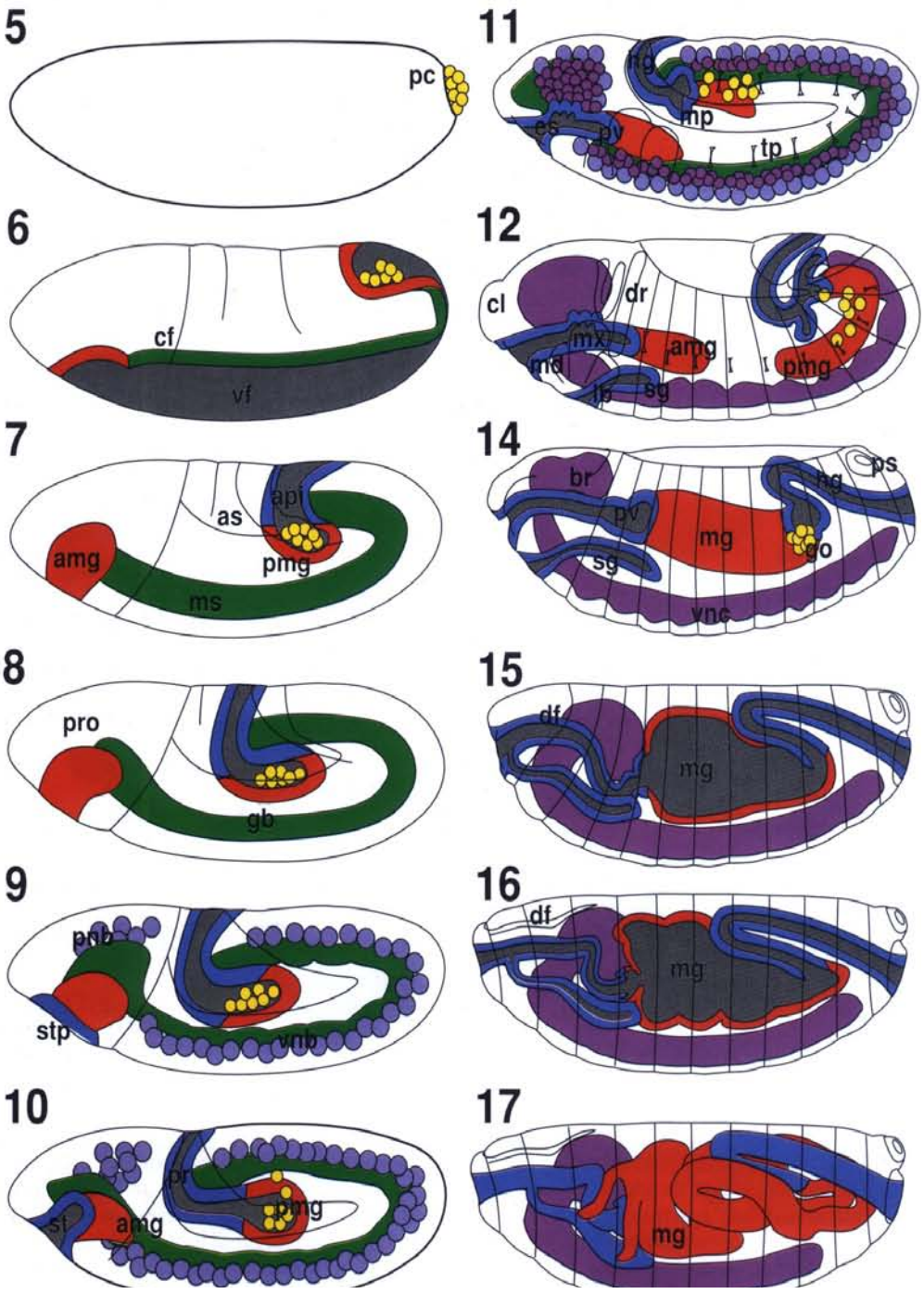

Fig. 8-2 Stages of embryonic development in *D.melanogaster.* All embryos are in lateral view (anterior to the left). (Red) Endoderm, midgut; (green) mesoderm; (purple) central nervous system; (blue) foregut, hindgut; (yellow) pole cells. (amg) anterior midgut rudiment; (br) brain; (cf) chephalic furrow; (cl) cypeolabrum; (df) dorsal fold; (dr) dorsal ridge; (es) esophagus; (gb) germ band, (go) gonads; (hg) hindgut; (lb) labial bud; (md) mandibular bud; (mg) midgut, (mt) Malphigian tubules; (mx) maxillary bud; (pc) pole cells; (pmg) posterior midgut rudiment; (pnb) procephalic neuroblasts; (pro) procephalon; (ps) posterior spiracle; (pv) proventriculus, (sg) salivary gland, (stp) stomodeal plate, (st) stomodeum; (tp) tracheal pits; (vf) ventral furrow, (vnb) ventral neuroblasts, (vnc) ventral nerve cord. (After Hartenstein, Drosophila Atlas)

8.4 Crossing scheme for rescue of *hedgehog* mutants

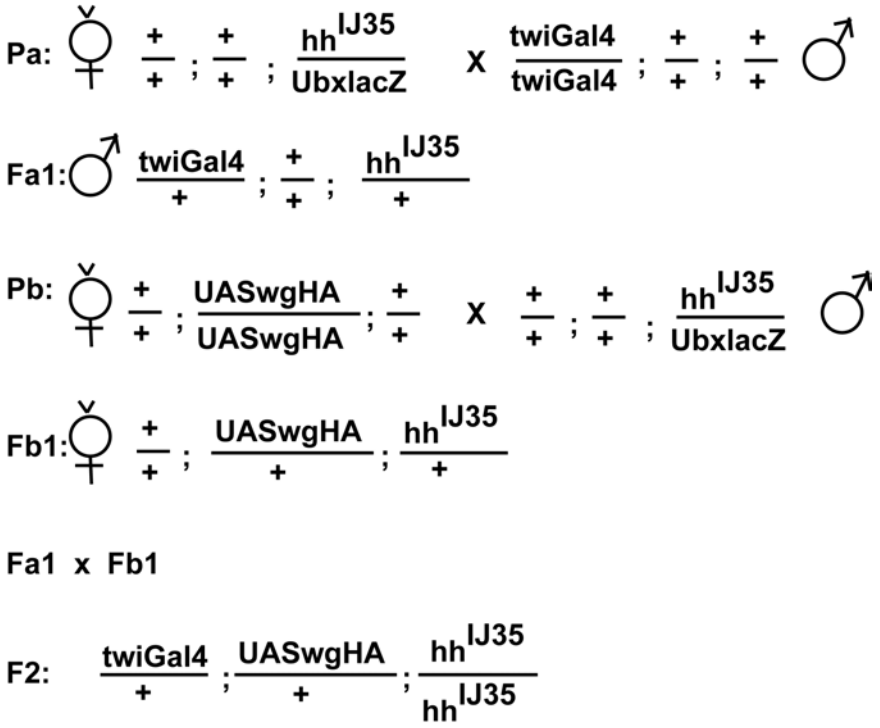

P = parental generation

F = filial generation

Table of Figures

Erklärung

Diese Dissertation wurde im Sinne von § 4 der Promotionsordnung vom 7.1.2004 am LIMES Institut / Universität Bonn unter der Leitung von Herrn Prof. M. Hoch angefertigt.

Hiermit versichere ich, dass ich die vorliegende Arbeit selbständig angefertigt habe und keine weiteren als die angegebenen Hilfsmittel und Quelle verwendet habe, die gemäß § 6 der Promotionsordnung kenntlich gemacht sind. Ferner wurde diese Arbeit an keiner anderen Hochschule als Dissertation eingereicht.

Bonn, im November 2008

Hildegard Lechner